The impact of terrestrial noise on the detectability and reconstruction of gravitational wave signals produced by core-collapse supernovae

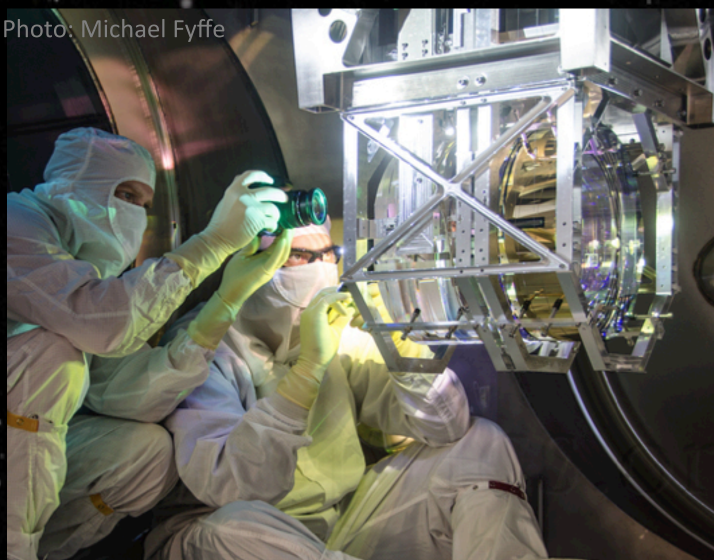
Photo: Michael Fyffe

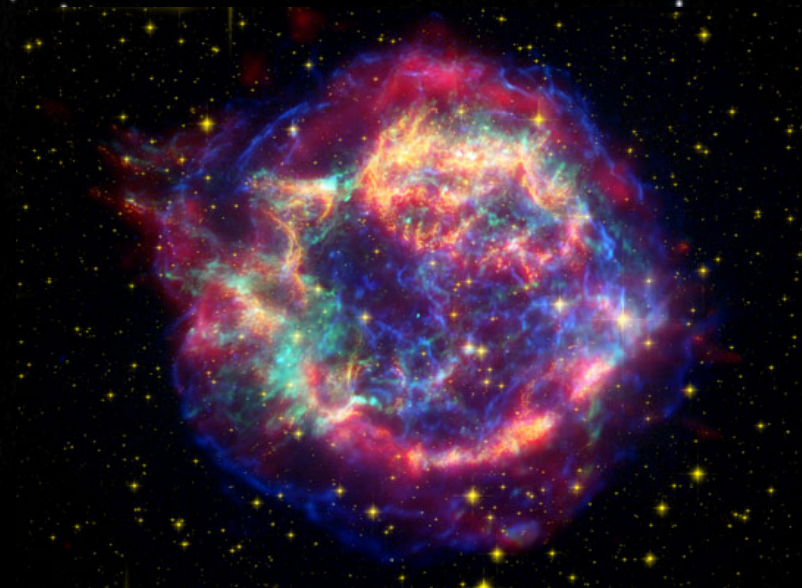

Jess McIver PhD defense

May 21, 2015

LIGO DCC P1500072

Outline

- Gravitational waves
- Interferometric detectors
- Core collapse supernovae
  - Models
  - Detectablity and waveform reconstruction
- Terrestrial noise and its impact
- Conclusions and future prospects

The centennial of General Relativity

The theory of General Relativity was first published by Albert Einstein in 1915

- Predicts the emission of *gravitational waves* by accelerating mass:
- ripples in the fabric of spacetime

Gravitational waves

- Solution to Einstein's field equations

$$G_{\mu\nu} = 8\pi\ T_{\mu\nu}$$

- Gravitational waves

$$h(t) = Ae^{i(2\pi ft - \mathbf{k}\cdot\mathbf{r})}$$

  - Propagate at speed of light
  - Induce spacetime strain measured as: $\dfrac{\Delta L}{L}$

Gravitational wave emission

- Produced by accelerating mass: $h(t) \propto \frac{1}{r}\frac{d^2 I_{ij}}{dt^2}$
- Weakly interacting

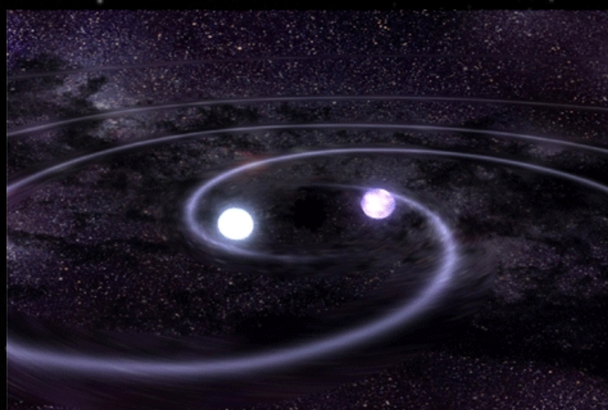

Binary black hole coalescence
h ~ 10^{-21} at 100Mpc for $10M_\odot$

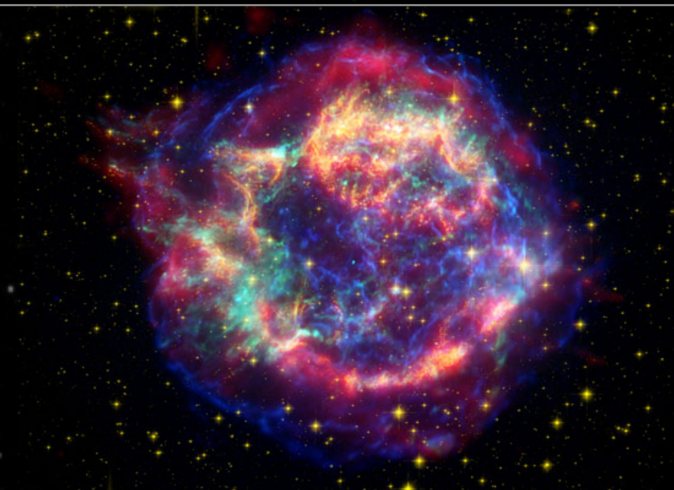

Core-collapse supernova
h ~ 10^{-21} at 10 kpc for rotating models

Gravitational wave manifestation

h(t) composed of cross and plus polarization

$$h(t) = \begin{pmatrix} 0 & 0 & 0 & 0 \\ 0 & h_+ & h_\times & 0 \\ 0 & h_\times & h_+ & 0 \\ 0 & 0 & 0 & 0 \end{pmatrix}$$

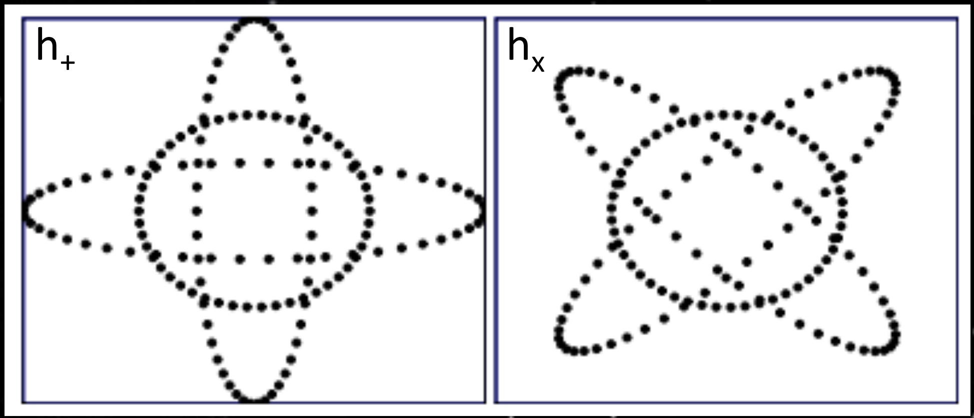

Observing GWs with interferometry

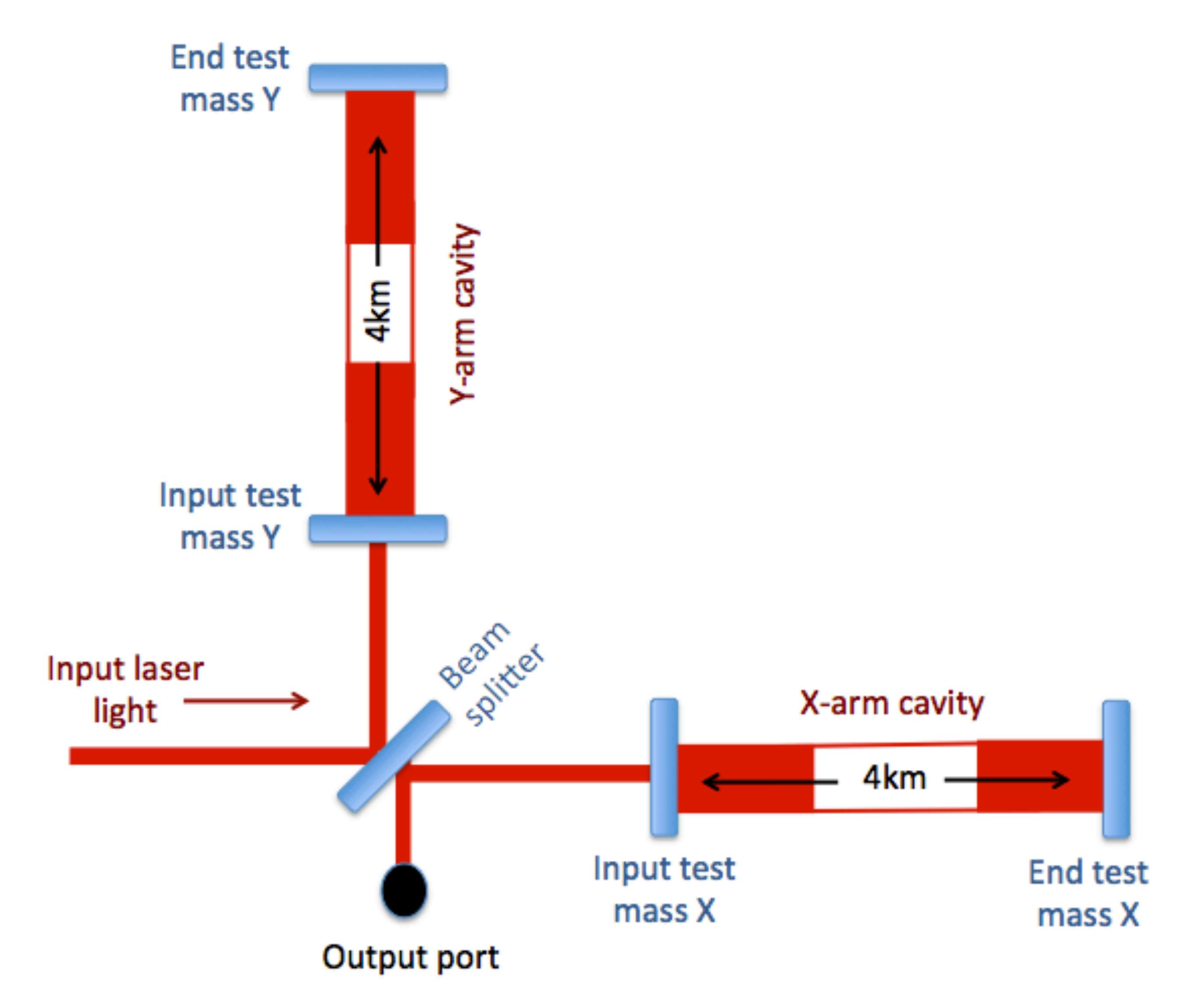

The LIGO detectors

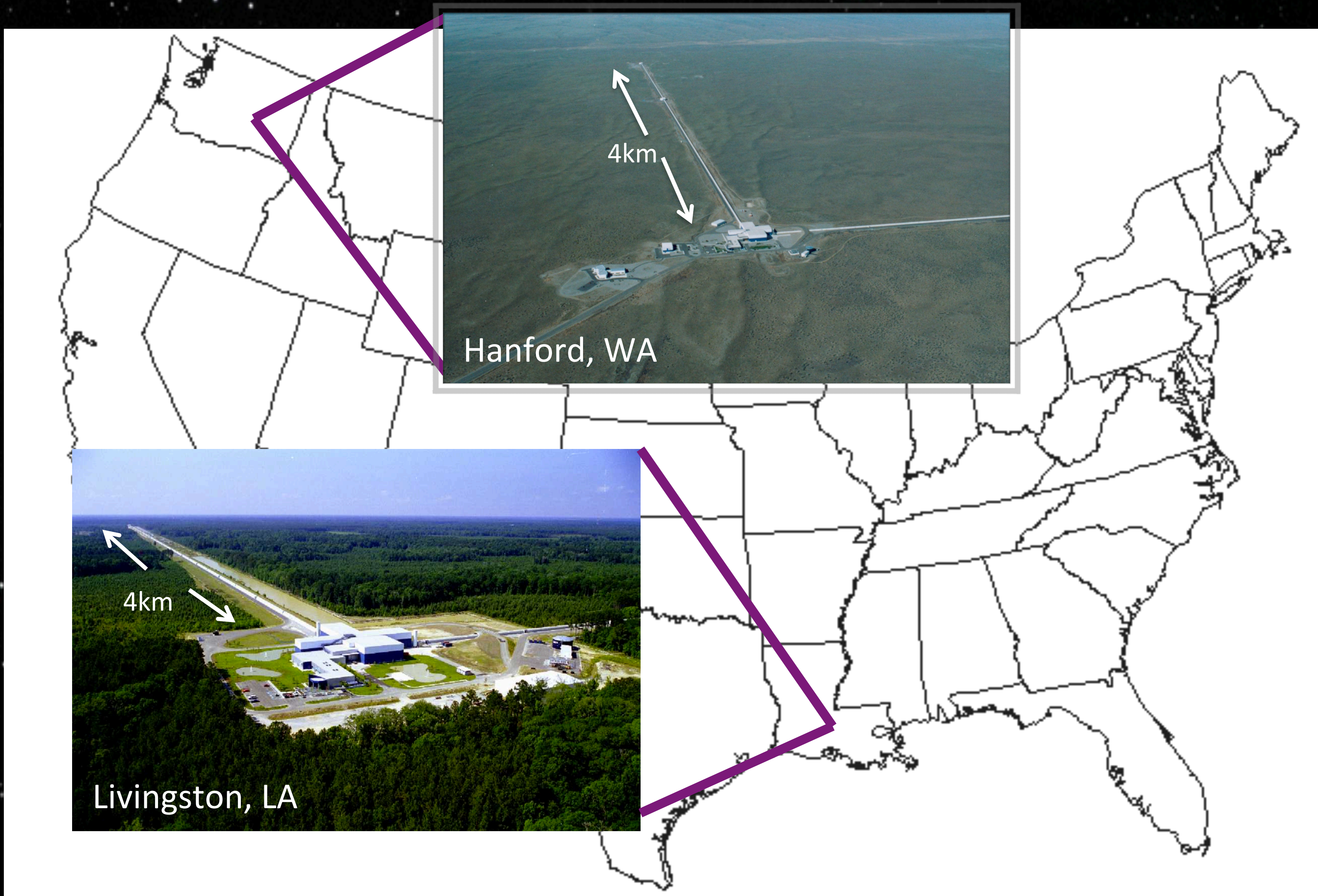

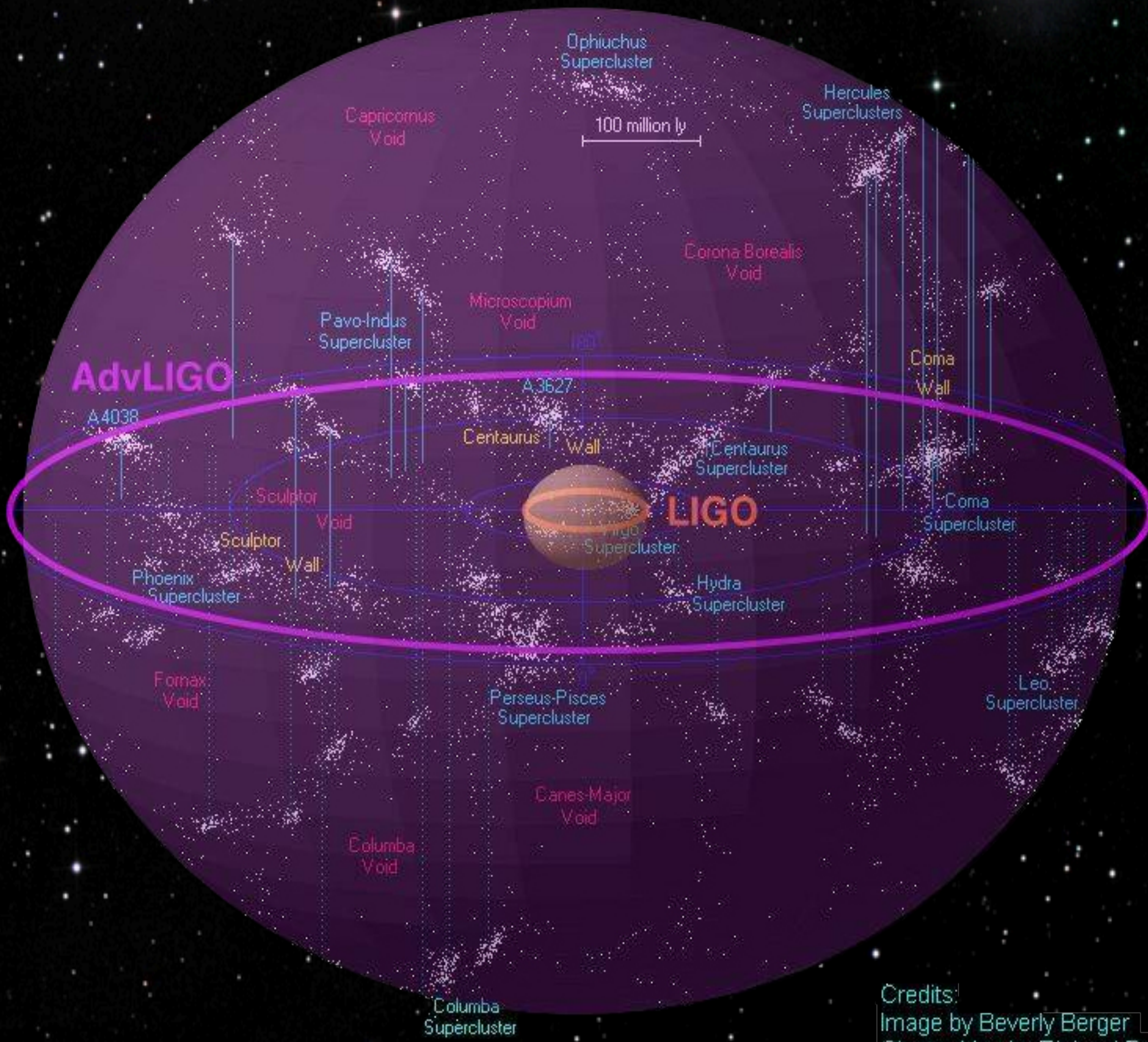

Credits:
Image by Beverly Berger
Cluster Map by Richard Powell

Sensitivity improvement

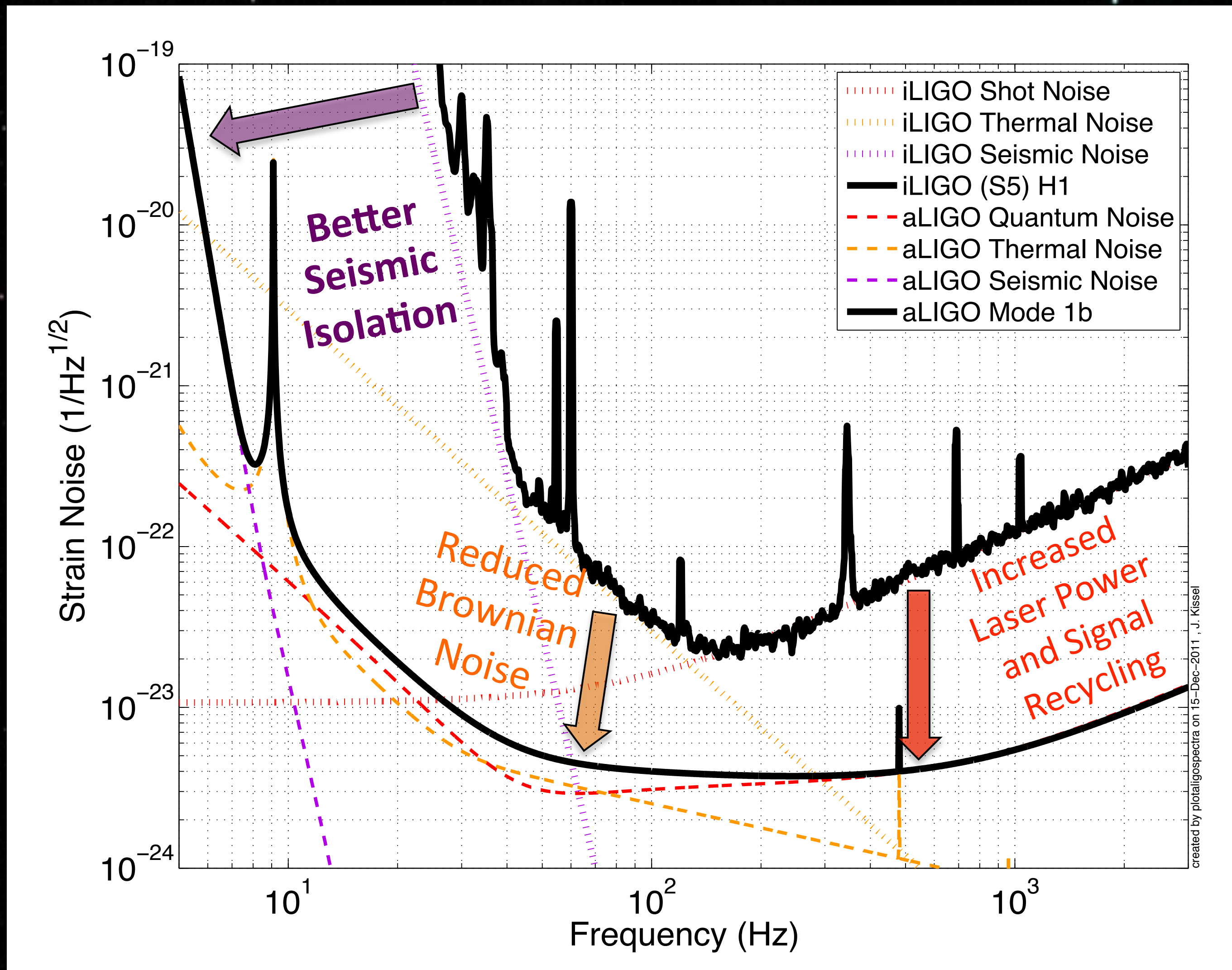

The global interferometer network

Network sensitivity

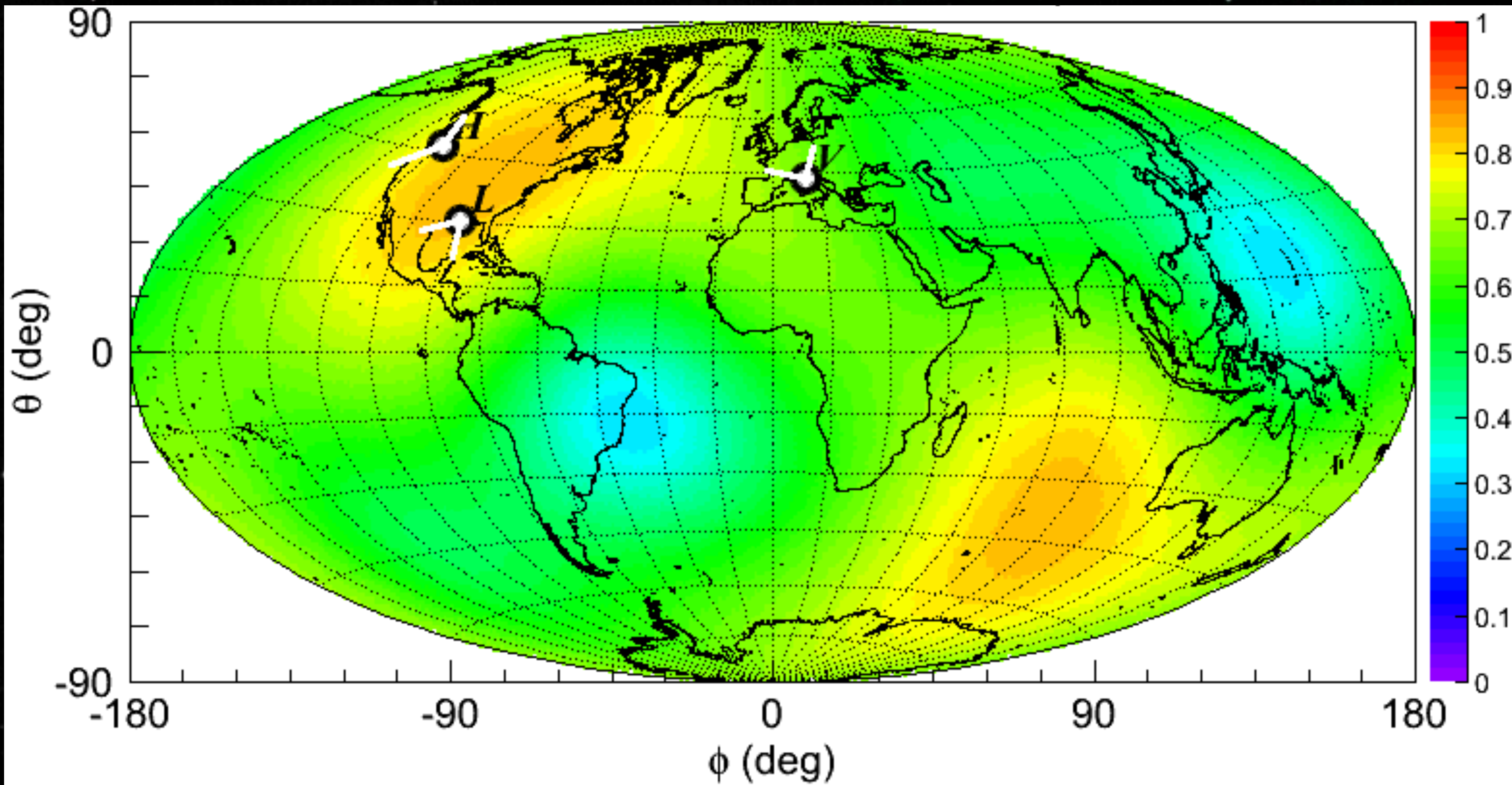

The gravitational wave sky

What sources will the Advanced detector network be sensitive to?

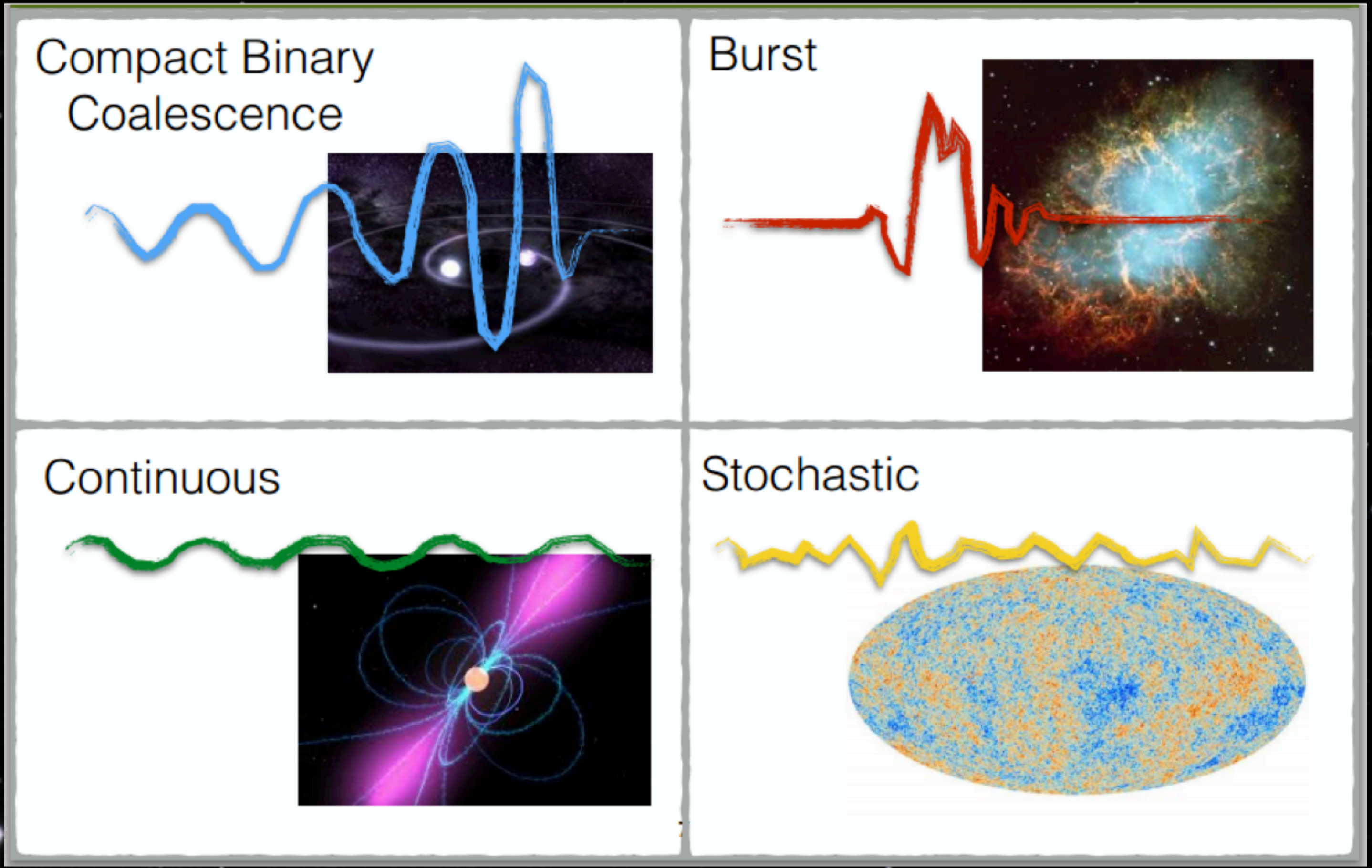

Core-collapse supernovae

- The iron core of massive stars burns out and the degeneracy pressure can no longer support the star against gravity.
- The gravitational core collapse releases an enormous amount of energy, 99% in the form of neutrinos of all flavors and forms a proto-neutron star.

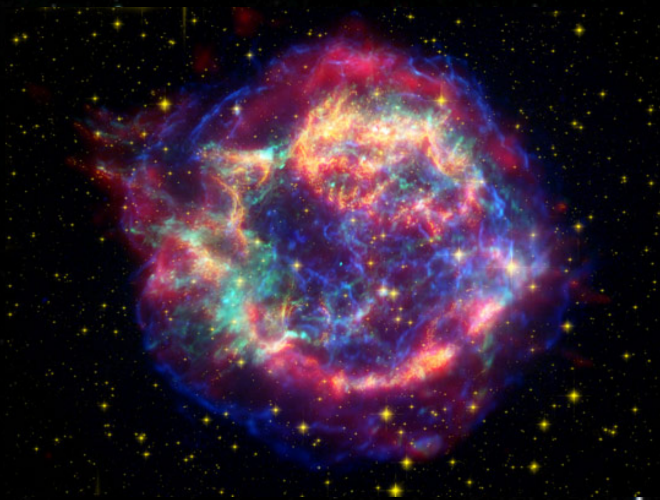

- Neutrinos observed during the 1987 supernova have confirmed this general model
- However, calculations robustly conclude that the shock wave loses energy to interactions with the outer layers and stalls

Key question: *what is the explosion mechanism?*

Explosion mechanism models

Neutrino-driven

- Assumes a small fraction of the energy emitted in the form of neutrinos is absorbed by the shock

Magnetorotational

- Differential rotation between the star core and outer layers induces magnetic field amplifications that cause jets of matter

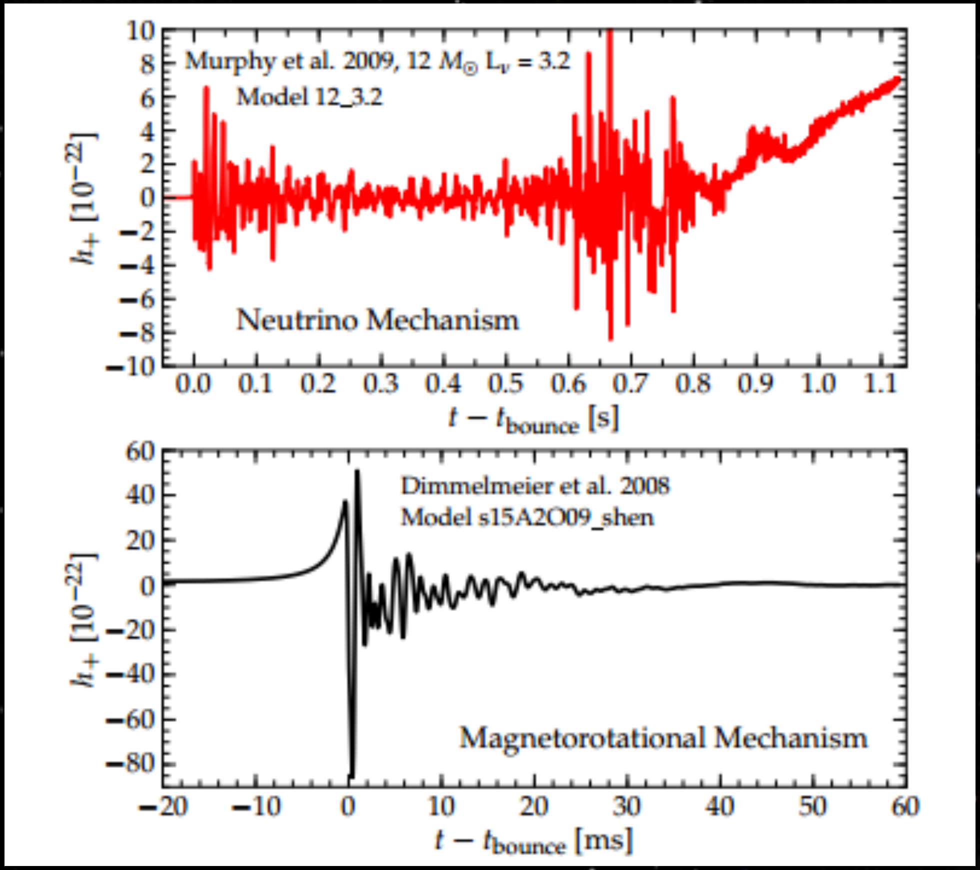

Study outline

Goal: Effective waveform reconstruction of gravitational wave signals will enable accurate interpretations of core-collapse supernovae (CCSN) physics

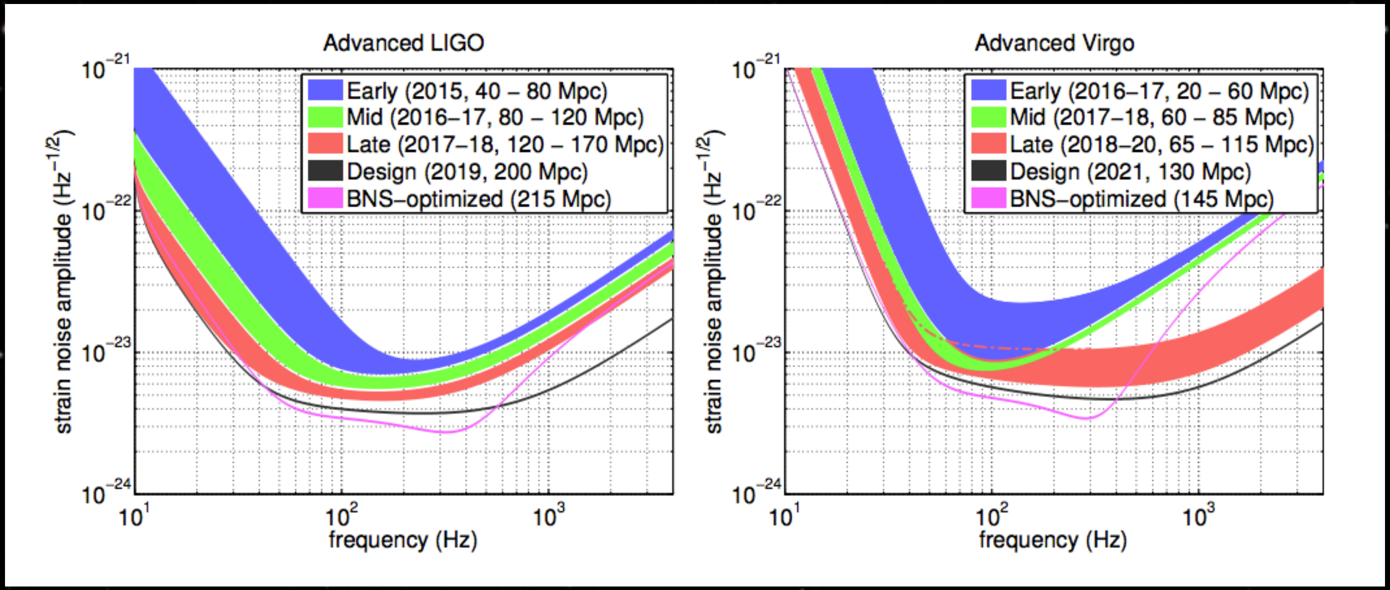

1. **Waveforms injected into Gaussian noise** colored with the expected Advanced LIGO and Advanced Virgo noise curves at design sensitivity
2. Injections recovered with burst waveform reconstruction algorithms

Included waveforms: Overview

The three considered waveform families:

Each simulated using different models.

1. Dimmelmeier

- 2D rotating core-collapse
- Produce the simplest, shortest GW signature ('wavelet-like')

2. Yakunin

- 2D neutrino driven
- Assumes star axis symmetry
- No well-defined amplitude peak

3. Mueller

- 3D neutrino driven
- Most realistic considered models
- Longest, most complex produced waveforms

Included waveforms

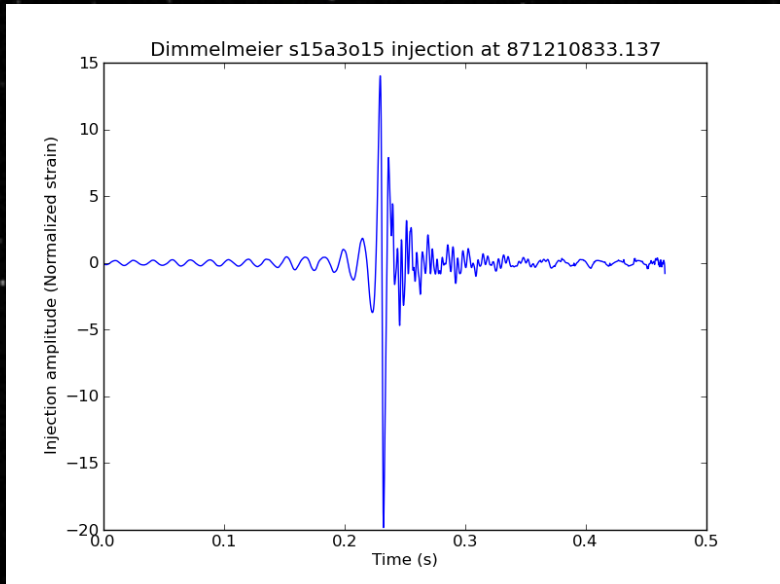

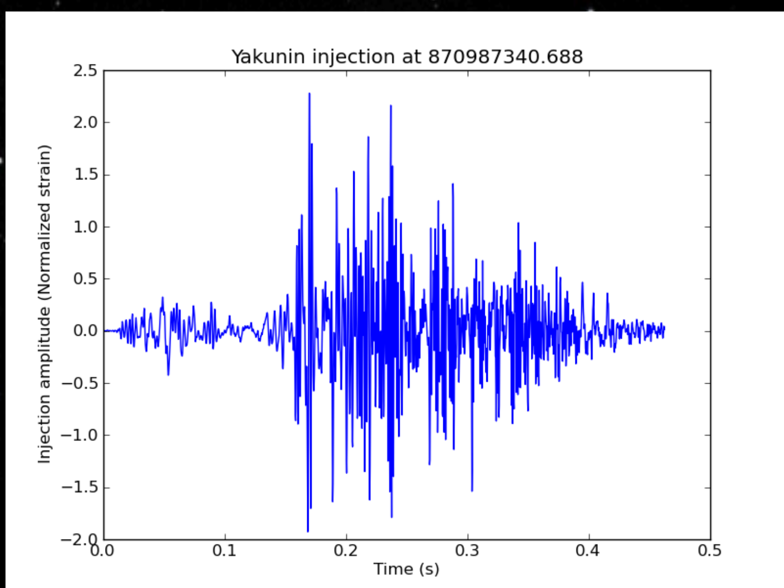

Dimmelmeier

- 2D axisymmetric rotating core-collapse
- 3 Dimmelmeier models: different rotation rates and profiles imposed on a progenitor star

Yakunin

- 2D axisymmetric non-rotating neutrino driven
- Strong signal due to standing accretion shock instabilities and non-radial accretion matter flows

Included waveforms

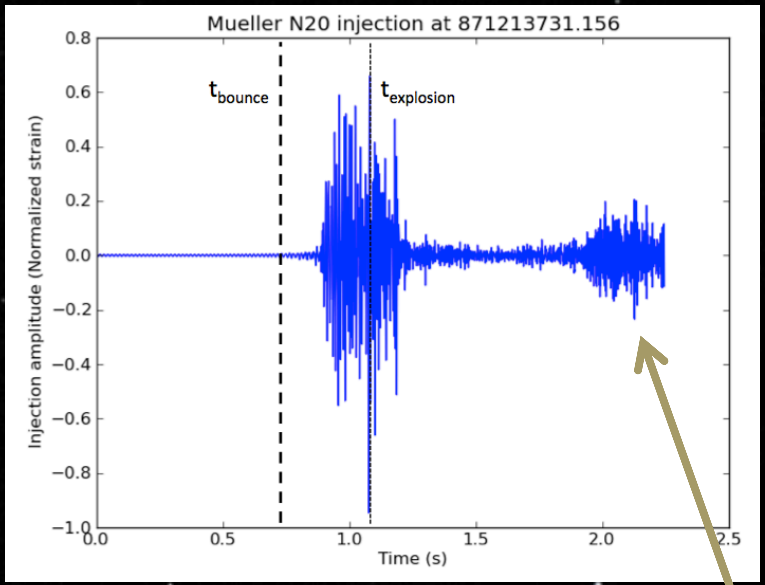

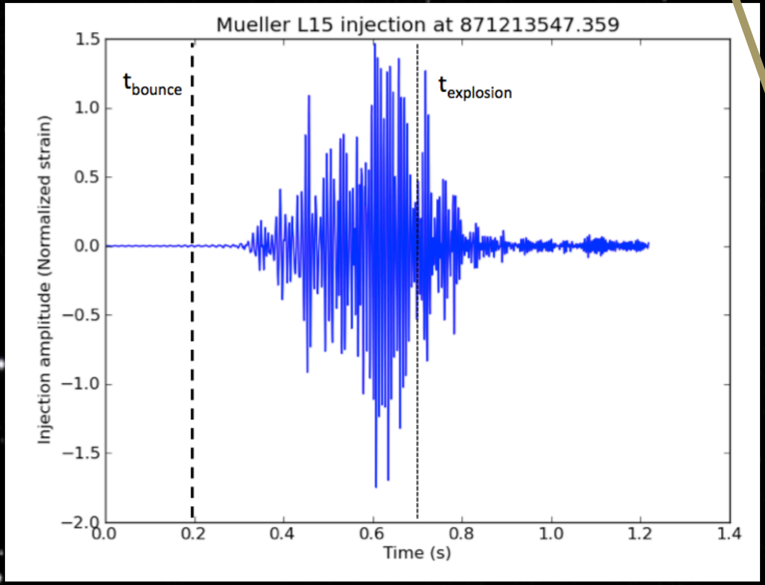

Mueller

- 3D non-rotating neutrino-driven
- 3 different progenitor stars evolved using the same input physics, initial symmetry perturbation, and matter equation of state
- Strong GW signal is due to non-radial matter flows produced by shock instability pre-explosion, and violent post-shock convection and PNS matter accretion post-explosion
- Two of three progenitor stars observe a delayed burst of GW signal due to PNS convection.

Targeted algorithms

cWB2G – the primary coherent burst all-sky search

- Identifies burst candidate events by tiling the data in time and frequency via a wavelet transform
- Extracts significant events using a coherent likelihood statistic maximized over all potential sky positions.

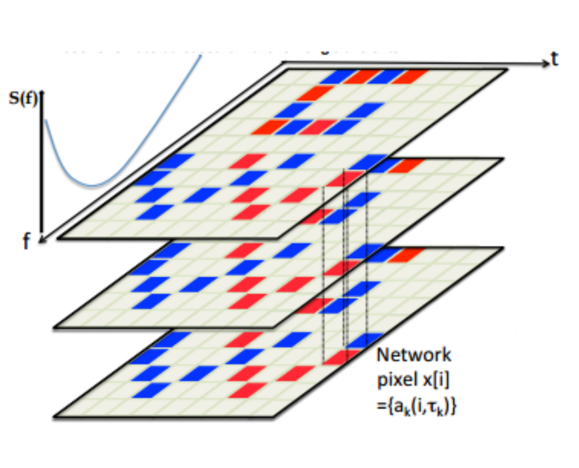

BayesWave – a Bayesian follow-up burst parameter estimation algorithm

- Estimates a posterior distribution for a recovered waveform inferred from the data and network antenna pattern.
- Reversible jump Markov-chain Monte Carlo algorithm explores a the application distribution of Morlet-Gabor wavelets and wavelet parameters to the signal fit

Figure of merit

Burst algorithm performance in reconstructing waveforms was judged by the **noise-weighted normalized overlap:**

$$\alpha = \frac{\langle \psi_{rec} | \psi_{inj} \rangle}{\sqrt{\langle \psi_{rec} | \psi_{rec} \rangle \langle \psi_{inj} | \psi_{inj} \rangle}}$$

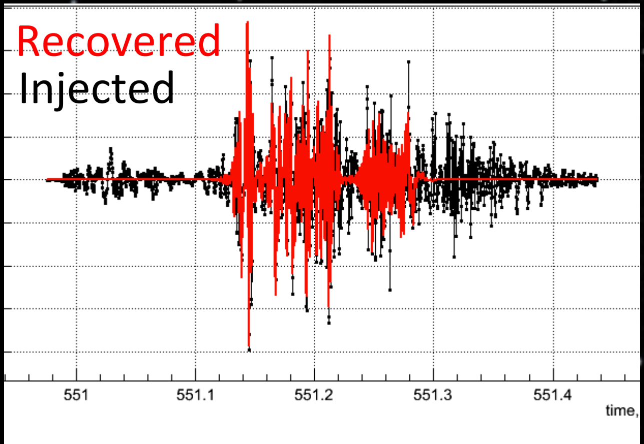

Where:

$$\langle \psi_{rec} | \psi_{inj} \rangle = \int \frac{\psi^*_{rec}(f)\ \psi_{inj}(f)}{S(f)}\, df$$

1 is perfect match, 0 is no match

Preliminary results in three parts:

1. Trends in detectability between different models
2. Trends for recovered overlap of different models by both algorithms
3. Trends for the recovered overlap by different algorithms of the same model

For these preliminary results, both cWB2G and BayesWave were run in configurations tuned for CCSN.

Detectability of the three included waveform families

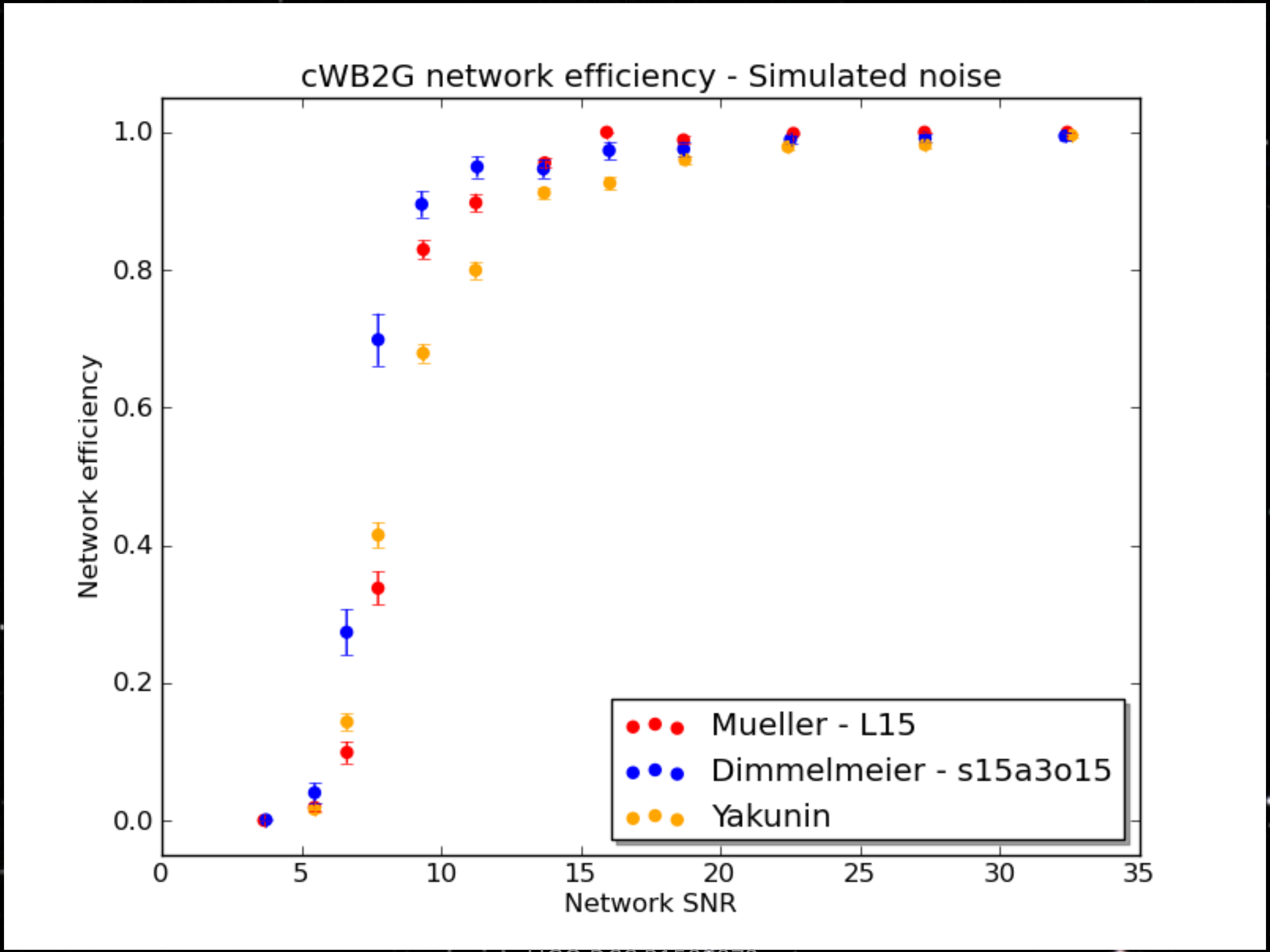

Detectability of the three included waveform families

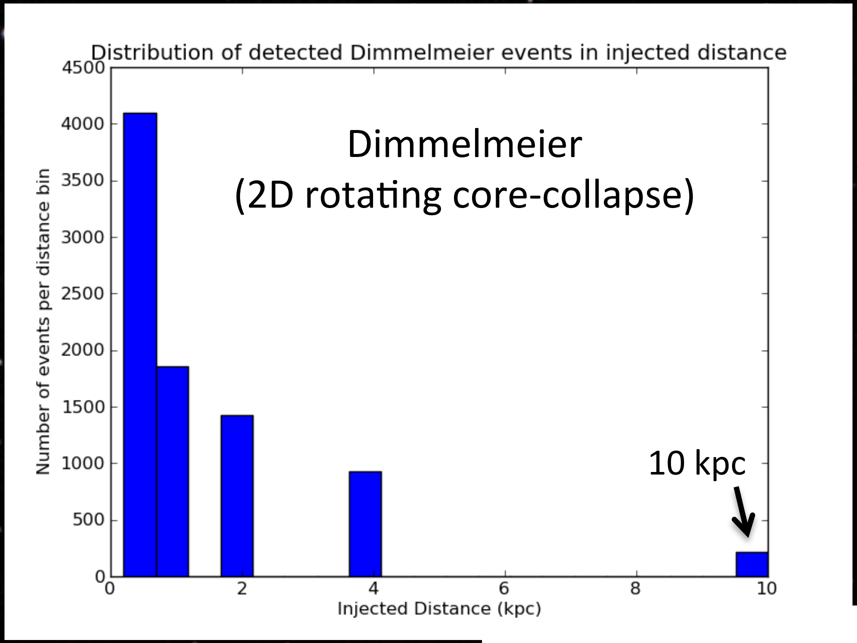

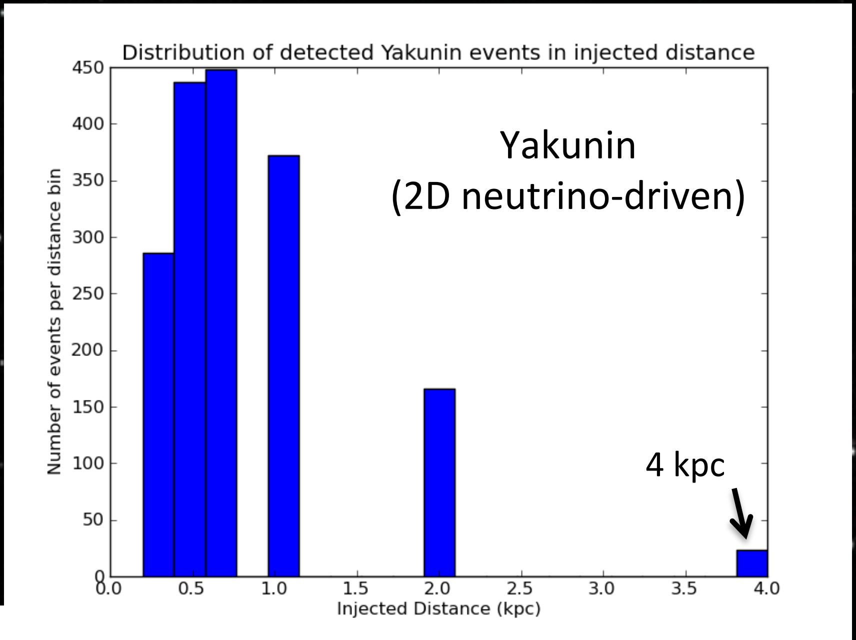

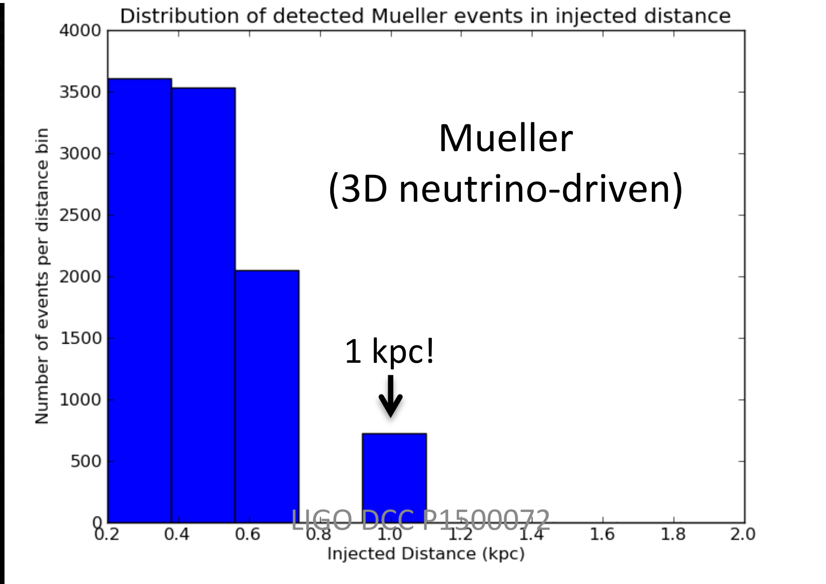

Reconstruction of the three included waveform families by cWB2G

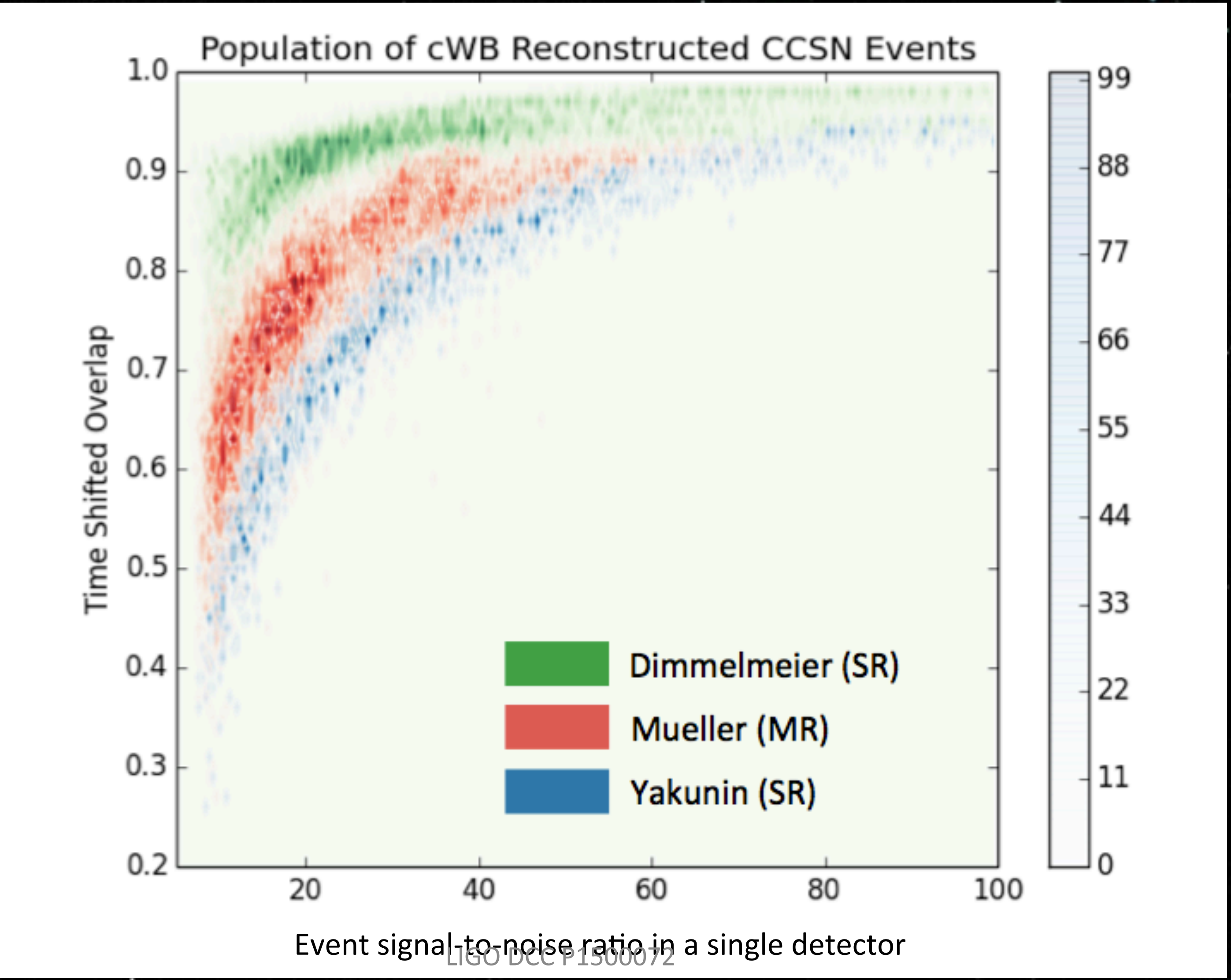

Dimmelmeier – rapidly rotating

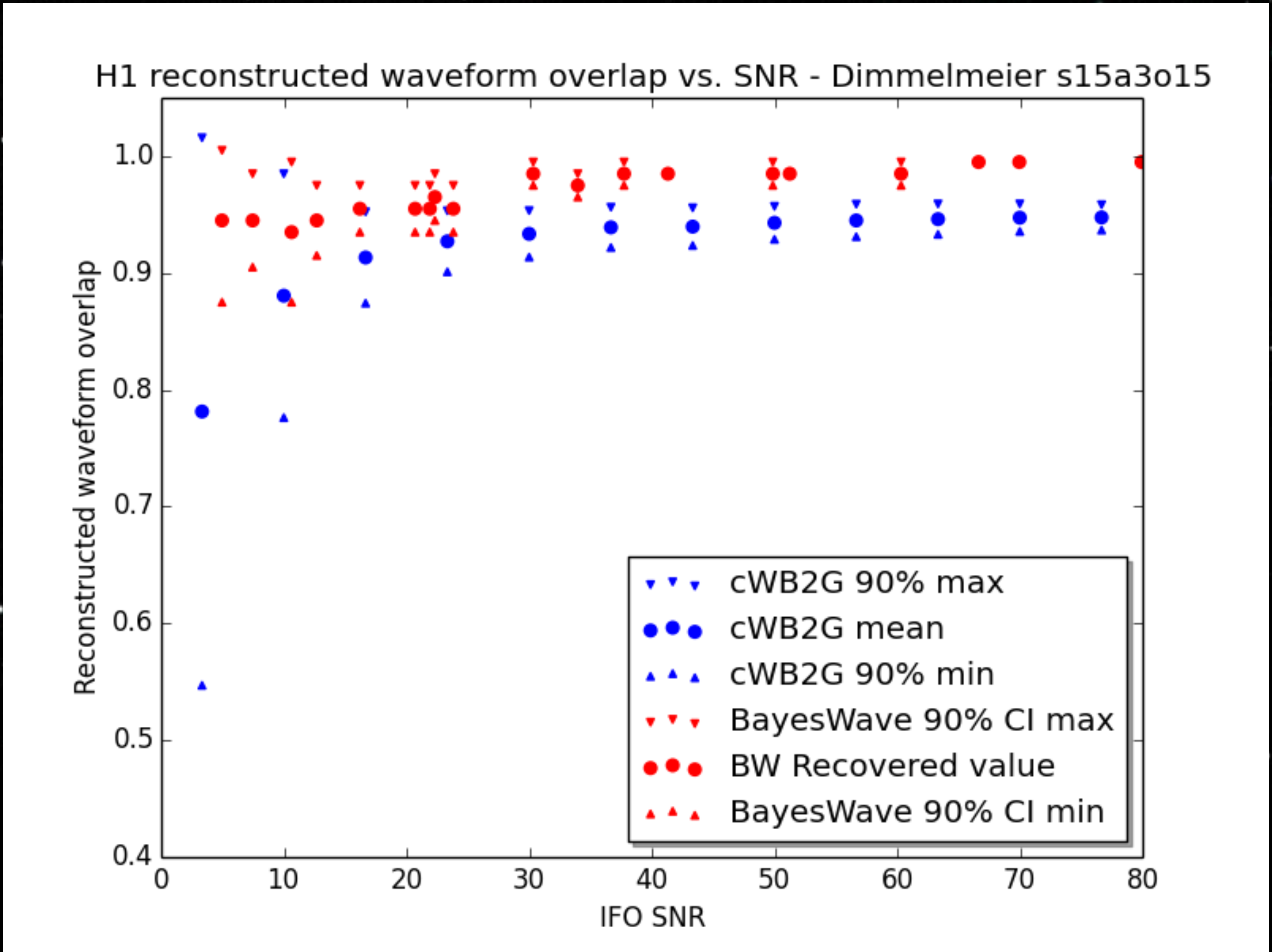

Dimmelmeier – rapidly rotating

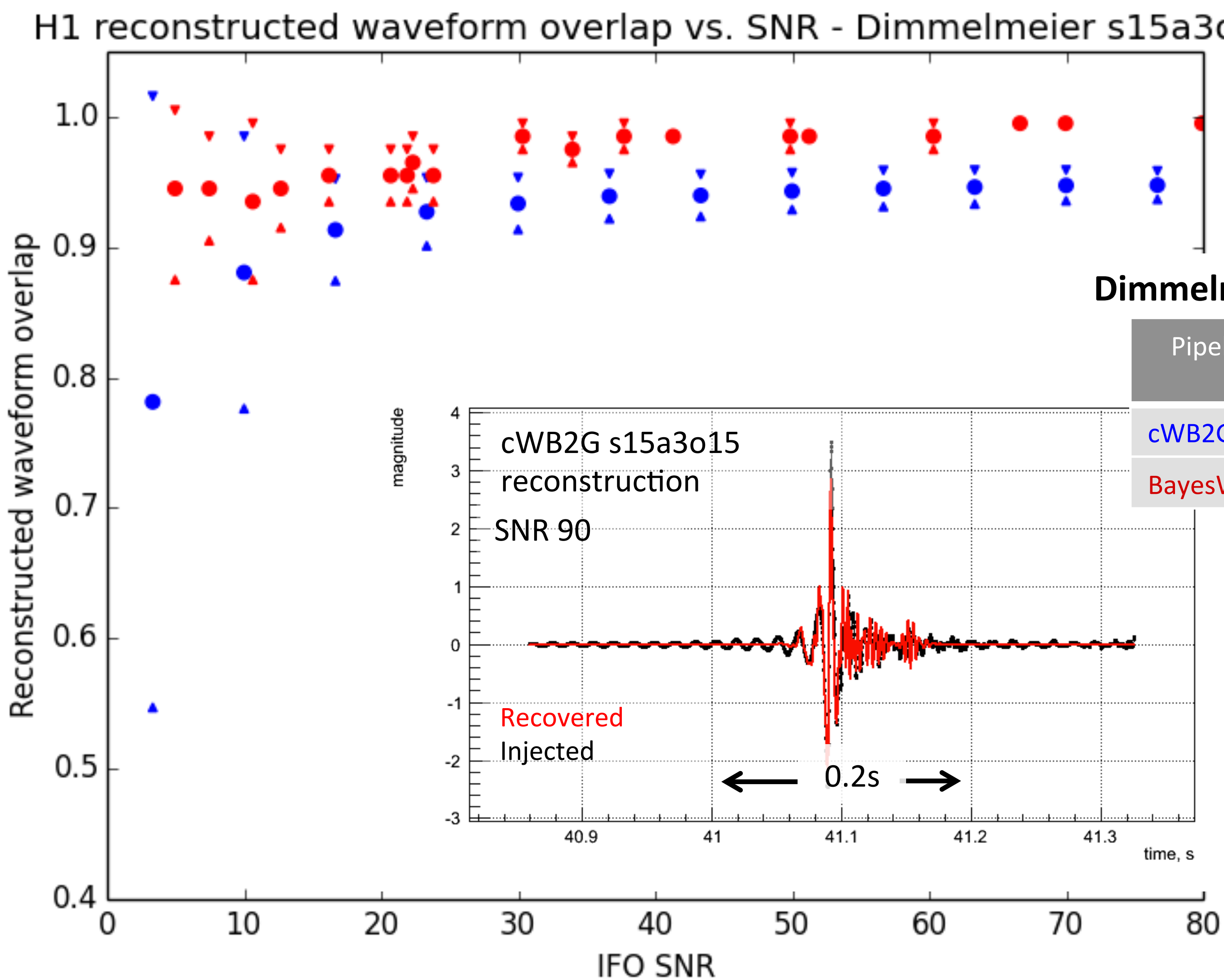

Dimmelmeier s15a3o15 – L1

Pipeline	Max overlap	Overlap at SNR8
cWB2G	95%	86%
BayesWave	99%	94%

Yakunin

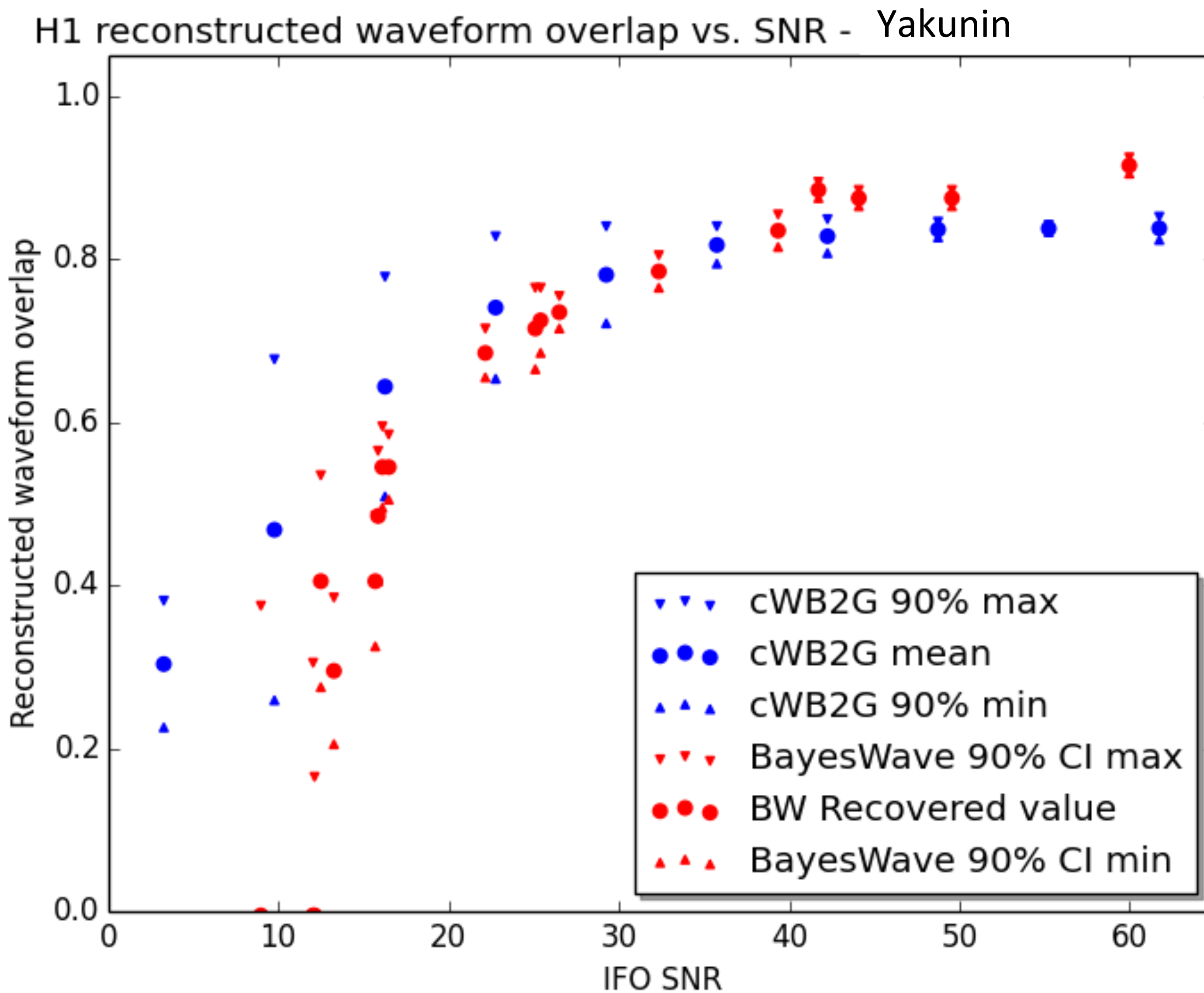

H1 reconstructed waveform overlap vs. SNR - Yakunin
Reconstructed waveform overlap
IFO SNR
0.0
0.2
0.4
0.6
0.8
1.0
0
10
20
30
40
50
60
cWB2G 90% max
cWB2G mean
cWB2G 90% min
BayesWave 90% CI max
BW Recovered value
BayesWave 90% CI min

Yakunin

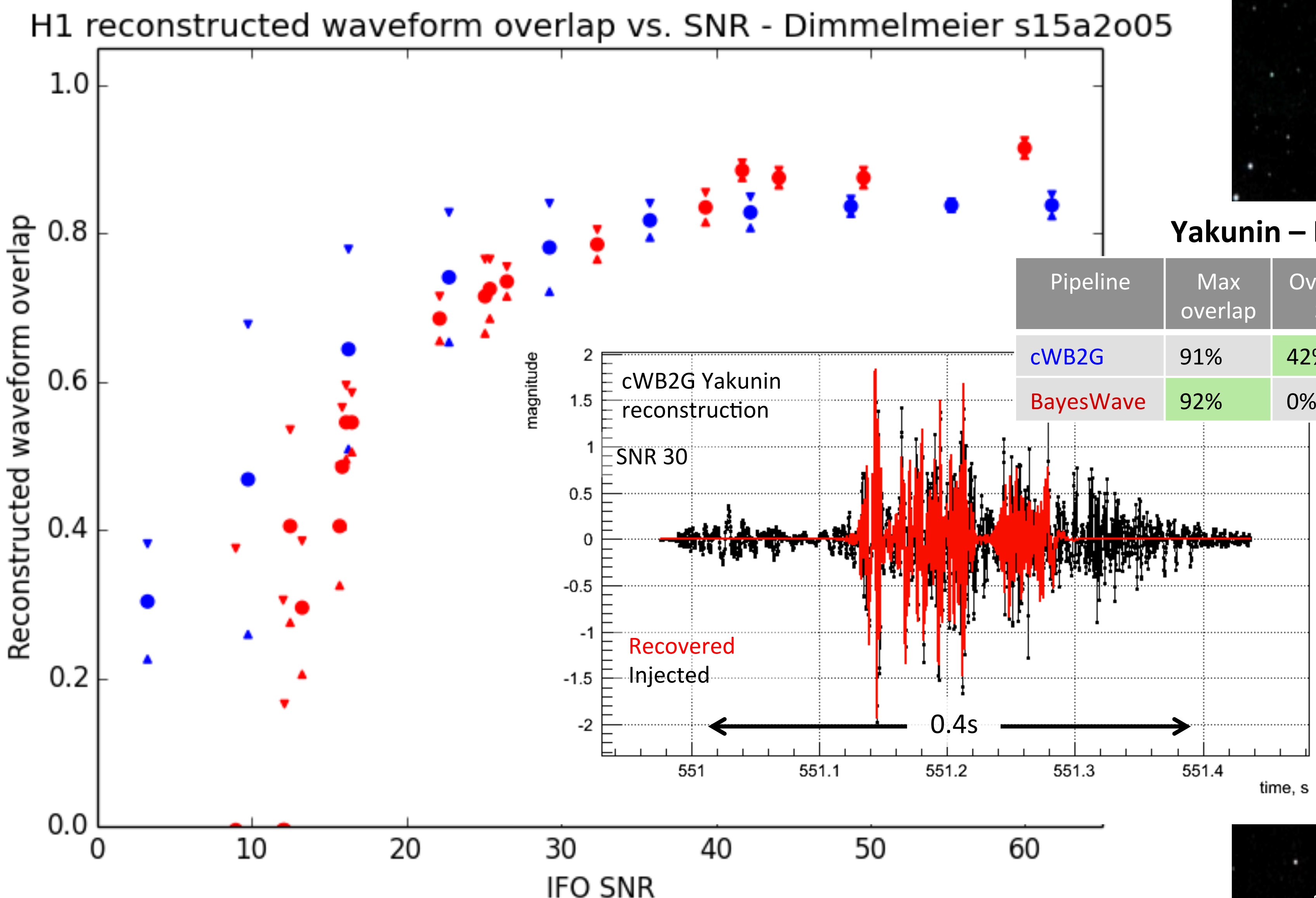

Yakunin – L1

Pipeline	Max overlap	Overlap at SNR8
cWB2G	91%	42%
BayesWave	92%	0%

Mueller – N20

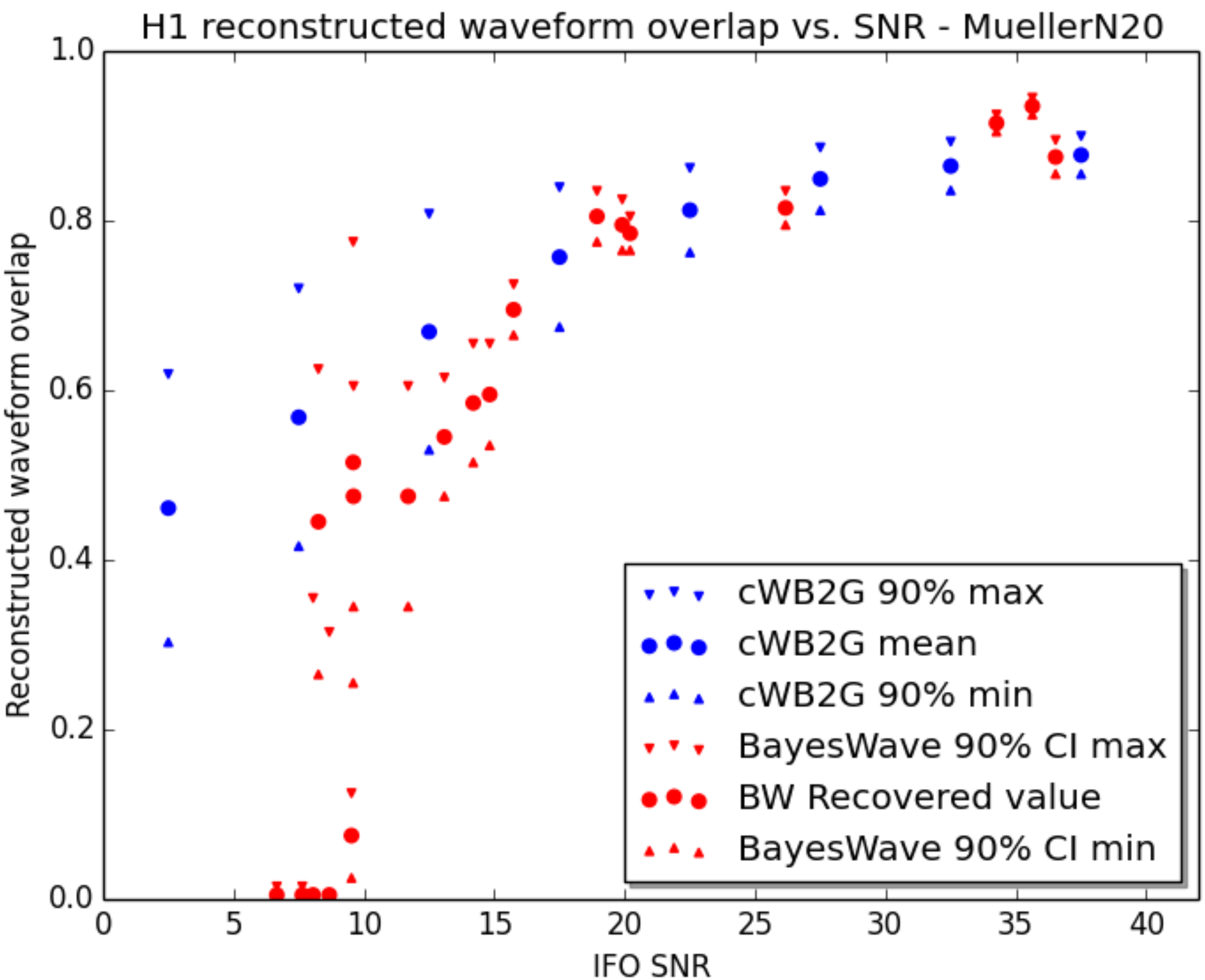

H1 reconstructed waveform overlap vs. SNR - MuellerN20
Reconstructed waveform overlap
IFO SNR
0.0
0.2
0.4
0.6
0.8
1.0
0
5
10
15
20
25
30
35
40
cWB2G 90% max
cWB2G mean
cWB2G 90% min
BayesWave 90% CI max
BW Recovered value
BayesWave 90% CI min

Mueller – N20

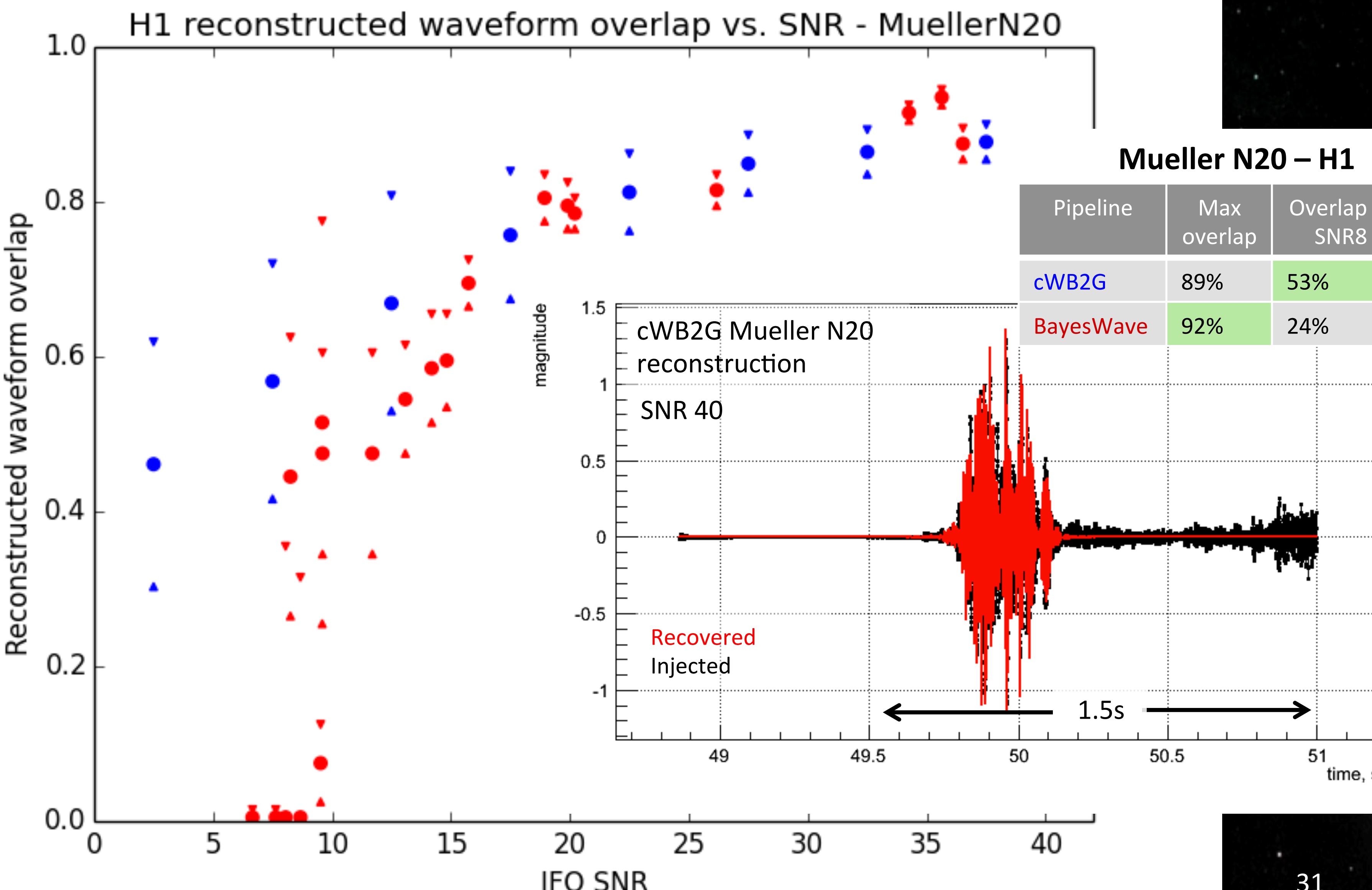

Mueller N20 – H1

Pipeline	Max overlap	Overlap at SNR8
cWB2G	89%	53%
BayesWave	92%	24%

Summary:
CCSN in aLIGO/aVirgo Gaussian noise

- For more realistic included waveforms in aLIGO/aVirgo noise the best average reconstruction (cWB2G) at realistic SNR (of ~8) is ~50-60% overlap.
- BayesWave, with more wavelet placement flexibility, tends to achieve a lower overlap at an SNR of 8.
- Both algorithms do not well reconstruct multiple bursts of energy distinct in time as one event.
- A lot of potential for significant improvement with BayesWave developing CCSN priors.

Terrestrial noise: a reality for GW searches

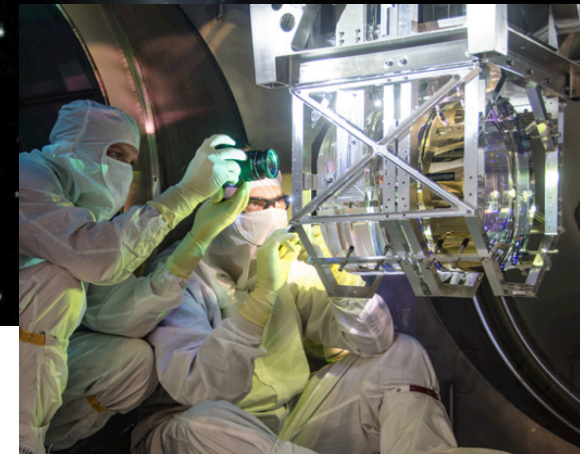

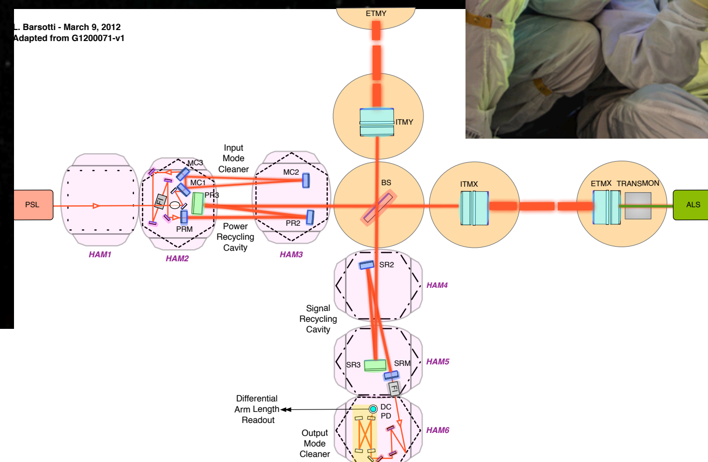

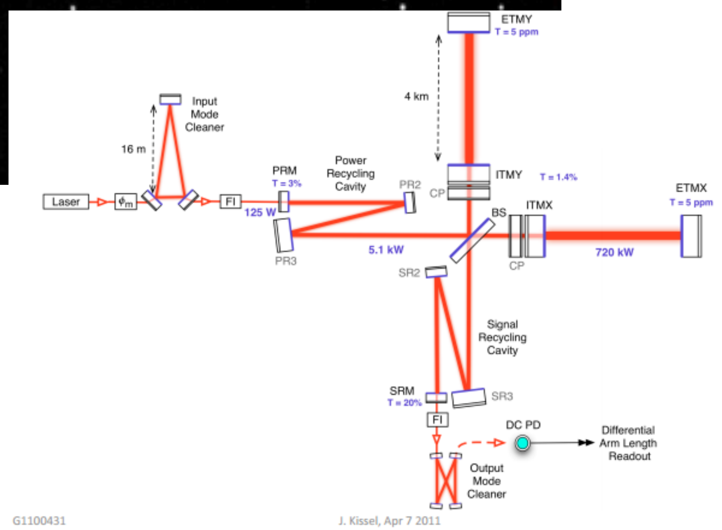

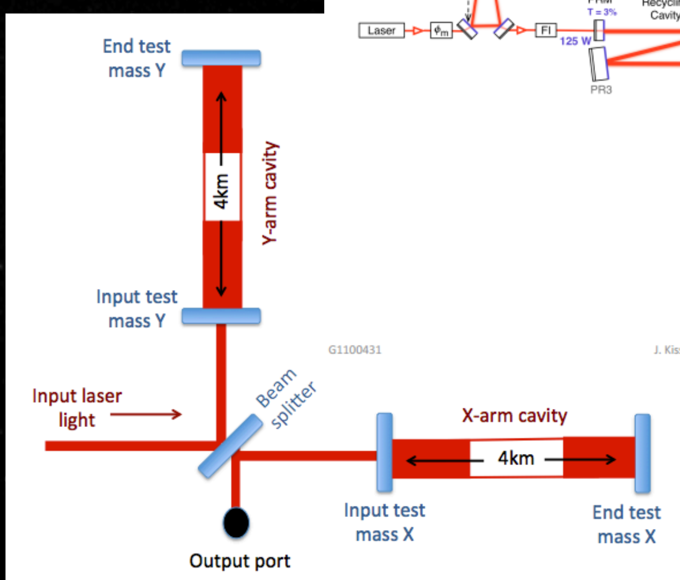

Reality

The challenges of terrestrial noise

- Many effects cannot be tested prior to large scale implementation
- Often noise sources stem from the interaction of different subsystems and cavities

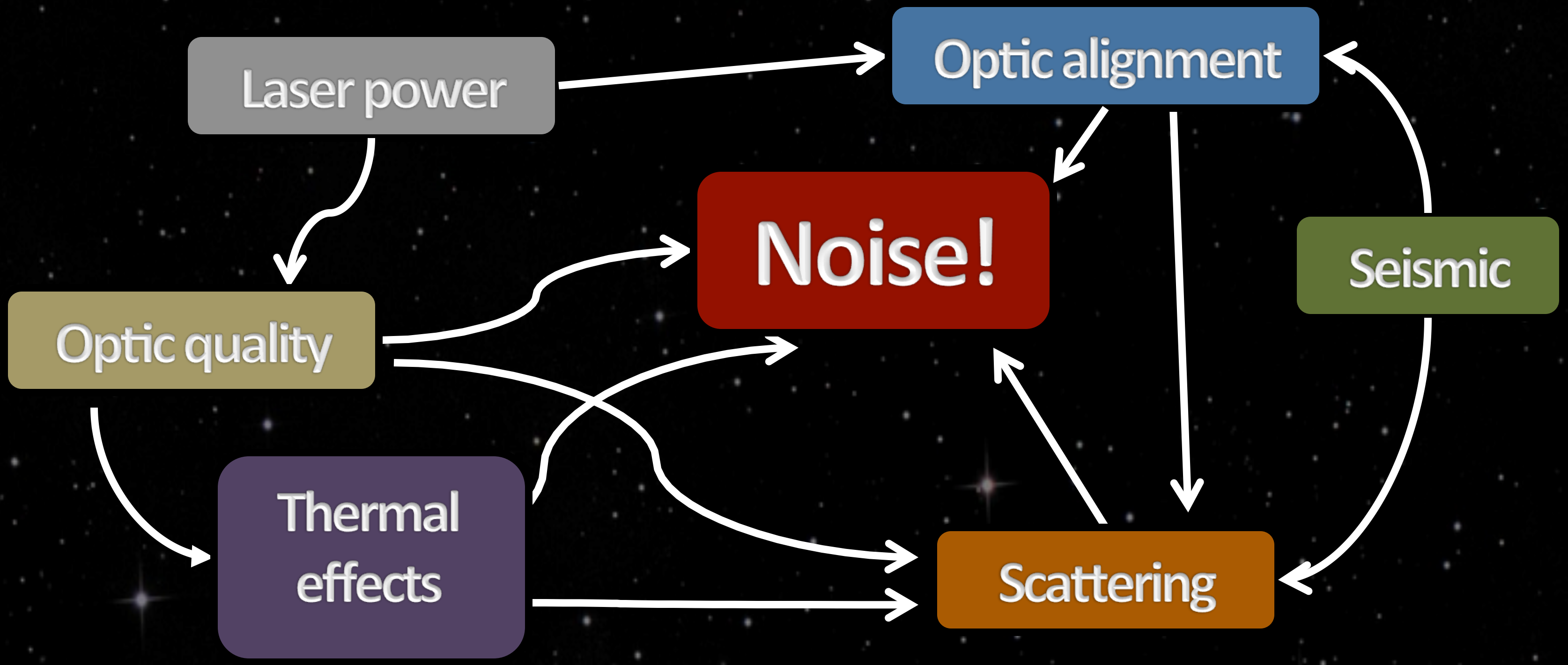

GW search pipelines are adversely affected by non-Gaussian data!

- Long tails (outliers) in all-sky GW burst search background triggers **greatly restrict achievable false alarm rate.**
- Non-Gaussian noise confuses parameter estimation for all transient searches.

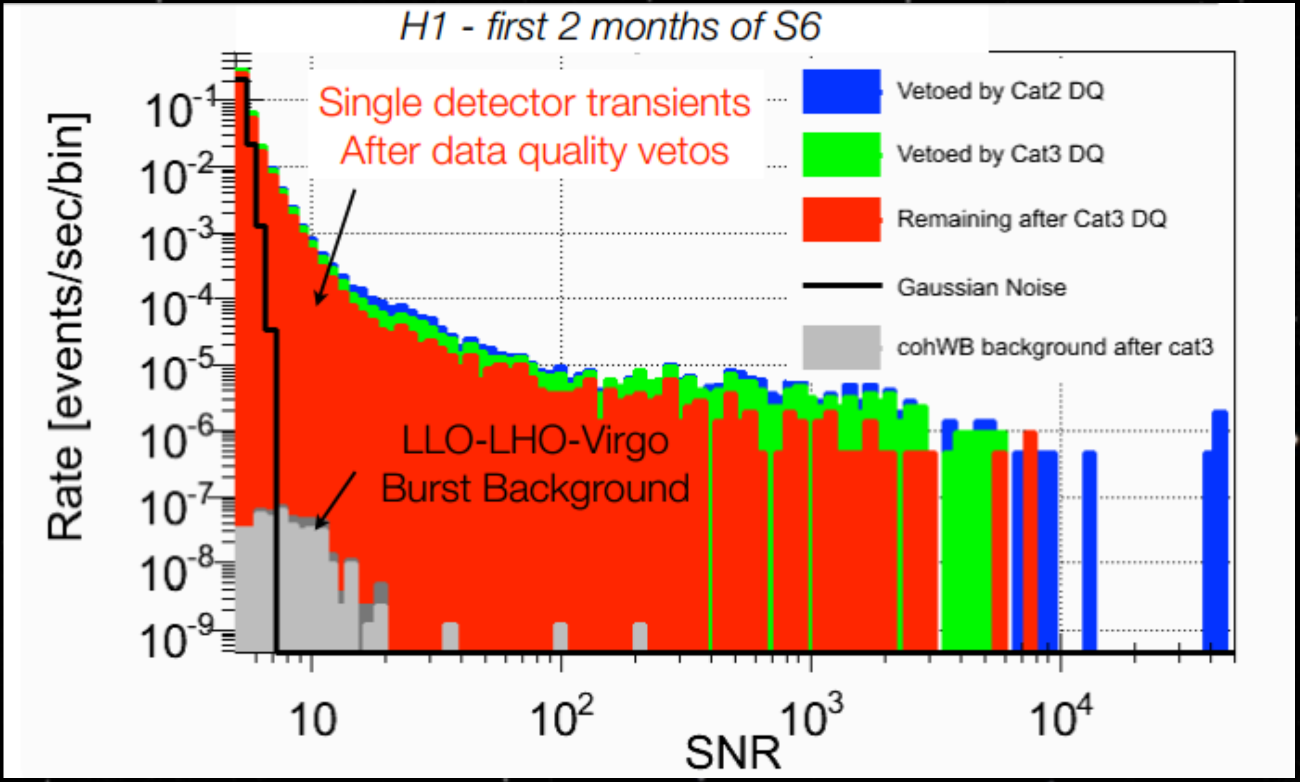

Example: NINJA2 search results

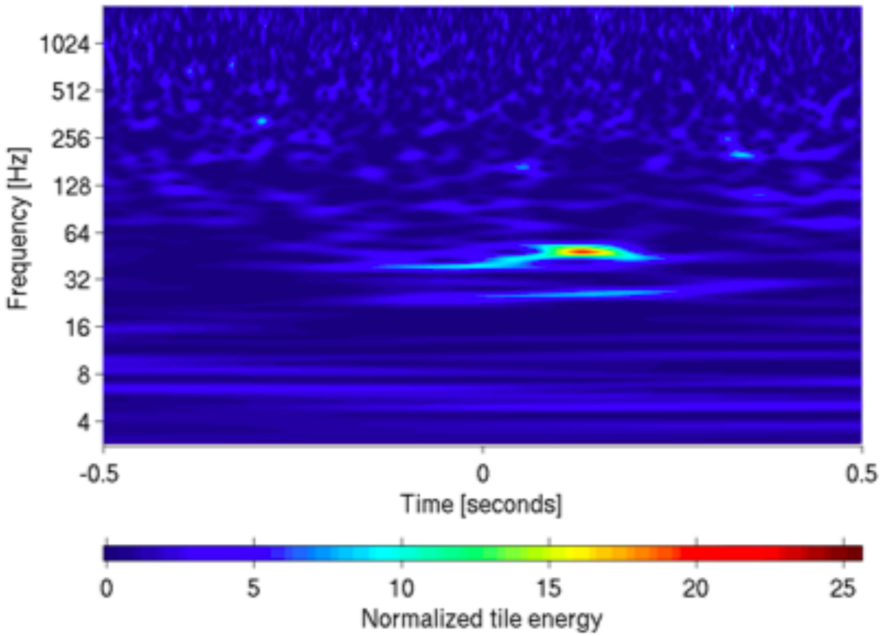

arvix 1401.0939

(a)

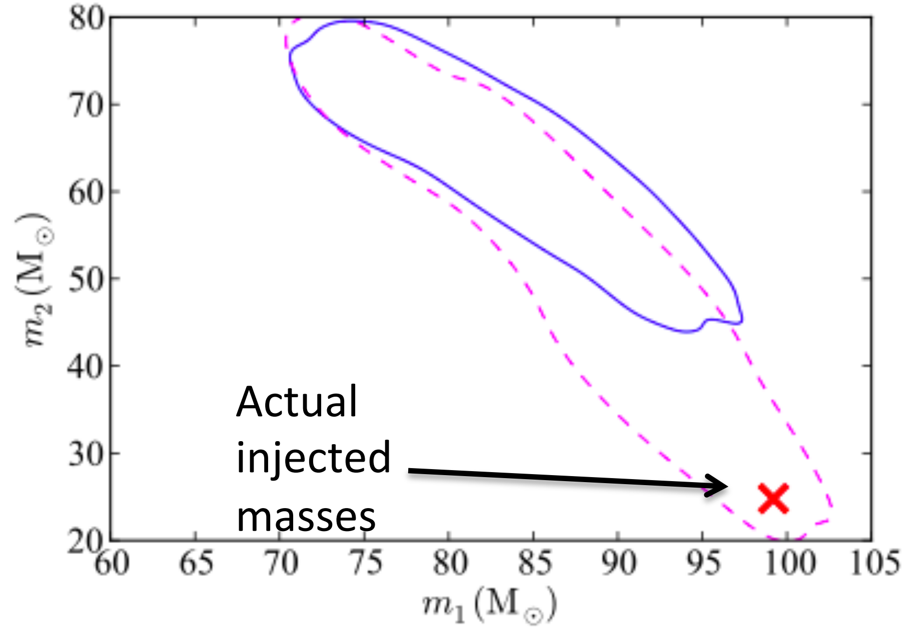

(b)

A normalized spectrogram of **Hanford recolored noise only** showing a transient event, or *glitch*, that happens to occur at the time of the injection.

Solid blue – the 95% credible region for mass estimation based on EOBNRv2 analysis using recolored noise.

Dashed pink – in Gaussian noise.

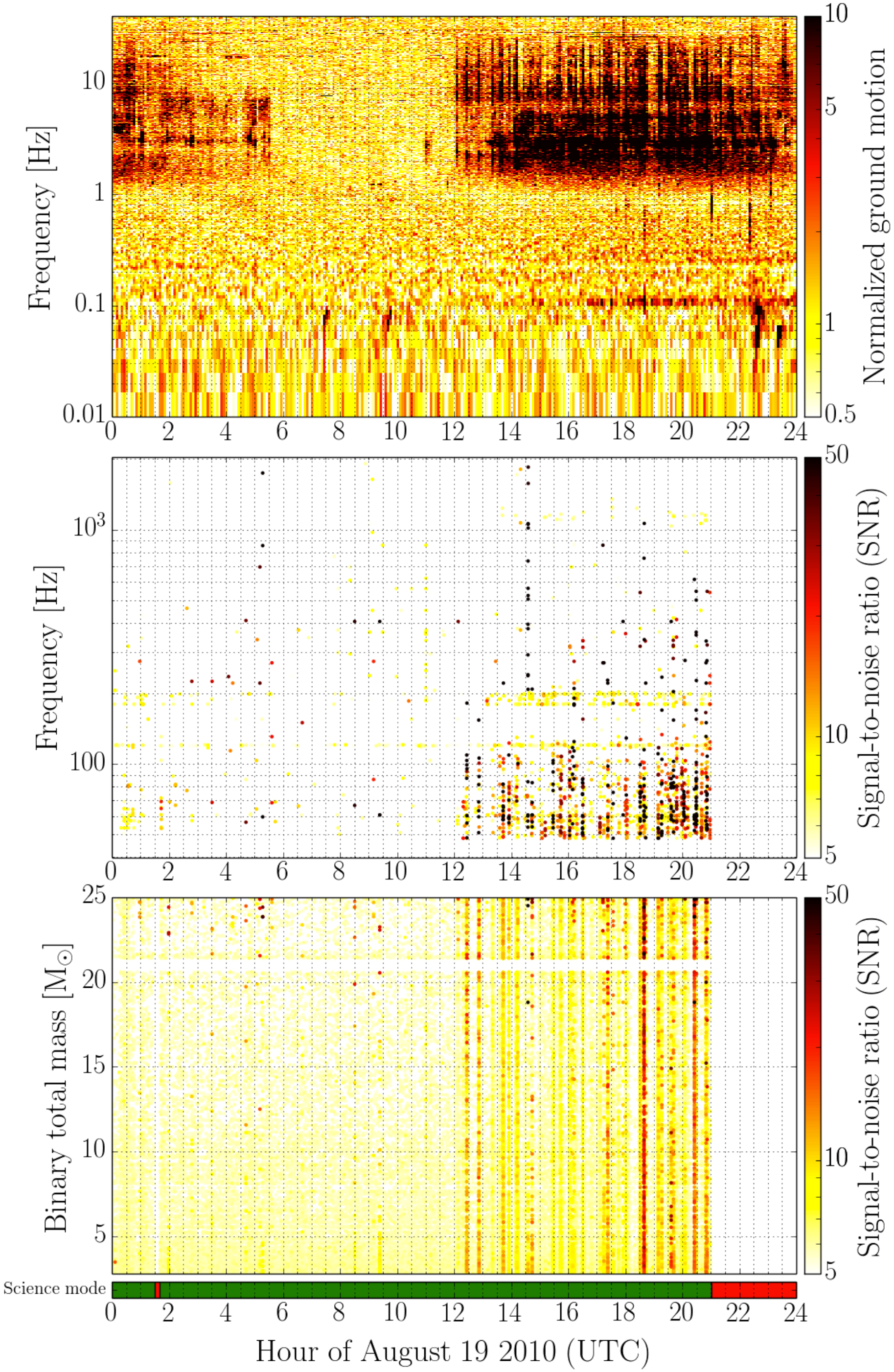

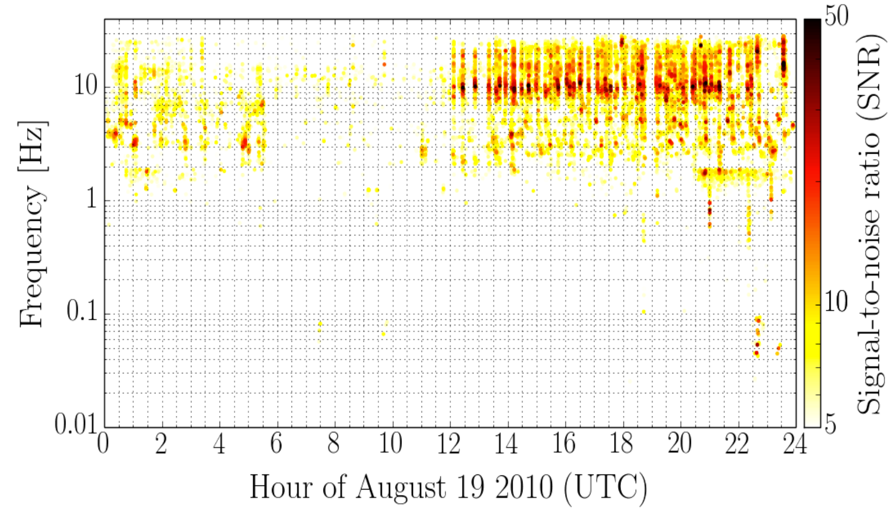

Data quality veto developed from application of burst analysis techniques (ETGs) was one of the **most effective vetoes** of S6:

Burst event SNR range	% events vetoed
SNR > 20	27%
SNR > 100	55%
SNR > 1000	85%

aLIGO seismic isolation instrumentation

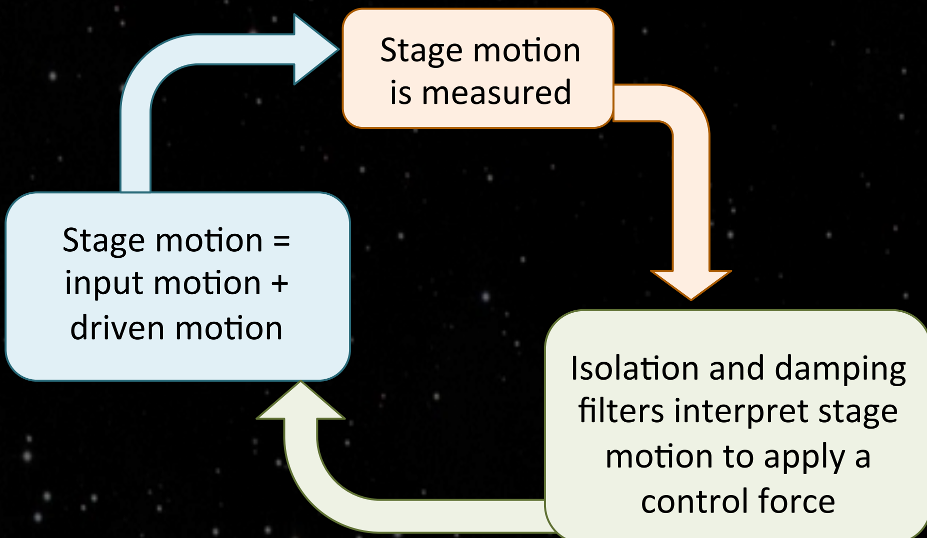

BSC chamber and test mass

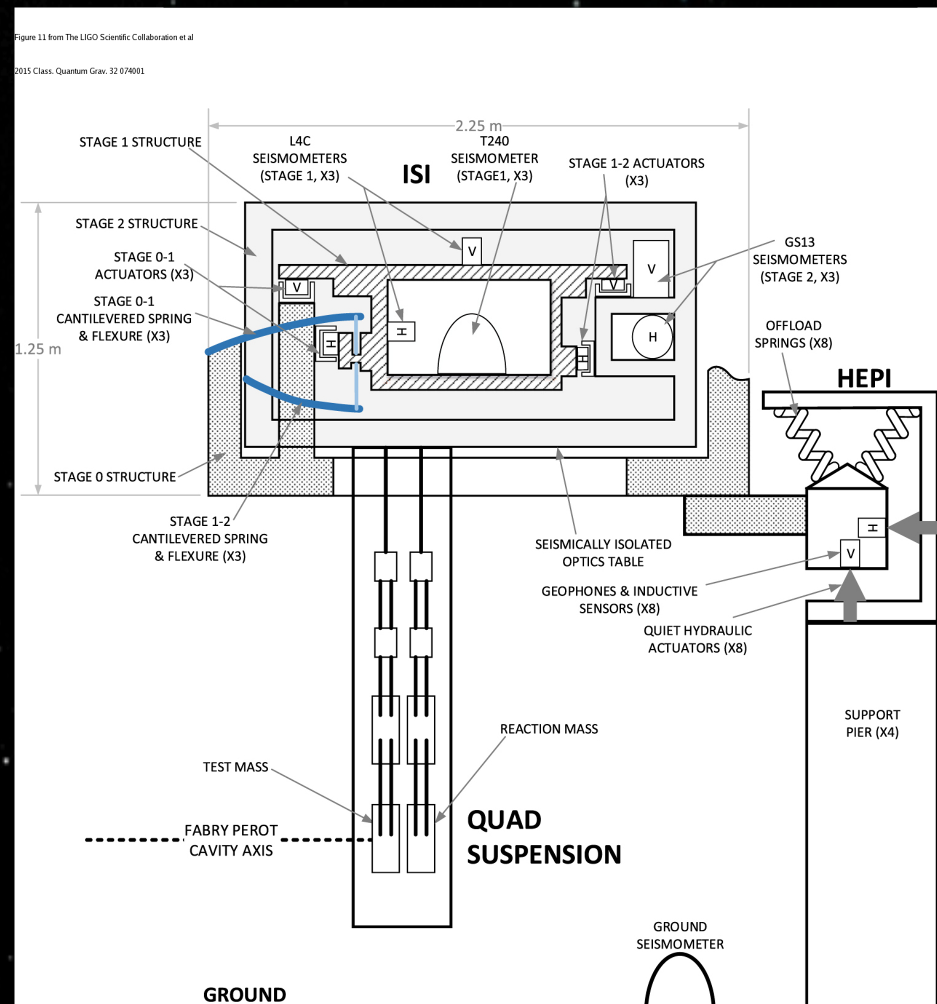

SEI transient propagation

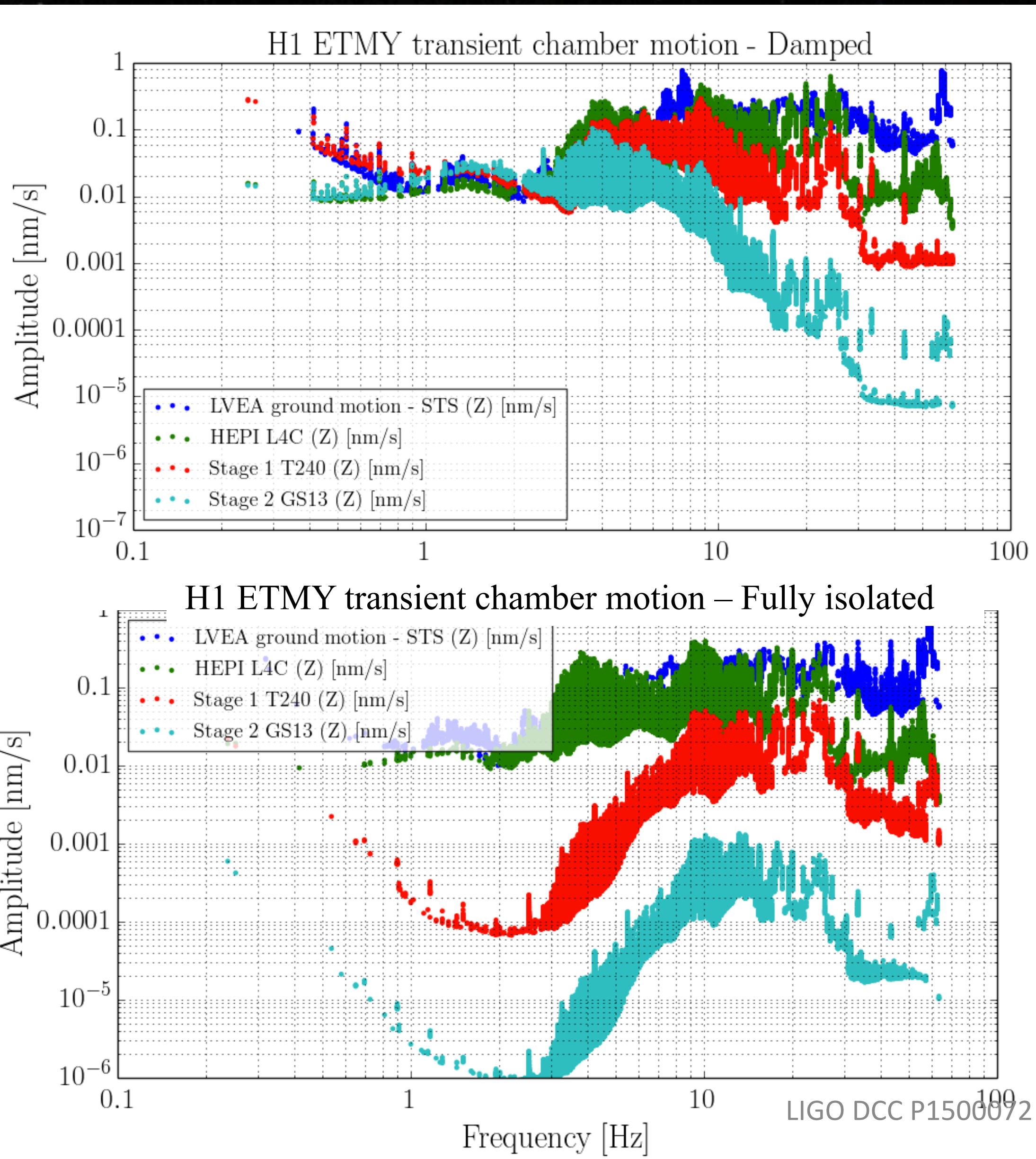

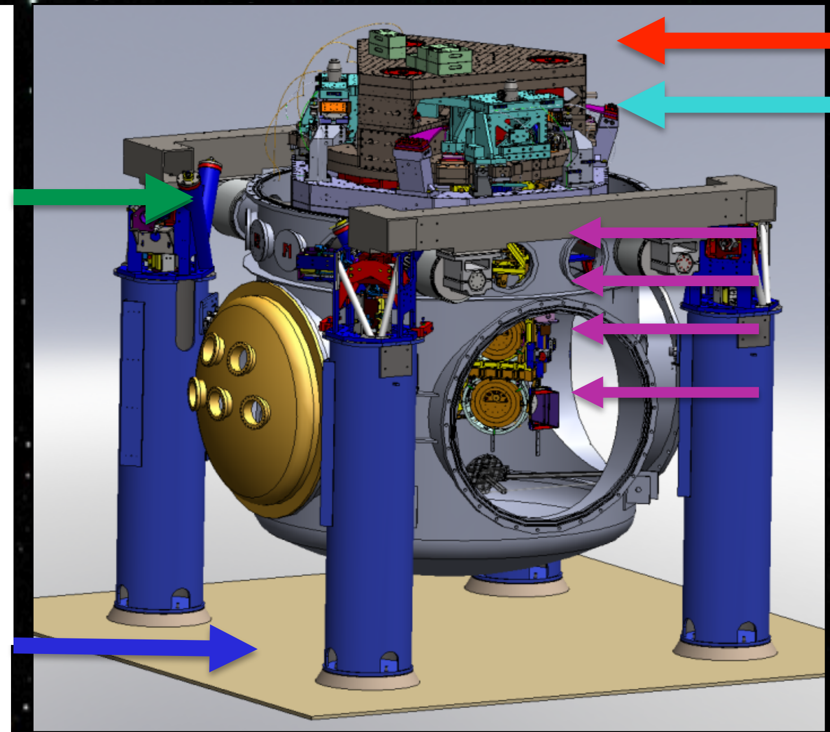

Tracing the transient motion from the ground to the optic table in various states of isolation loop aggression.

More aggressive isolation mitigates transients well < ~15Hz

LIGO DCC P1500072

Windy vs. Quiet time transient SEI study at LHO

Most of the day, Oct 11, high microseism, low wind (~5MPH)

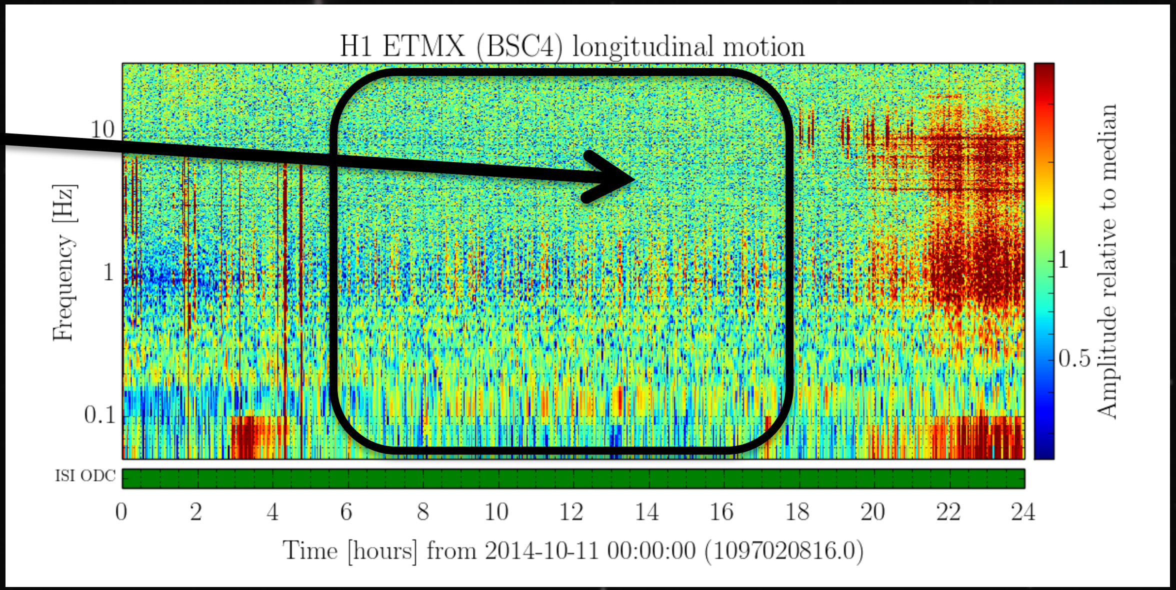

Windy vs. Quiet time transient SEI study at LHO

Most of the day, Oct 11, high microseism, low wind (~5MPH)

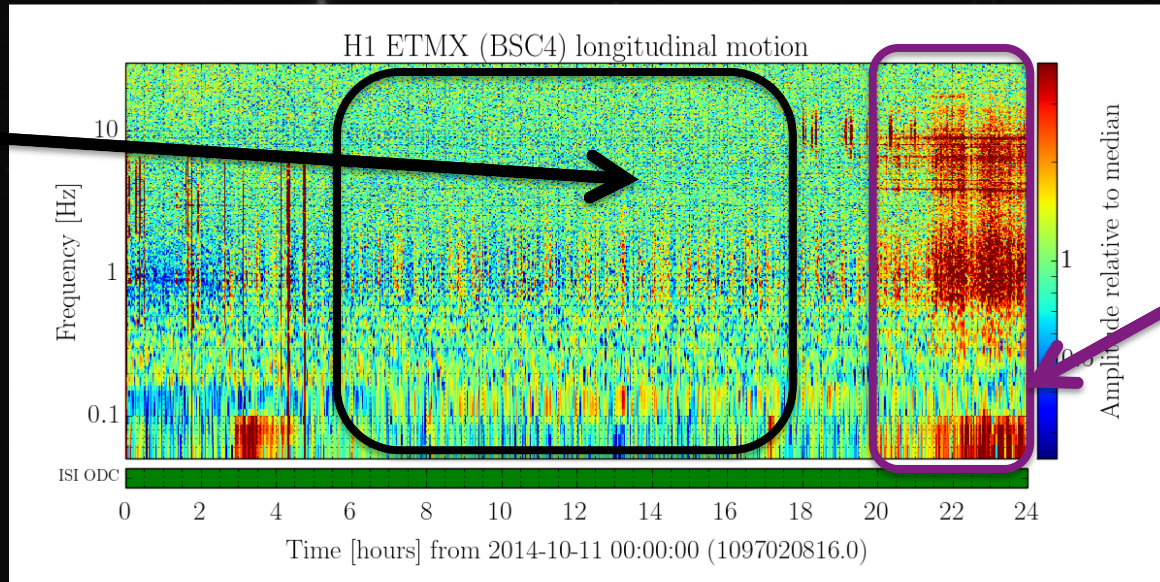

After~20:00 UTC, **high wind** (~30MPH)

Below are Omicron triggers of two hours of “quiet” time (left) and “windy” time (right). Each dot is a transient event. Transient motion amplitude is very elevated during high wind for events of freq < ~30Hz.

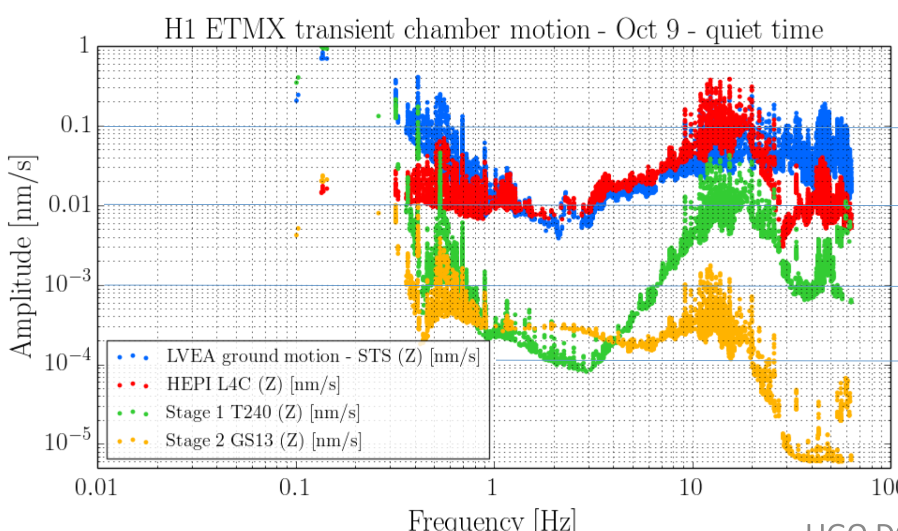

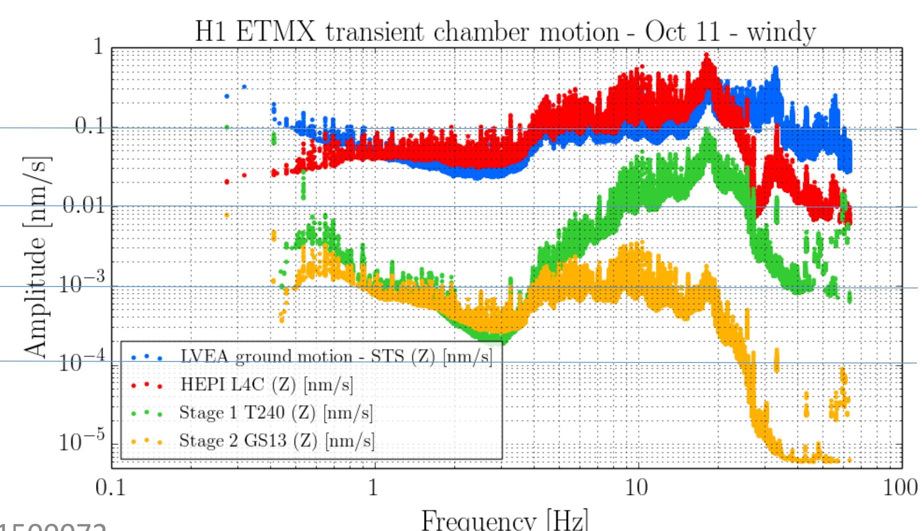

LIGO DCC P1500072

Note: these plots show ETMX local ground motion, not LVEA

The rate of transient motion events also increases dramatically during windy time – by over a factor of 10 in optic table motion at end X.

Stage	Quiet* (# trigs)	Windy* (# trigs)	Factor increase
Ground motion	30,755	116,601	3.8
HEPI (L4C)	21,317	74,624	3.5
ISI ST1 (T240)	7,791	57,948	7.4
ISI ST2 (GS13)	3,924	49,562	12.6

* For a two hour period of relatively quiet or windy time

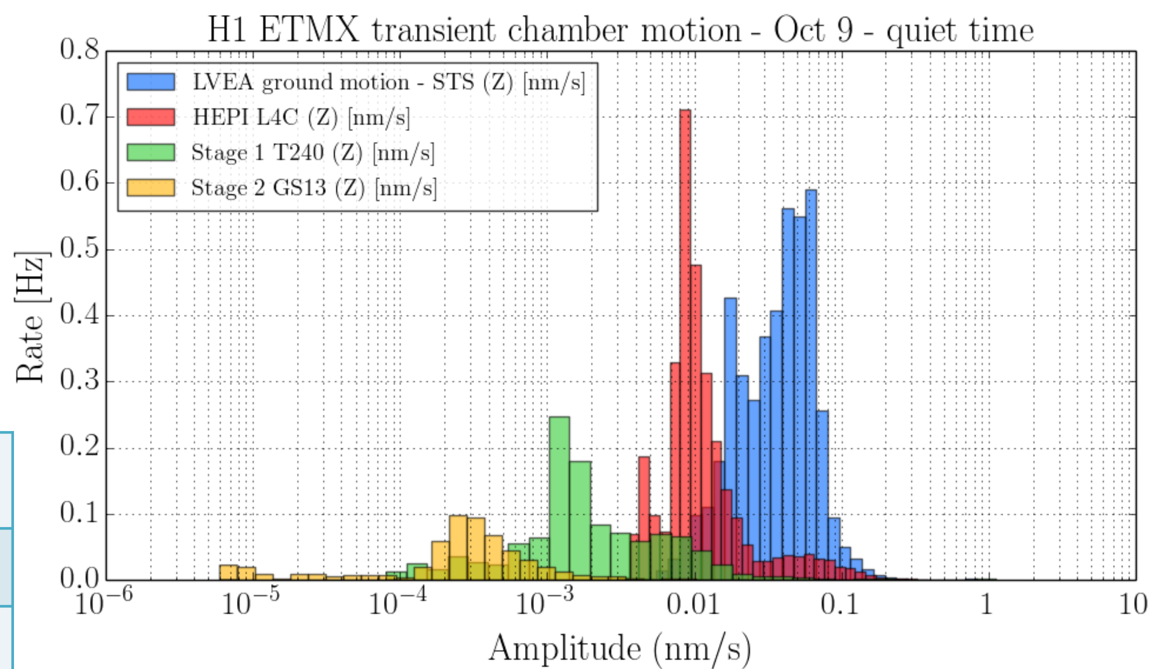

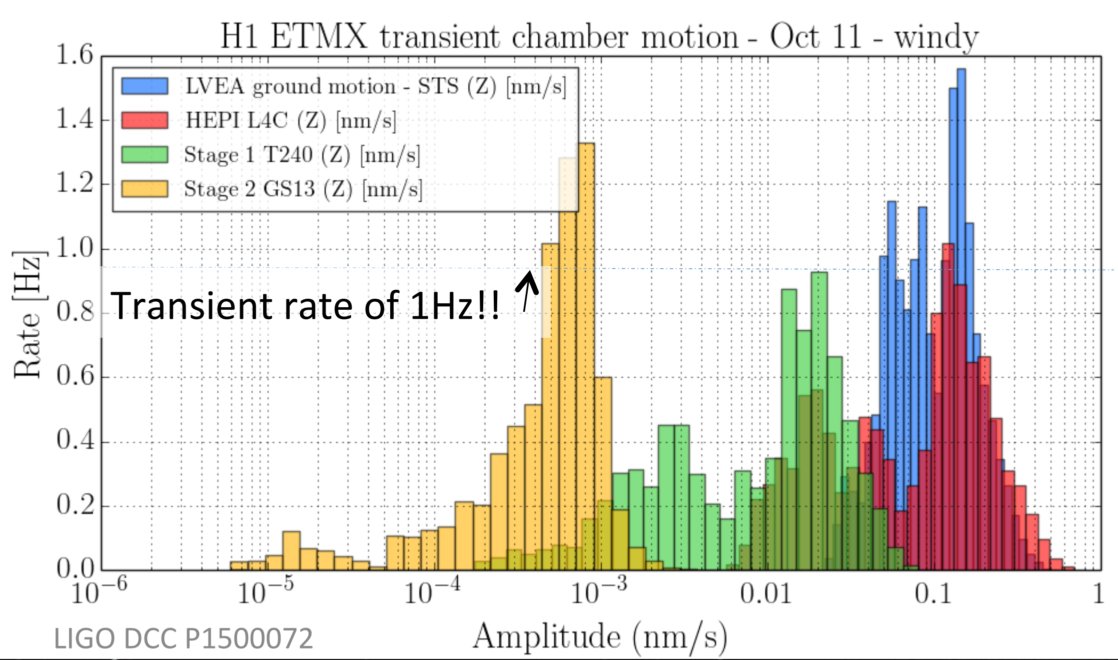

Isolated stages see a much greater increase in the rate of transients than ground motion during windy time.

Note: these plots show ETMX local ground motion, not LVEA

LIGO DCC P1500072

Conclusions for windy vs. quiet SEI transient study:

Ultimately, at the optic table the transient motion amplitude per event isn't significantly increased above 10-15Hz, but the **rate** of transients is greatly increased

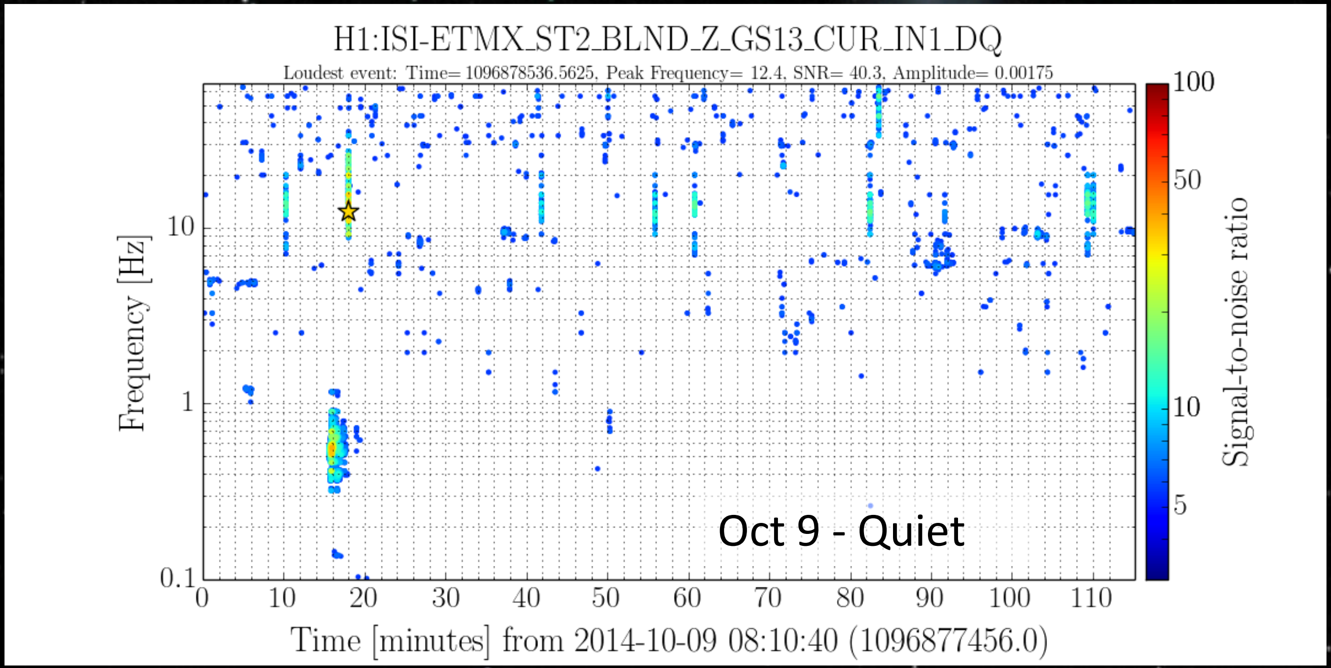

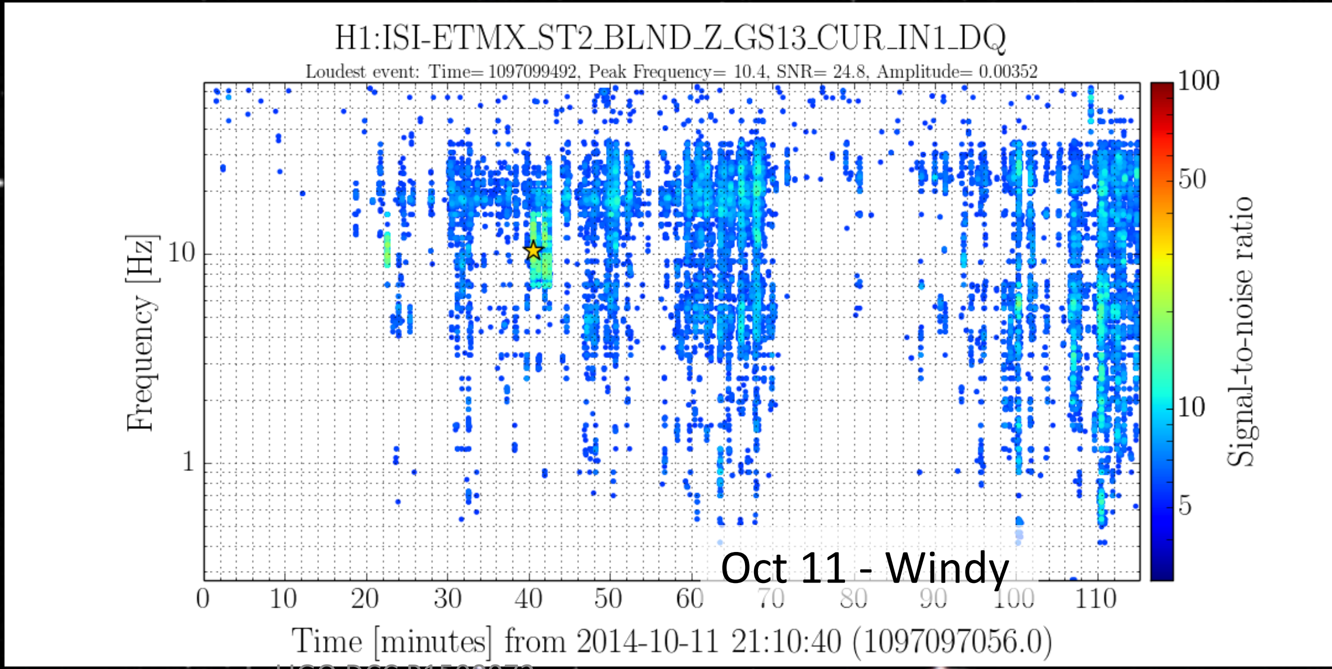

Livingston ER6 -Dec 16 lock

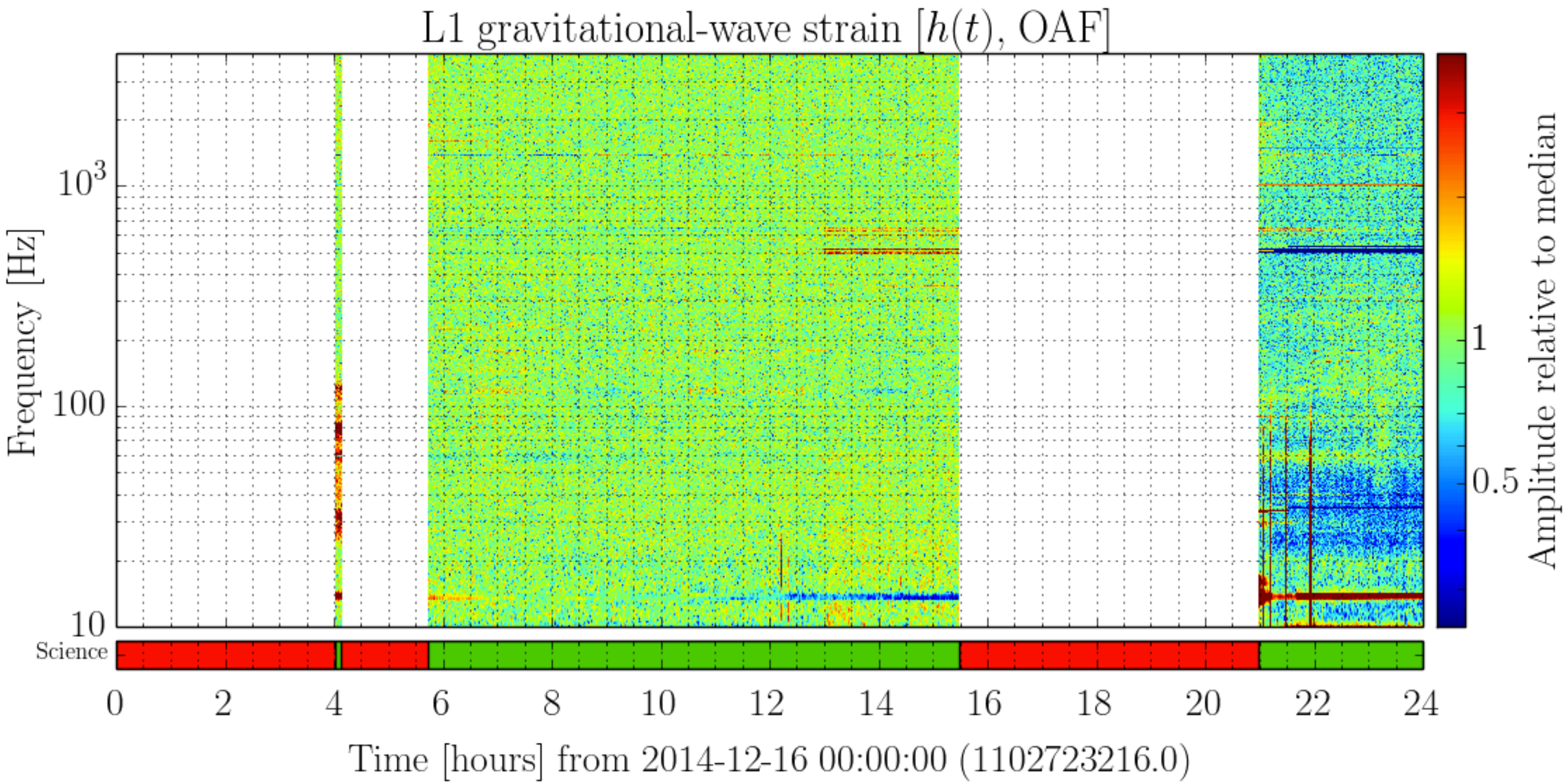

Violin modes caused high trigger rate in inspiral and burst searches

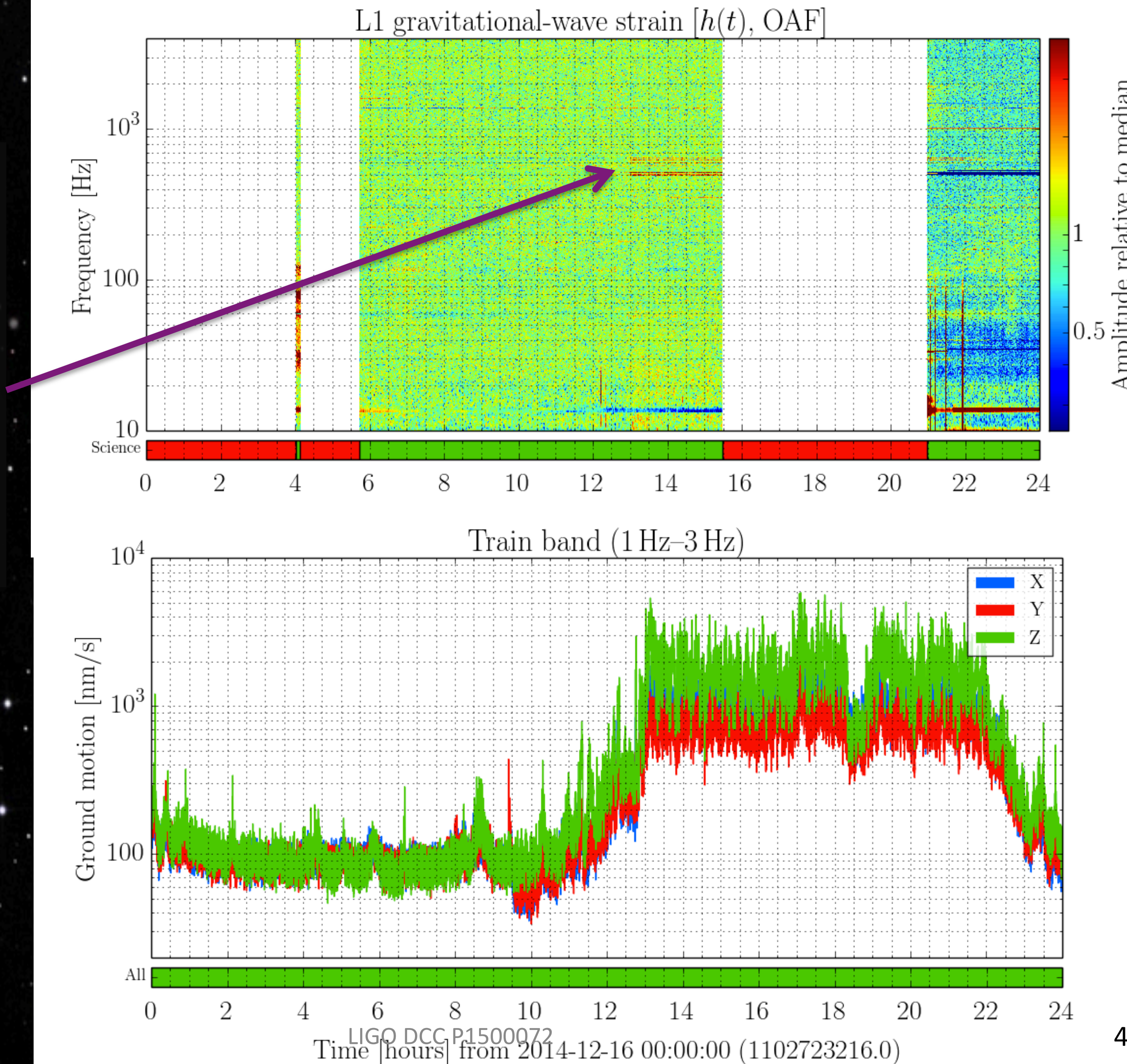

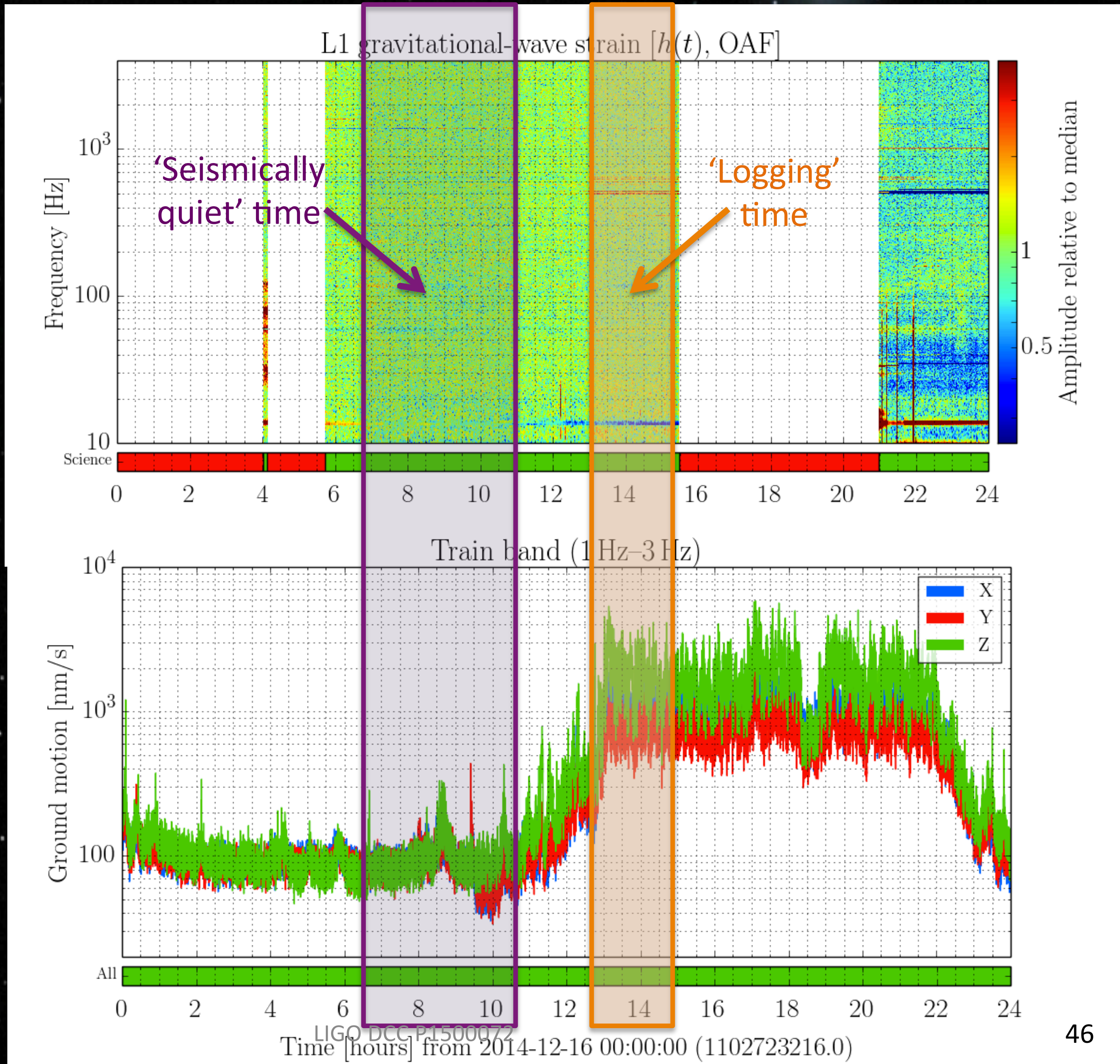

LIGO DCC P1500072

Seismically quiet part of lock

Logging stretch of lock

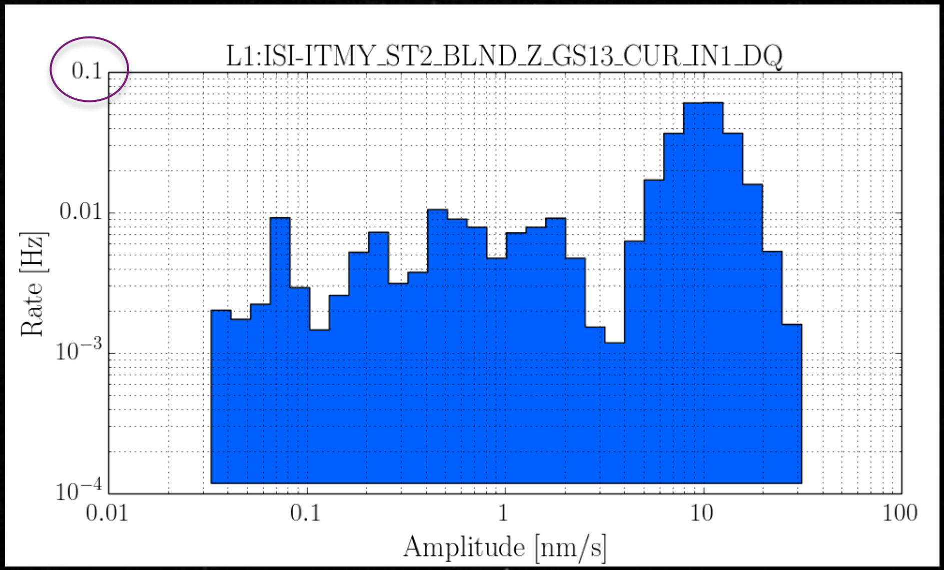

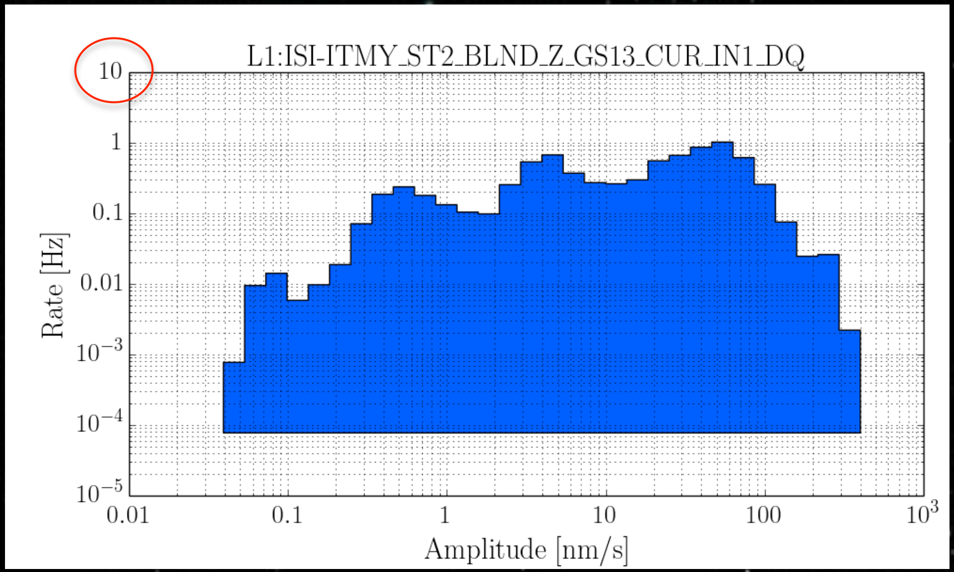

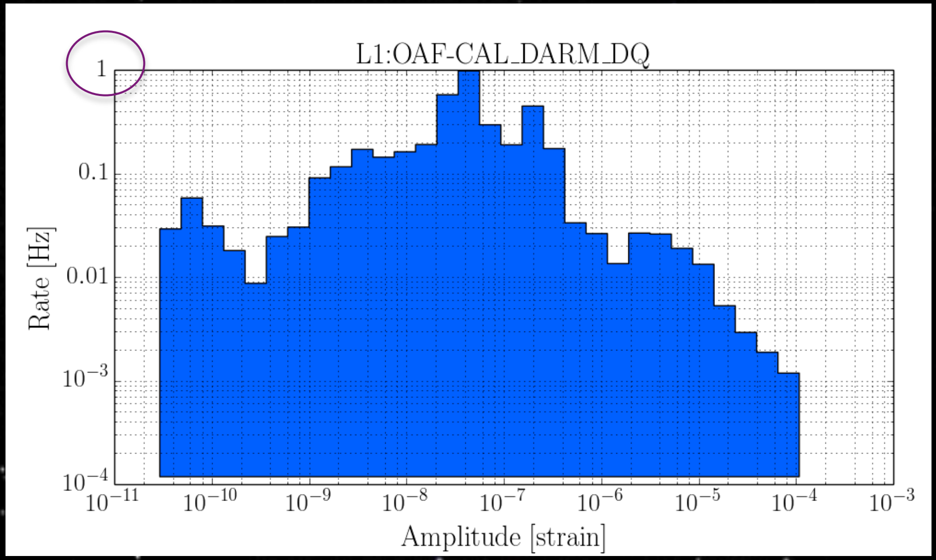

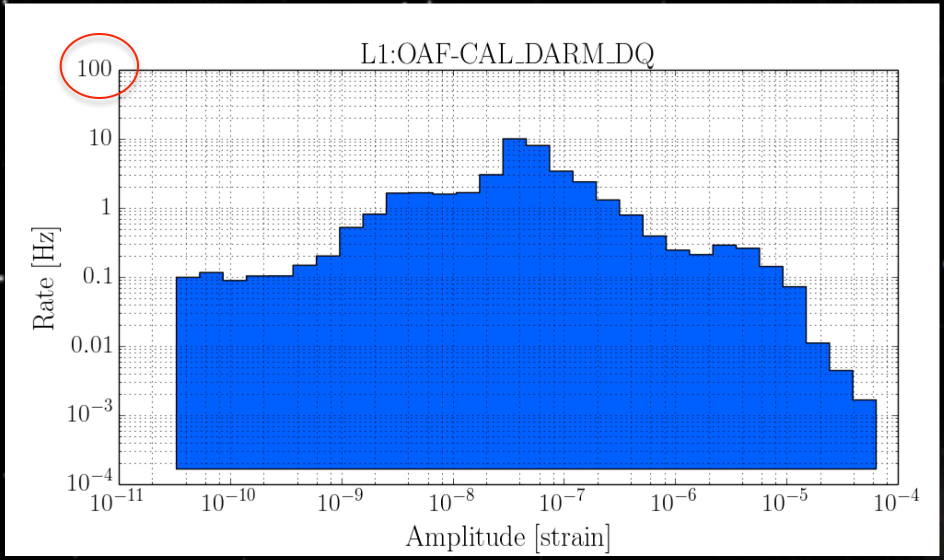

Summary:
Terrestrial noise and its impact on generic burst searches

- In previous science runs, seismic noise was a major contributor to glitch pollution of transient GW searches.
- Advanced LIGO seismic isolation instrumentation does mitigate seismic noise, drastically reducing average motion and increasing observation time.
- However, elevated ground motion is still shown to affect DARM by increasing the glitch rate.
- Efforts are underway to tune the instrumentation configuration and control loop settings to better mitigate this.
- ETGs are a critical tool in this effort.
-

CCSN recovery in realistic noise

Representative results for the same set of waveforms injected into real non-Gaussian data from a prior science run, re-colored to aLIGO design sensitivity

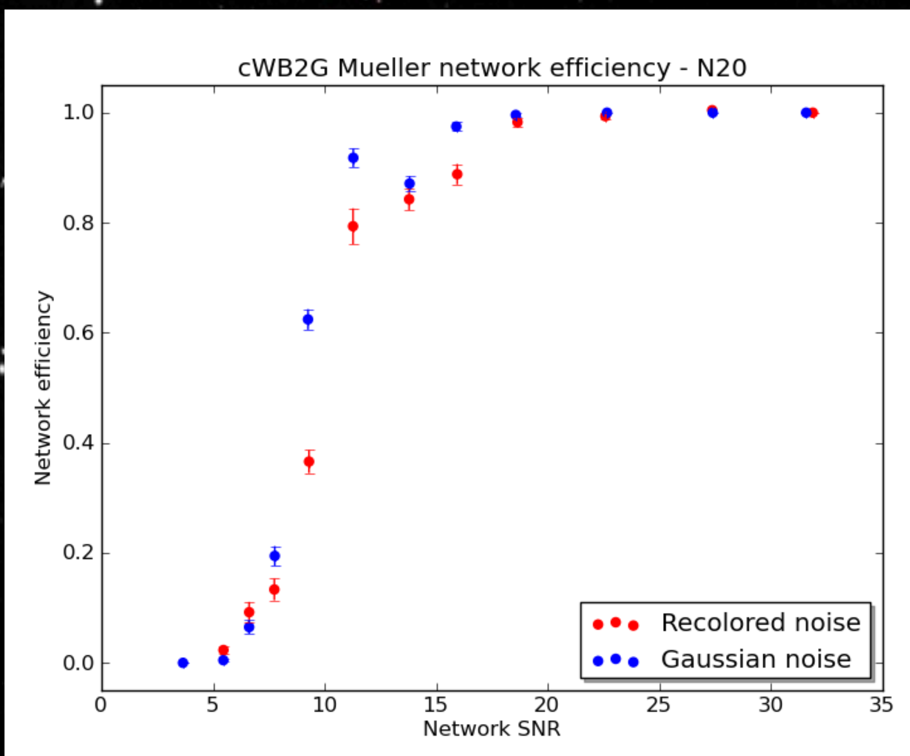

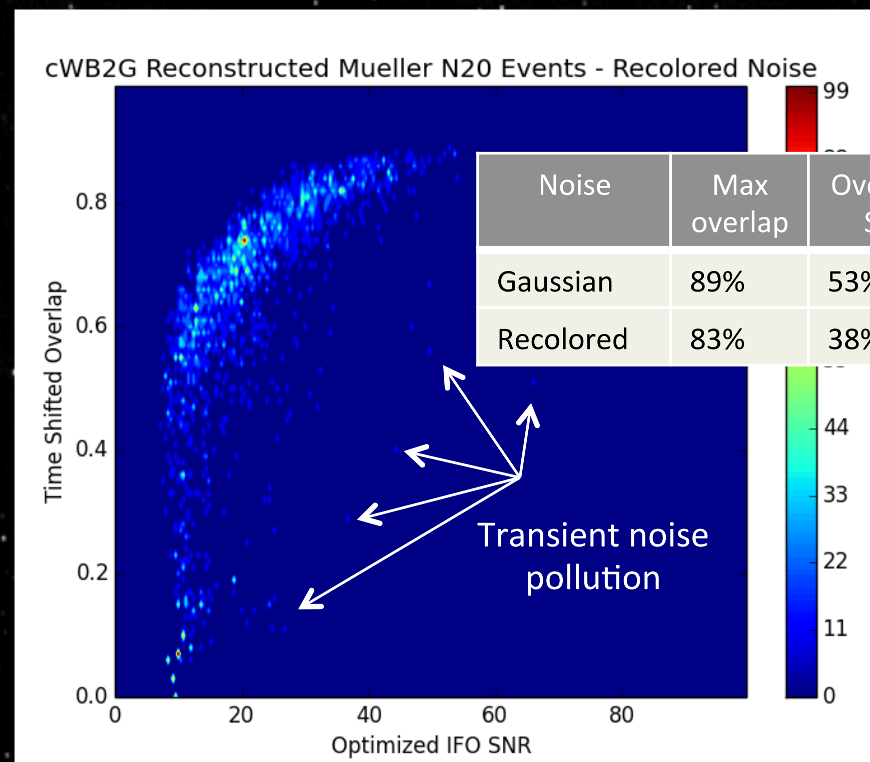

Noise	Max overlap	Overlap SNR8
Gaussian	89%	53%
Recolored	83%	38%

Example outlier event

L1 reconstruction stats: single ifo **SNR 17.5, overlap 30%**

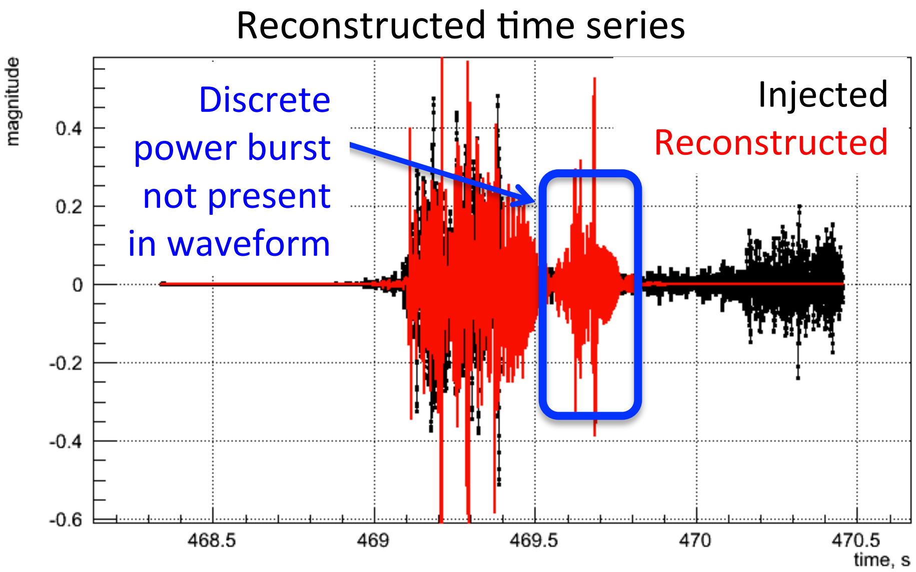

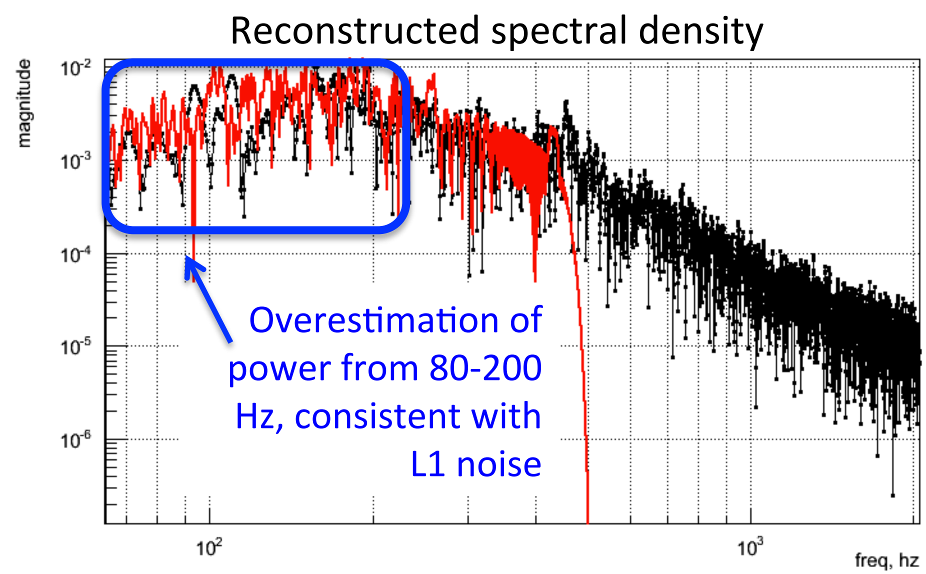

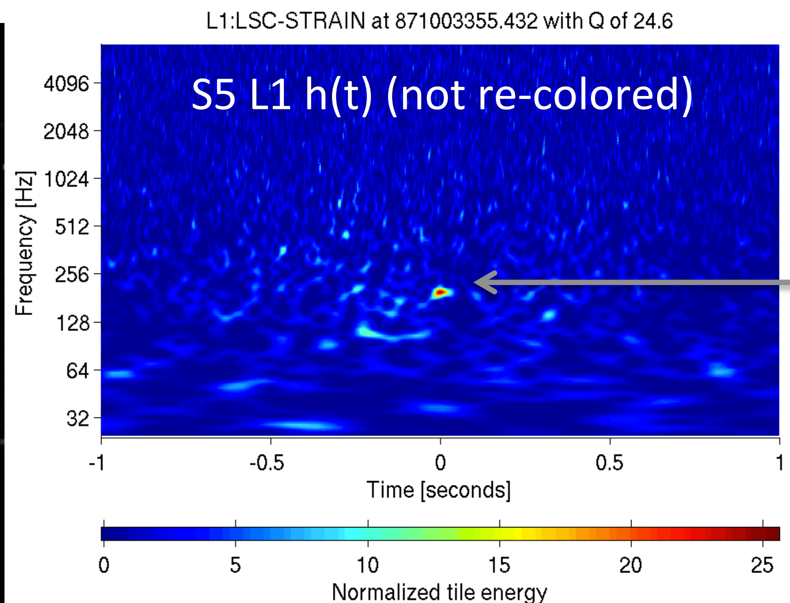

Example event (SNR 17, overlap 30%) with excess power from 80-200Hz and a distinct glitch at ~150Hz in L1.

Future prospects

This work identified two major areas that need improvement:

- Burst waveform reconstruction algorithms
- Transient noise mitigation

Major efforts in progress ahead of O1 and O2 to address these:

- cWB2G and BayesWave tuning and guided development
- ETG performance testing, tuning, and improvement
- Noise mitigation studies and instrument tuning informed by the data quality needs of the transient GW searches

Acknowledgements

My advisor:

- Laura Cadonati

My committee:

- Ben Brau
- David Kastor
- Alex Pope

My thesis readers:

- Laura Nuttall
- Josh Smith
- James Clark
- Sarah Gossan
- Florent Robinet
- Laura Cadonati

Contributors:

- Josh Smith
- James Clark
- Duncan Macleod
- Jeff Kissel
- Sarah Gossan
- Florent Robinet
- Claudia Lazzaro
- Jonah Kanner
- Tyson Littenberg
- Chris Pankow
- John Zweizig
- Joey Key
- Daniele Triferio
- Amber Stuver

LIGO supporters:

- Laura Nuttall
- Andy Lundgren
- TJ Massinger
- Ryan Fisher
- Marissa Walker
- Thomas Abbott
- Brian Lantz
- Fabrice Matichard
- Rich Mittleman
- Dan Hoak
- Gaby Gonzalez
- Joe Giaime
- Peter Saulson
- Hugh Radkins
- Celine Ramet
- Sebastien Biscans
- Arnaud Pele
- Matt Heintze
- Janeen Romie

Team thesis:

- Alex Lombardi
- Preema Pais
- Brendan Gavin
- Szu-Chia Chen
- Sarah Zuraw
- Kalina Nedkova
- Elizabeth Drellich
- Cathy Walker

Jane Knapp and the UMass physics staff

Family and friends

Tom

Next up:

Extra slides

Core-collapse supernovae

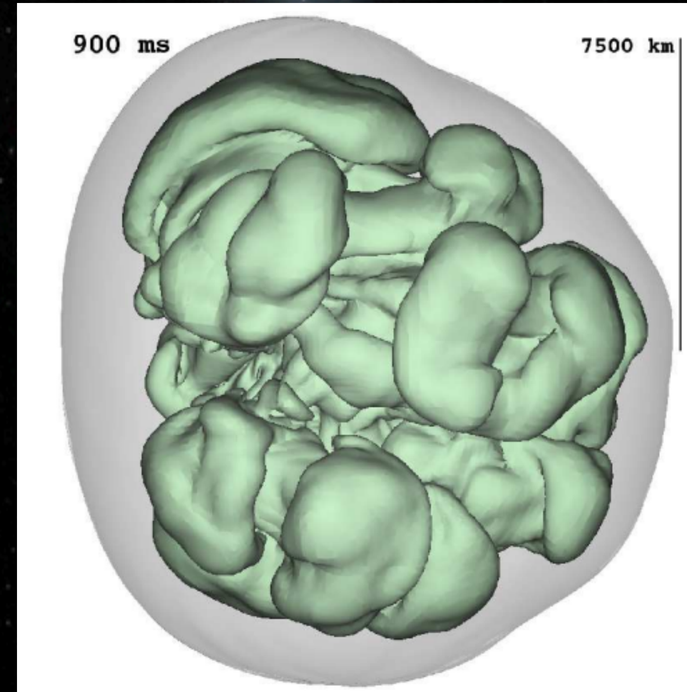

Relative timing of astronomy messengers

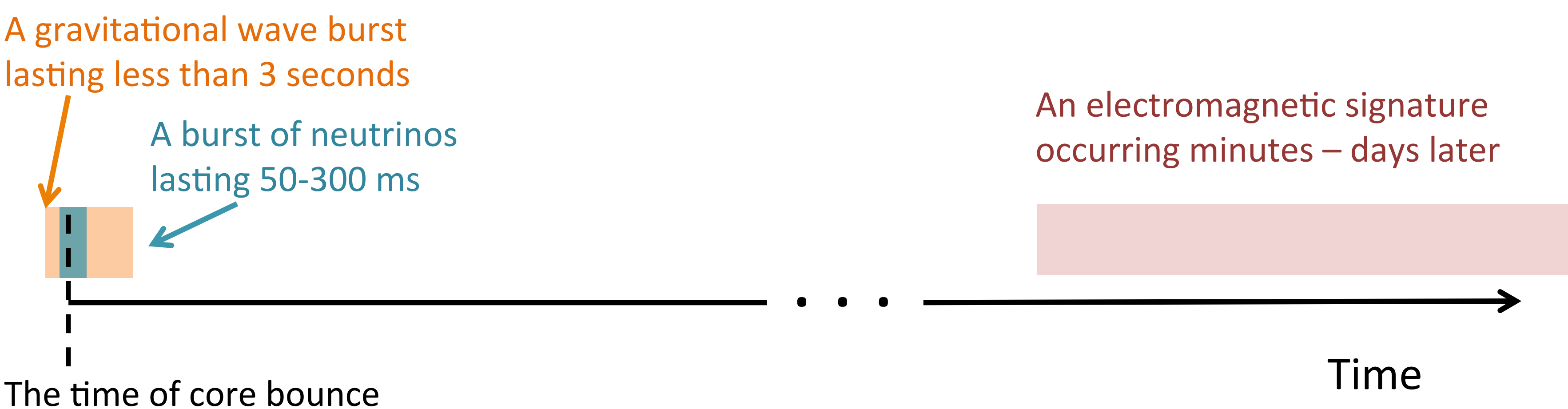

Dimmelmeier –slowly rotating

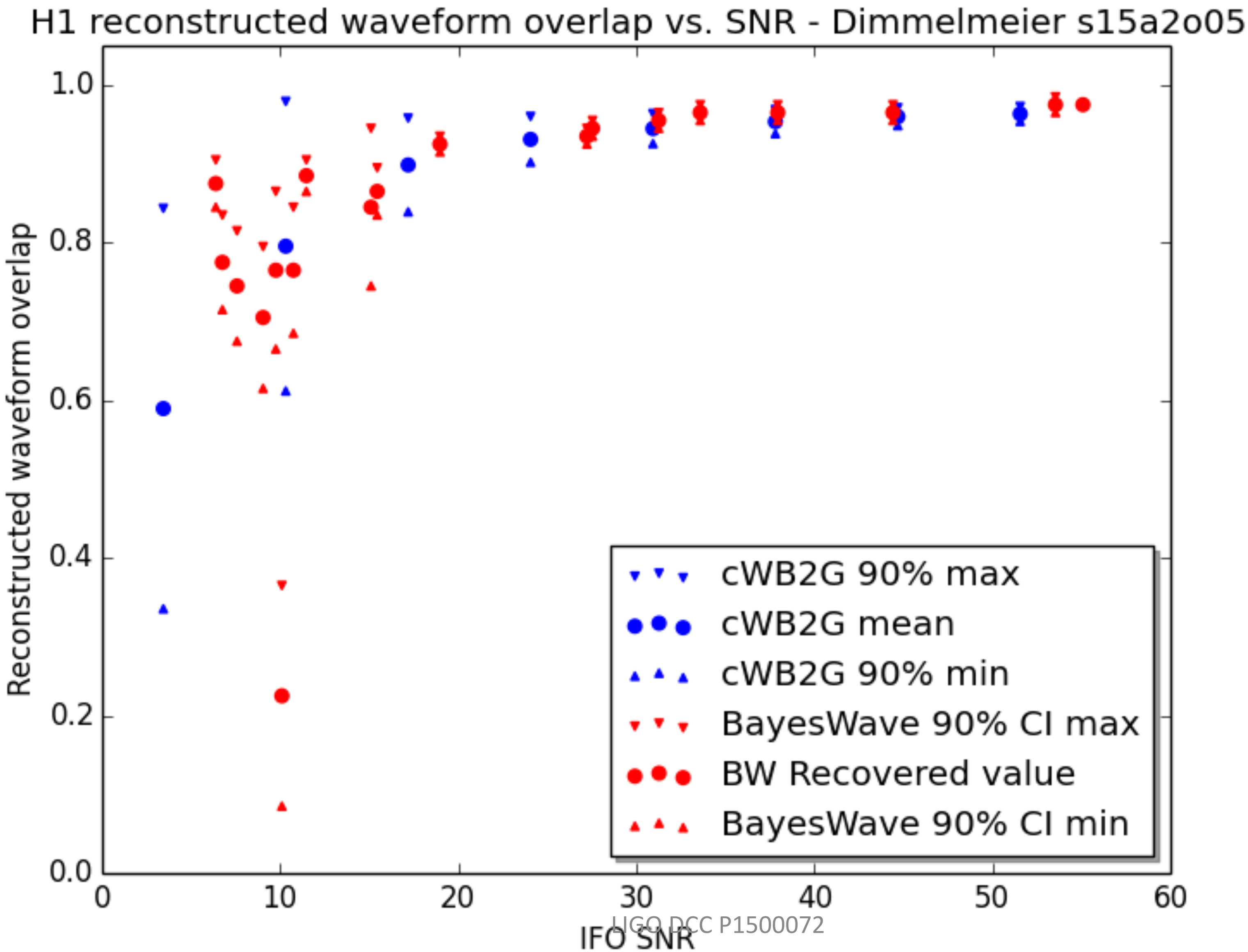

Dimmelmeier –slowly rotating

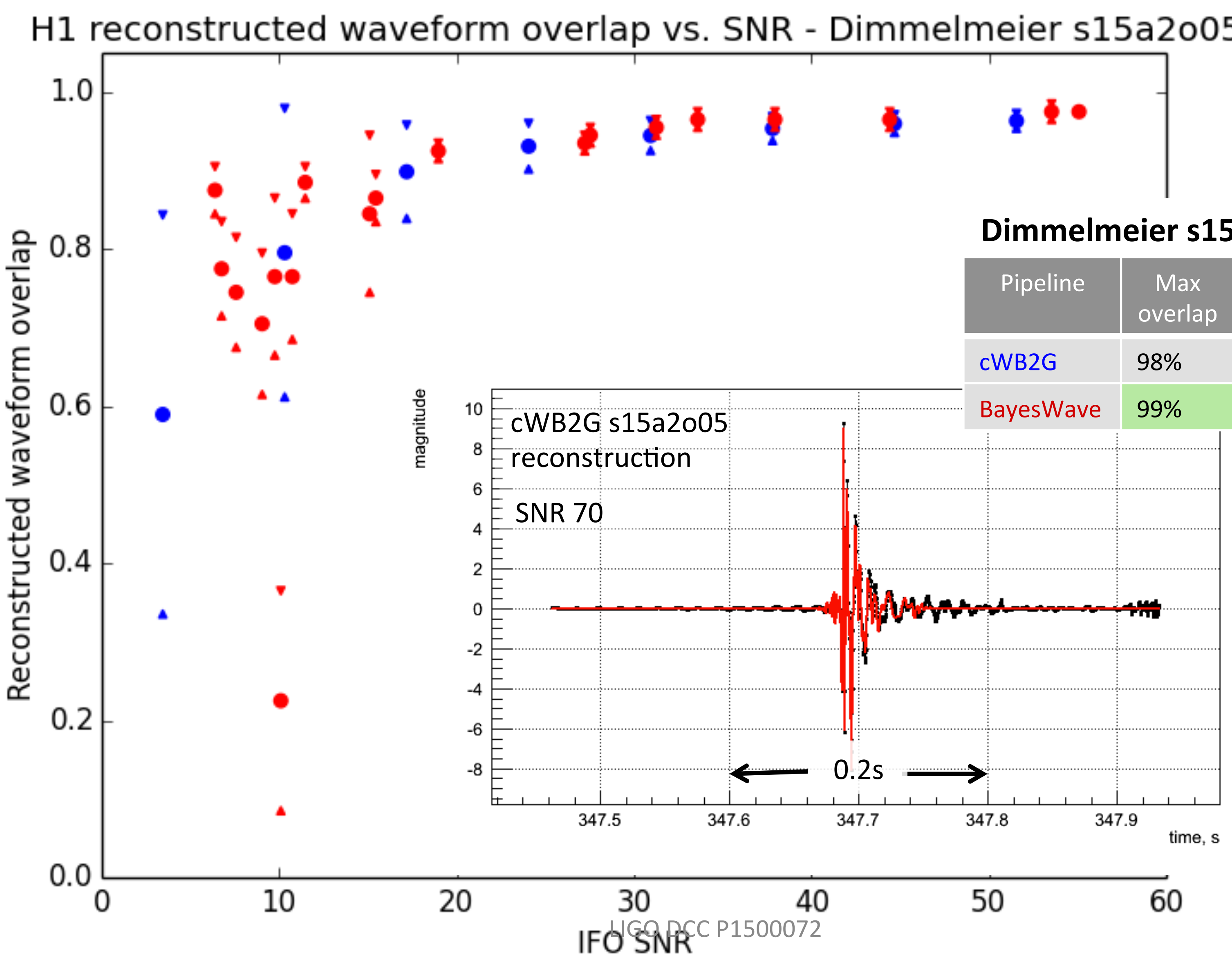

Dimmelmeier s15a2o05 – L1

Pipeline	Max overlap	Overlap at SNR8
cWB2G	98%	71%
BayesWave	99%	79%

Mueller – L15

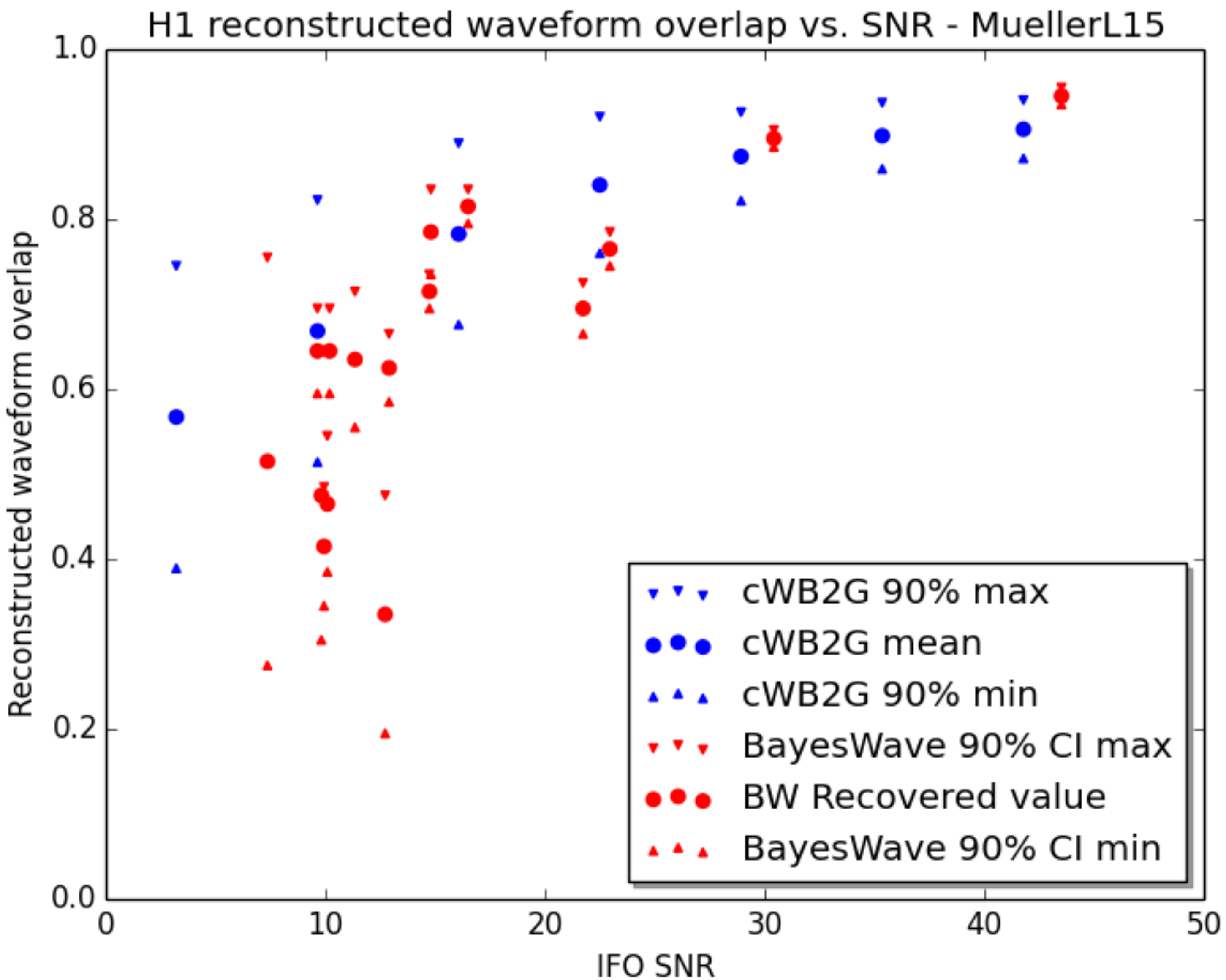

H1 reconstructed waveform overlap vs. SNR - MuellerL15
Reconstructed waveform overlap
IFO SNR
1.0
0.8
0.6
0.4
0.2
0.0
0
10
20
30
40
50
cWB2G 90% max
cWB2G mean
cWB2G 90% min
BayesWave 90% CI max
BW Recovered value
BayesWave 90% CI min

Mueller – L15

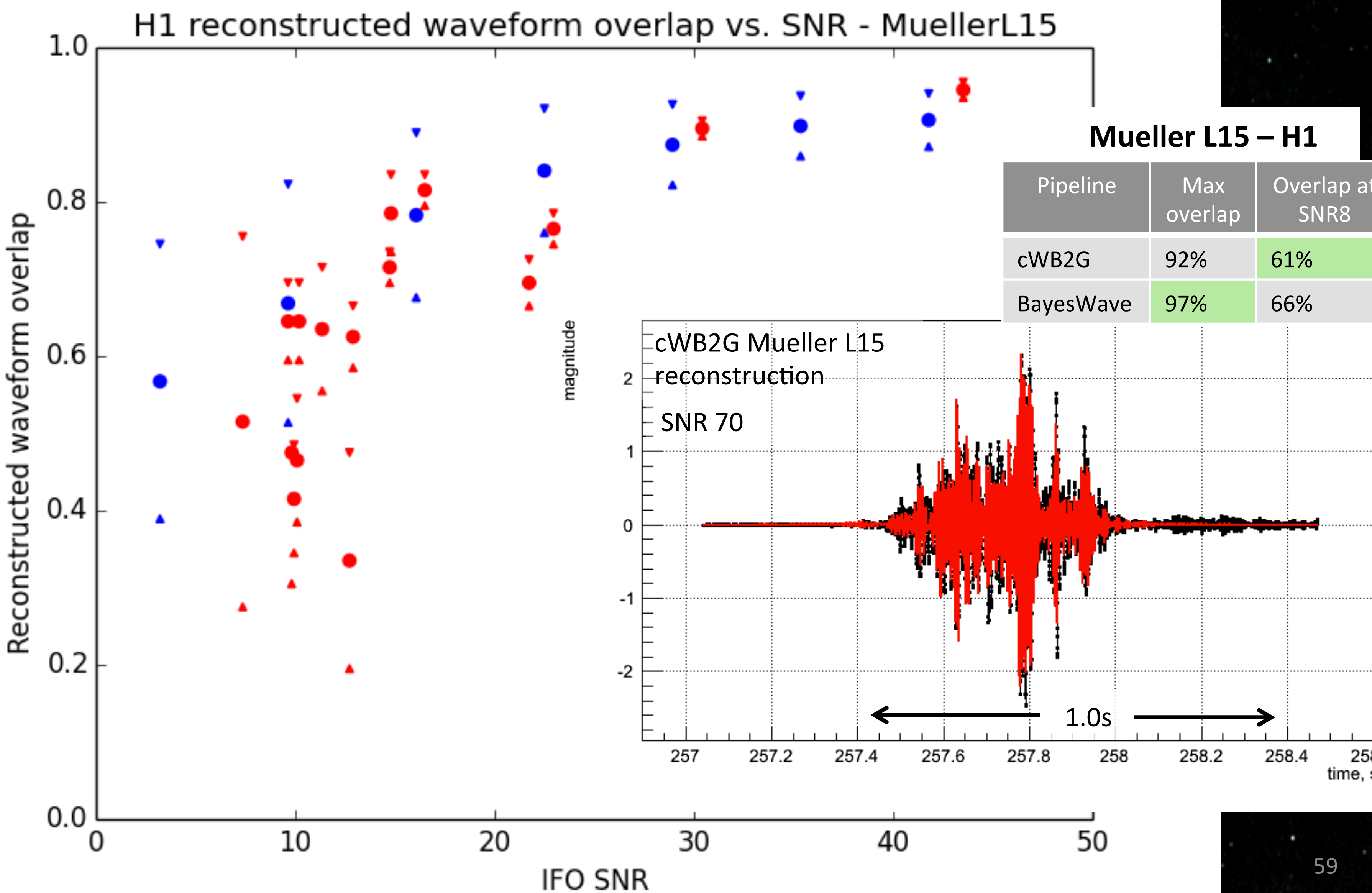

Mueller L15 – H1

Pipeline	Max overlap	Overlap at SNR8
cWB2G	92%	61%
BayesWave	97%	66%

Timeline: the lead up to the first observing run

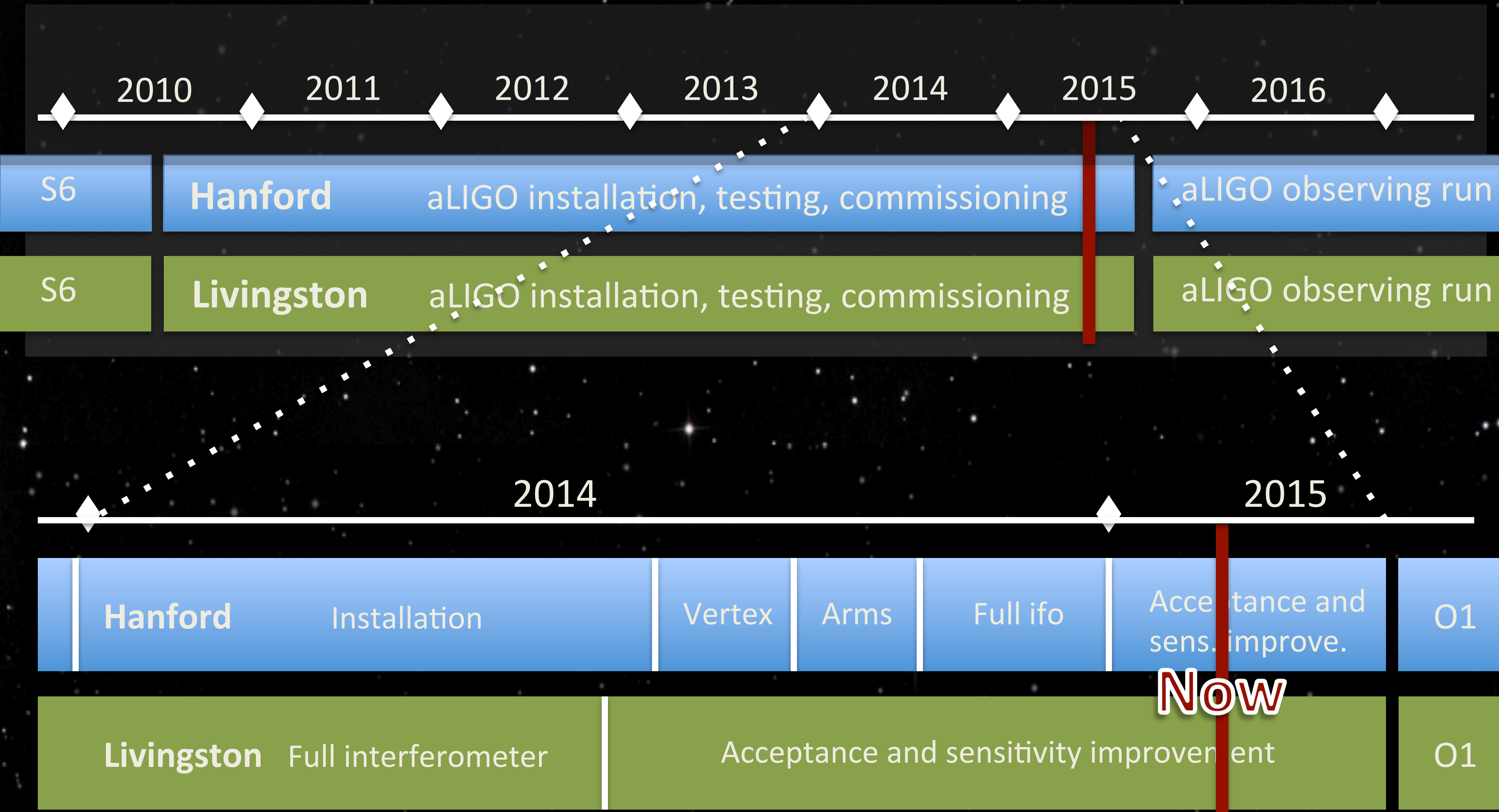

Event Trigger Generators

- Single-interferometer burst algorithms that identify excess power events well-localized in time and assign a characteristic event time, frequency, and measure of loudness signal-to-noise ratio (SNR)

ETGs tile the data in time and frequency, generally with multiple difference aspect ratios.

The data is projected onto some basis that provides an adequate potential match for a target signal.

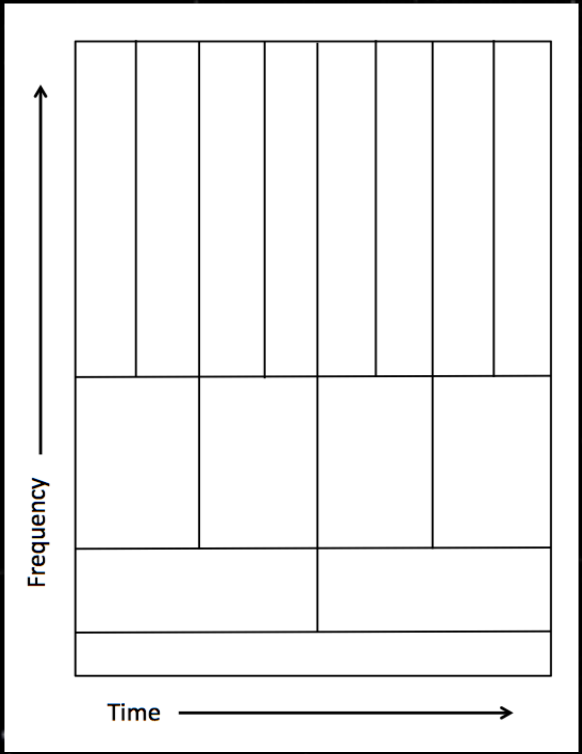

The ETG Omicron

- Omicron uses a sine-Gaussian basis which provides low mis-match between burst-like signals and the basis functions.
- Omicron identifies burst events very well – especially at higher SNR

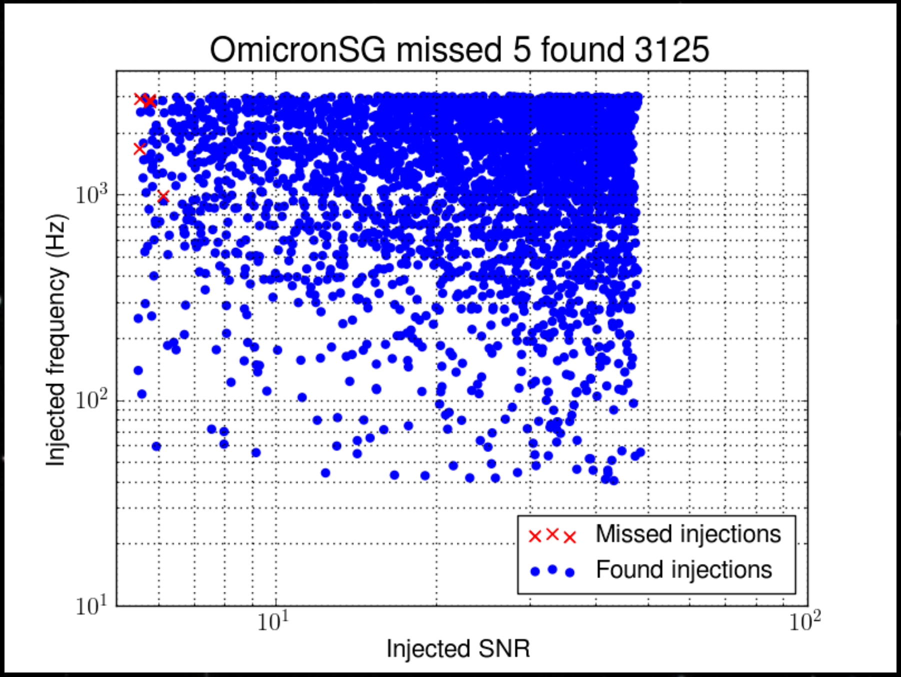

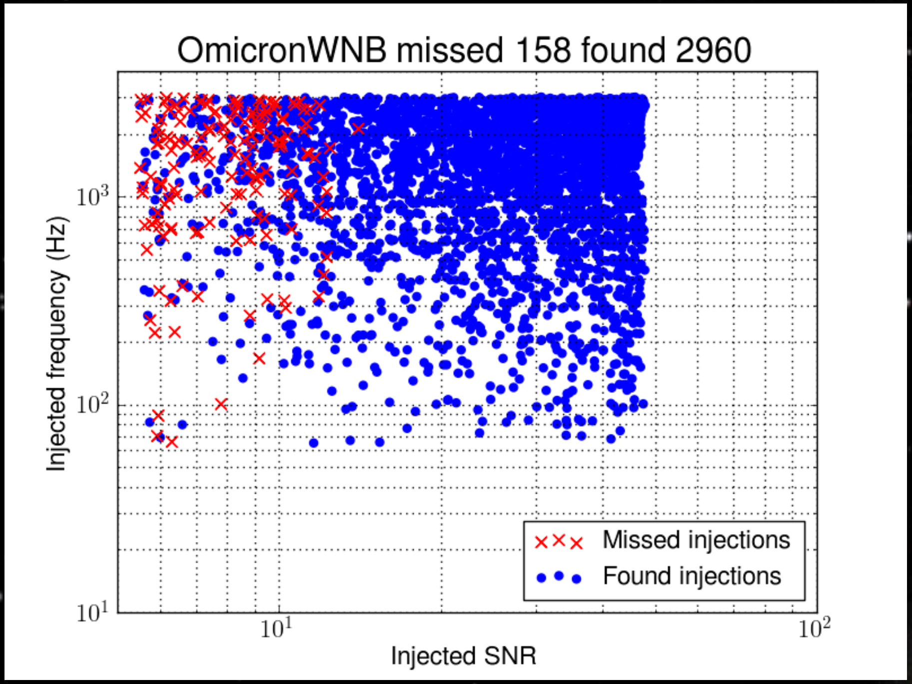

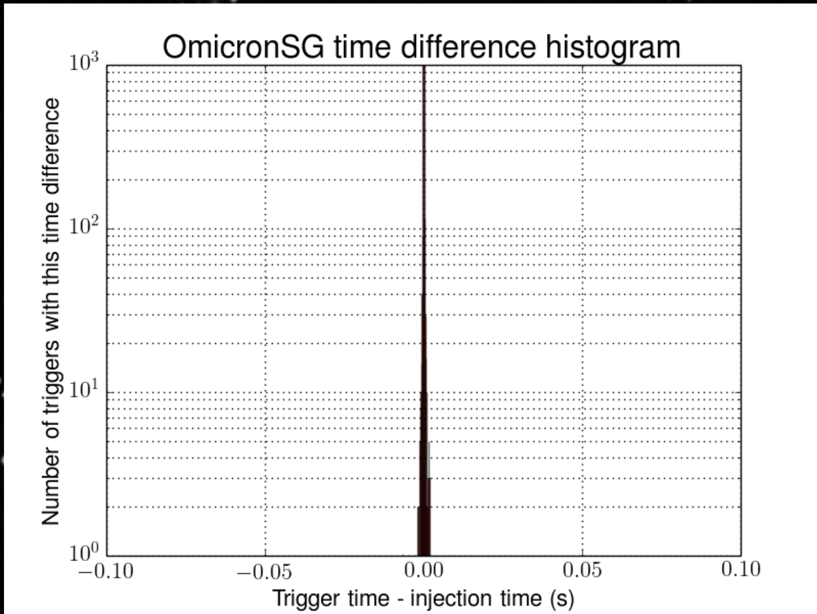
OmicronSG time difference histogram
Number of triggers with this time difference
Trigger time - injection time (s)
10^0
10^1
10^2
10^3
−0.10
−0.05
0.00
0.05
0.10

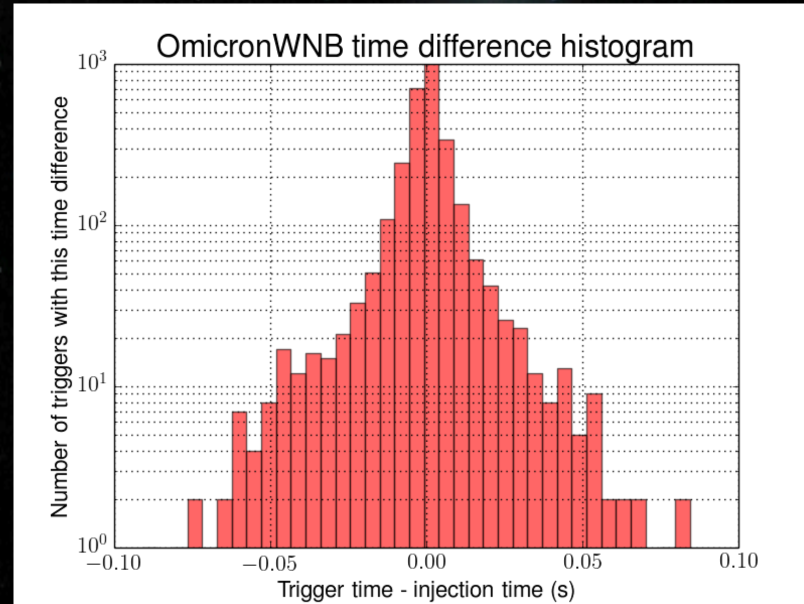
OmicronWNB time difference histogram
Number of triggers with this time difference
Trigger time - injection time (s)
10^0
10^1
10^2
10^3
−0.10
−0.05
0.00
0.05
0.10

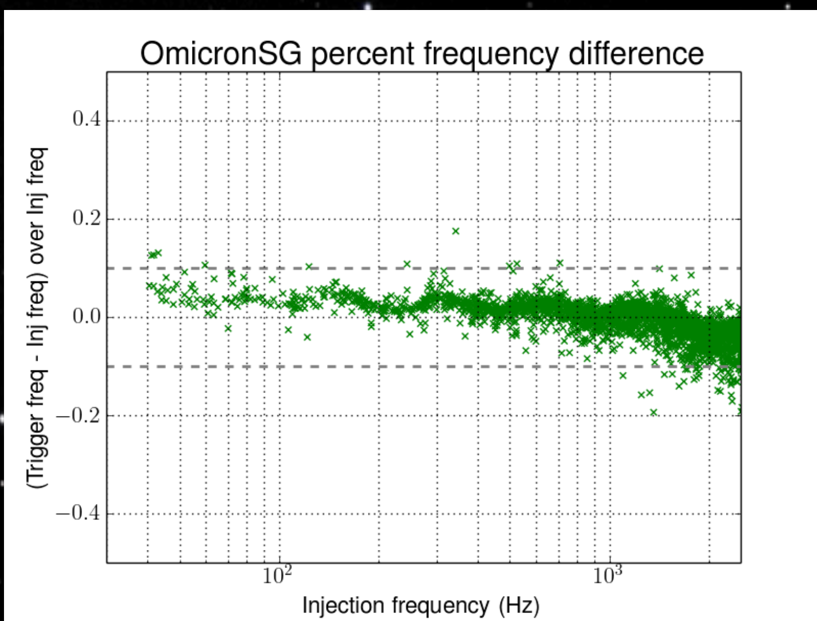
OmicronSG percent frequency difference
(Trigger freq - Inj freq) over Inj freq
Injection frequency (Hz)
0.4
0.2
0.0
−0.2
−0.4
10^2
10^3

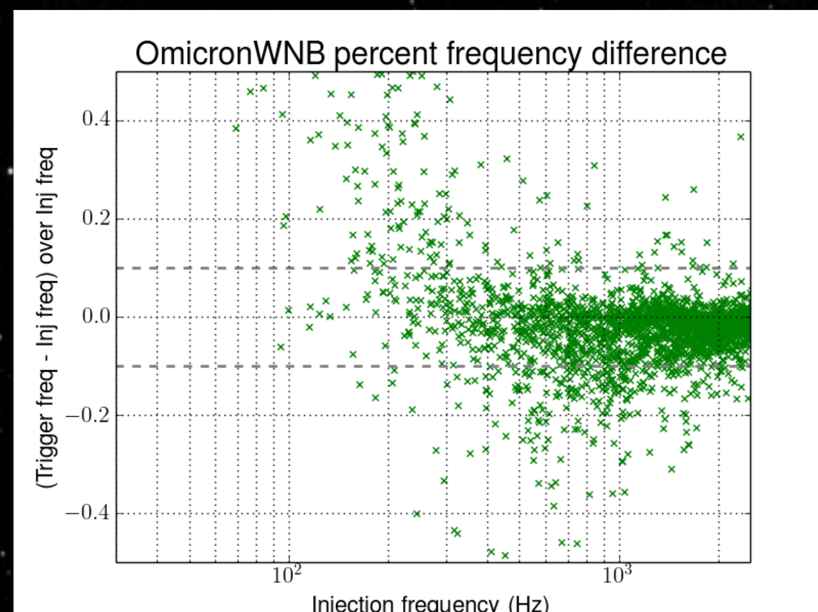
OmicronWNB percent frequency difference
(Trigger freq - Inj freq) over Inj freq
Injection frequency (Hz)
0.4
0.2
0.0
−0.2
−0.4
10^2
10^3

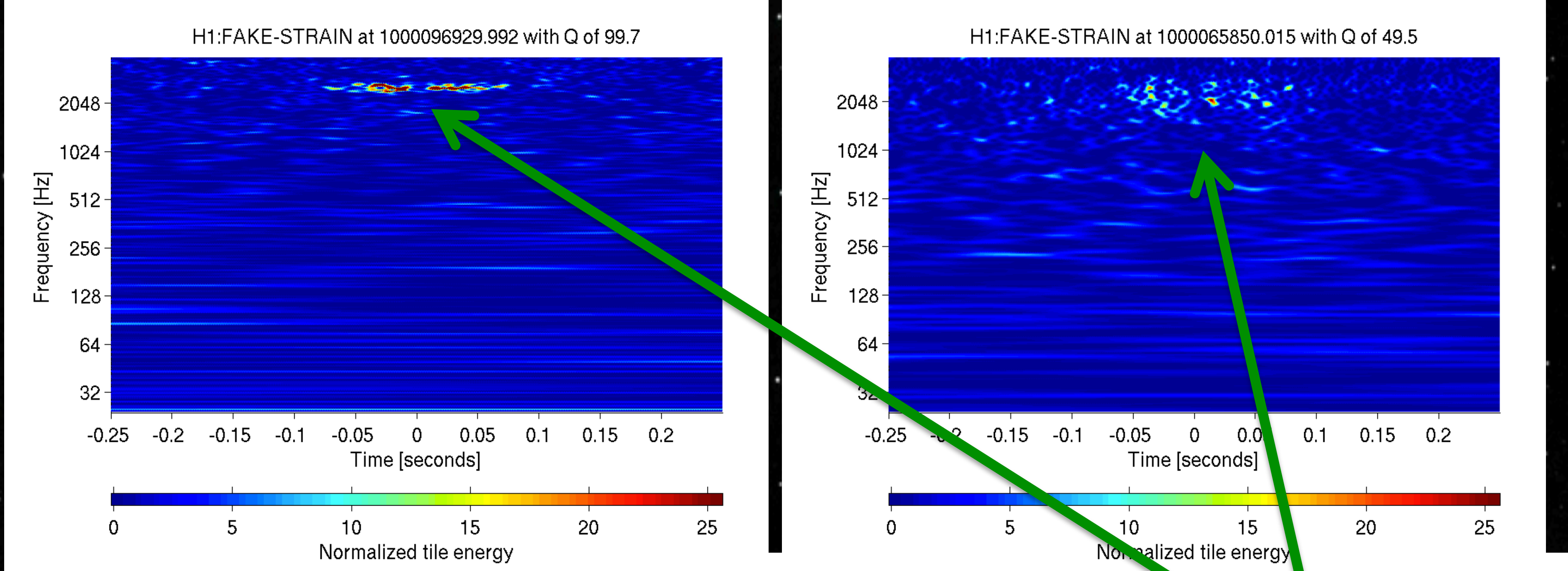

Loud WNBs missed by Omicron

- Tend to be higher frequency than ExcessPower loud missed WNBs
- Tend to be more long duration, narrow bandwidth than ExcessPower missed WNB events
- Efficiency may be significantly improved by accounting for injection duration in matching

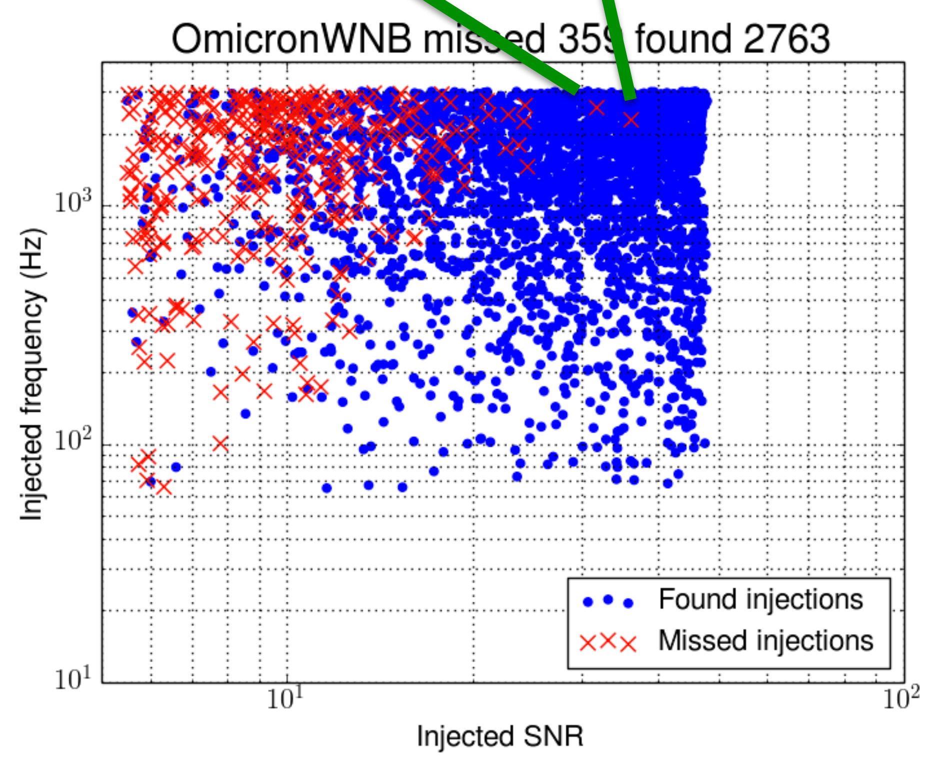

Timing resolution

- All ETGs have better timing resolution for SGs (with the exception of BayesWave, which has some timing offset for SGs)
- The Greeks (Omicron, Omega) have comparable timing resolution – the best for both SGs and WNBs

ETG	SG (s)	WNB (s)
Omicron	3.4e-4	9.8e-3
Excess Power	0.014	0.056
DMT Omega	5.4e-4	6.2e-3
BayesWave	0.055	0.045
PCAT	7.9e-4	0.010

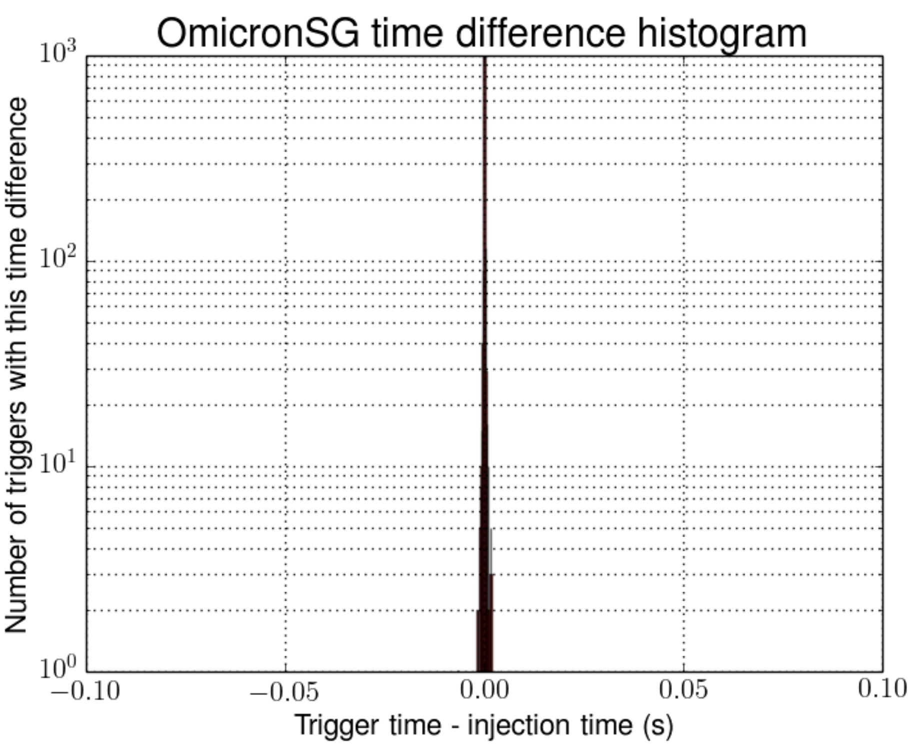

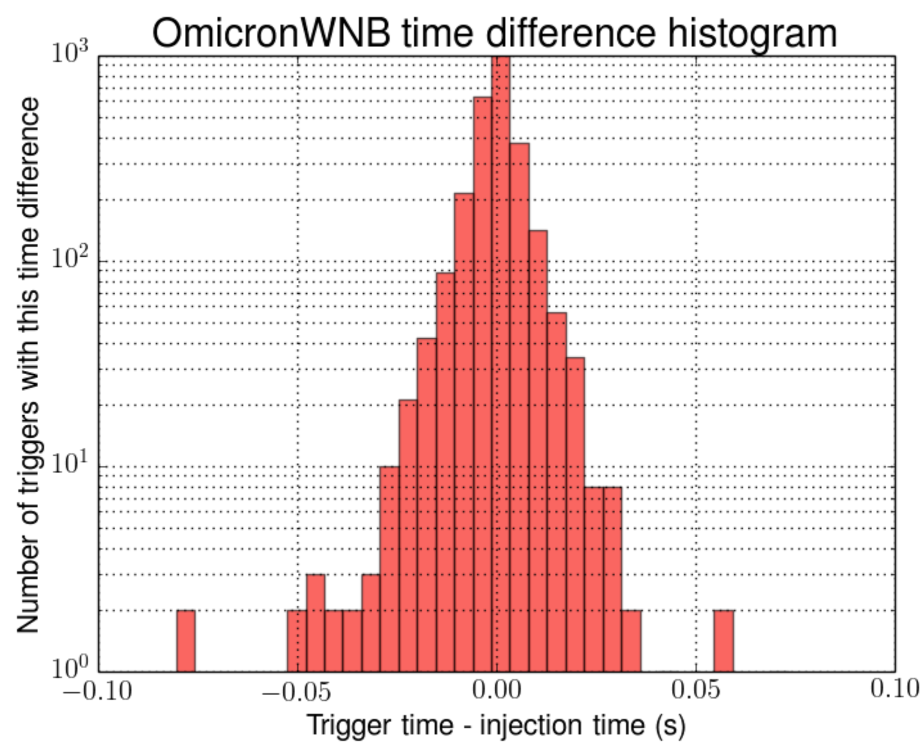

Frequency resolution - I

Summary

- All ETGs have more accurate frequency resolution for SGs (BayesWave has some skew for both)
- The Greeks (Omicron, Omega) again have the best resolution for both SG and WNB frequency

ETG	SG (Hz)	WNB (Hz)
Omicron	82	152
Excess Power	196	544
DMT Omega	93	150
BayesWave	48	115
PCAT	142	121

There are some noticeable tiling artifacts for **Omicron** and **DMT Omega** SG freq resolution

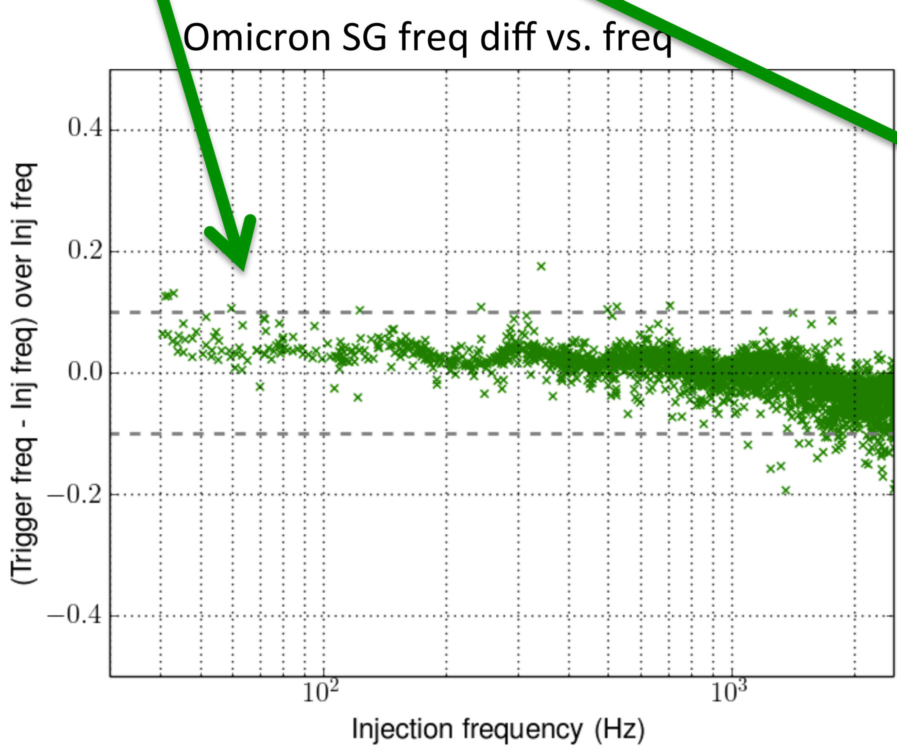

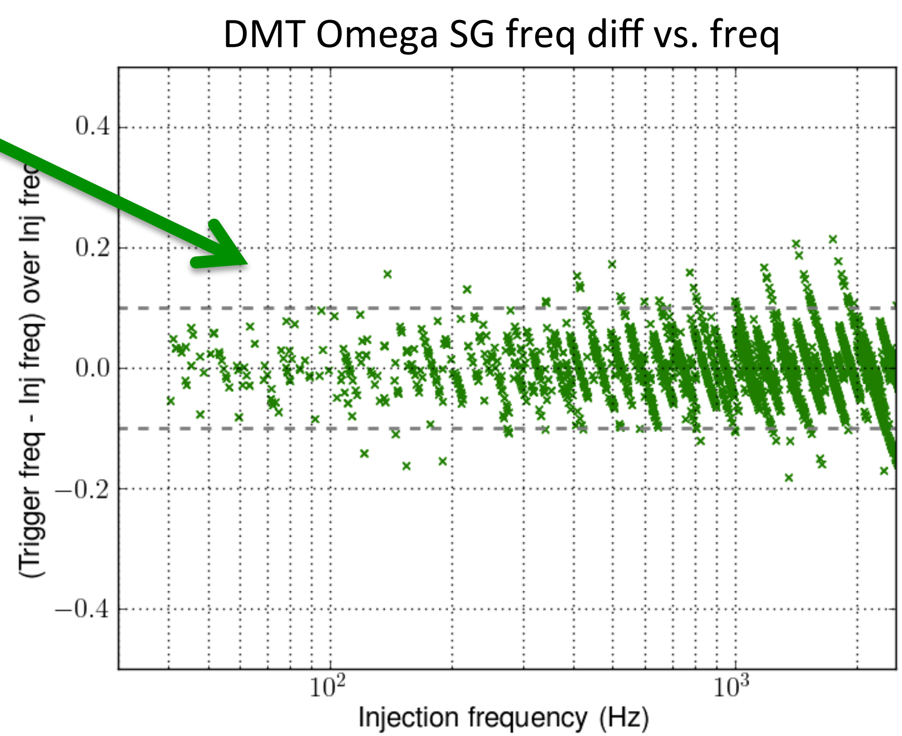

Frequency resolution - II

- **ExcessPower** has a strong artifact in frequency resolution for WNBs and SGs
- **BayesWave** has a skew toward overestimating frequency at lower freq (and underestimating at high freq)
- **PCAT** seems to have no noticeable artifacts for WNBs or SGs

ExcessPowerAll freq diff vs. freq

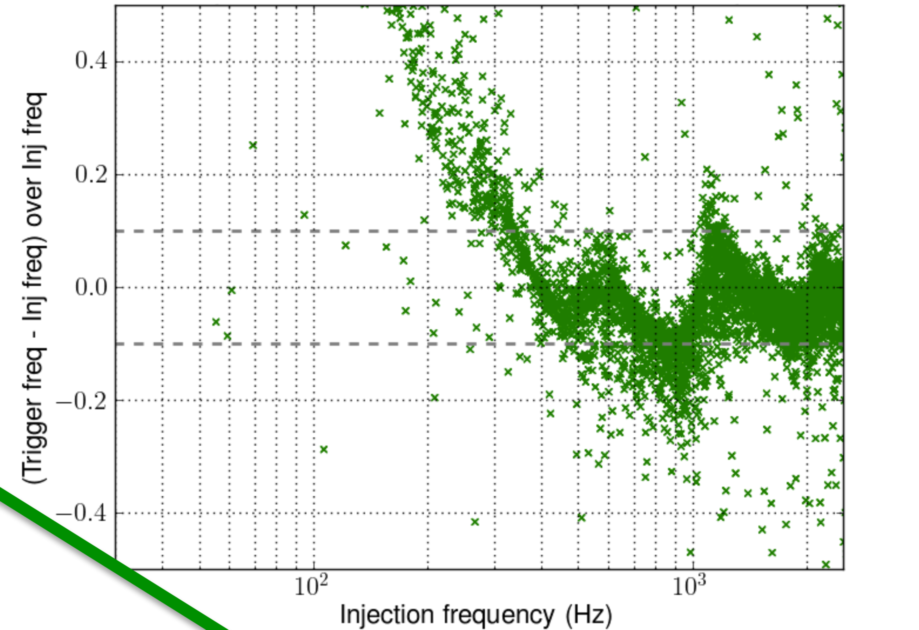

PCAT SG freq diff vs. freq

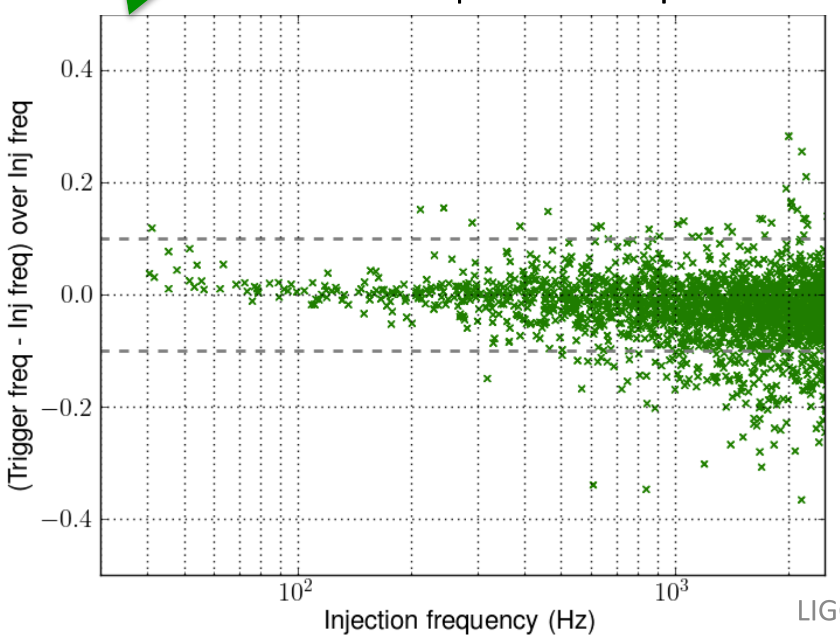

BayesWave2000Hz SG freq diff vs. freq

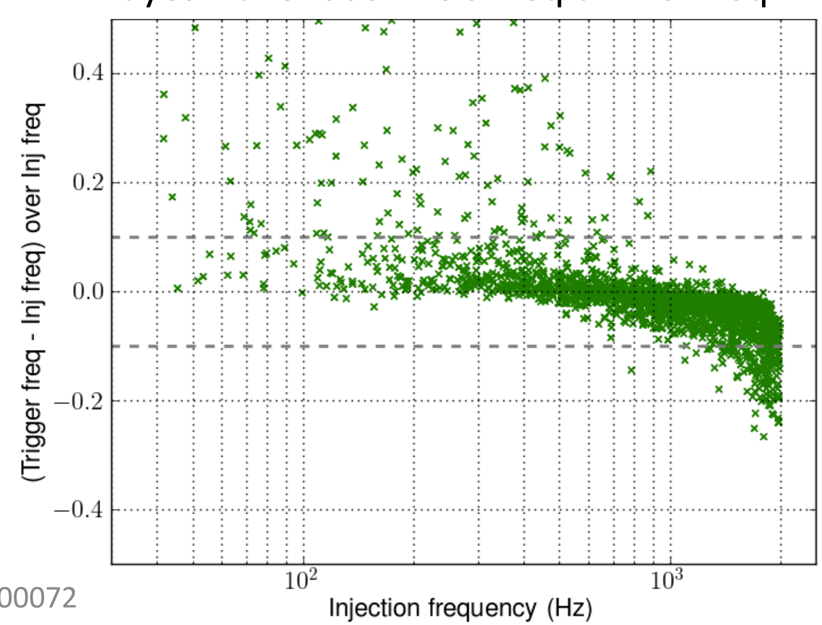

Missed injections

Omicron | Excess Power

White noise bursts

Sine Gaussians

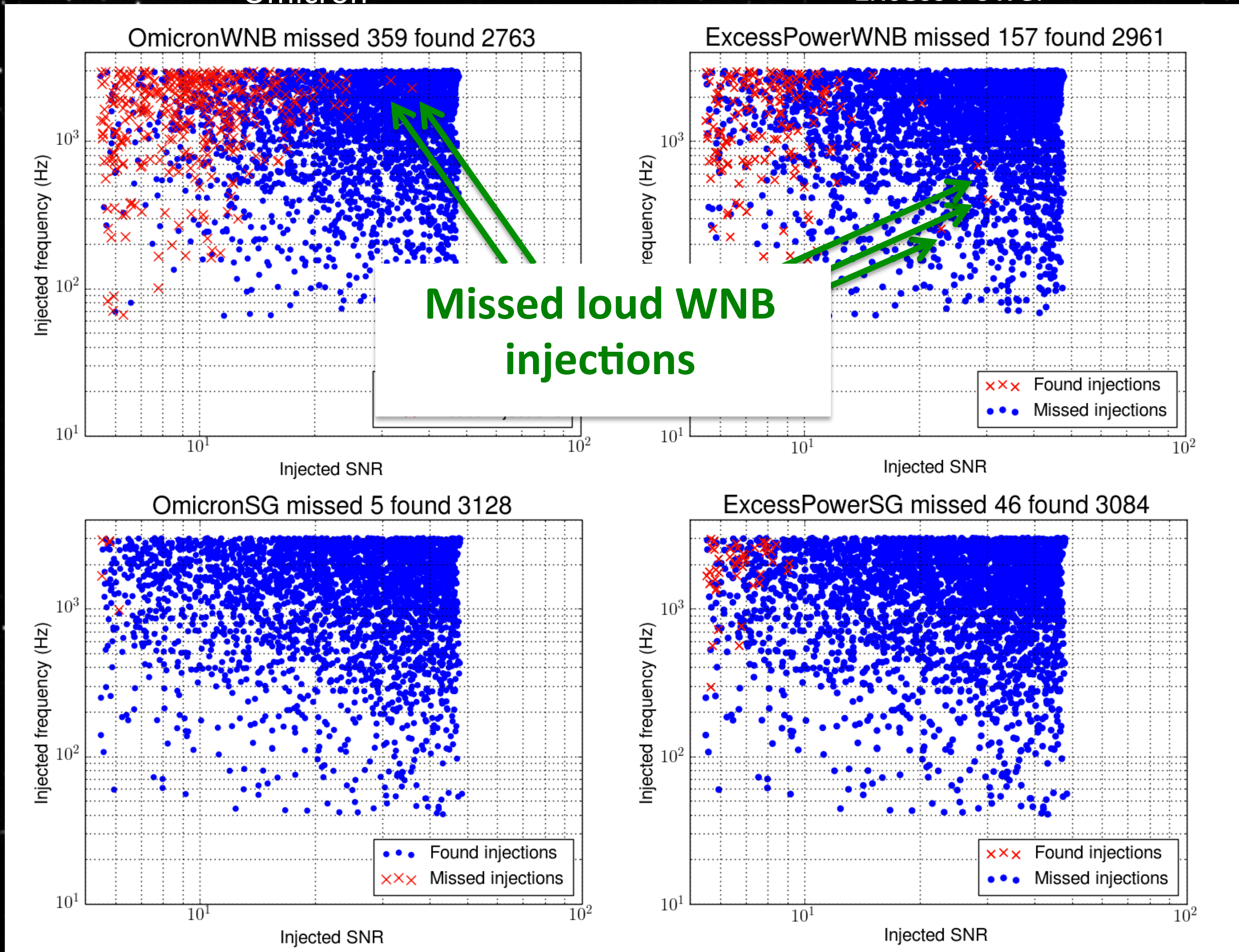

Advanced LIGO instrumentation

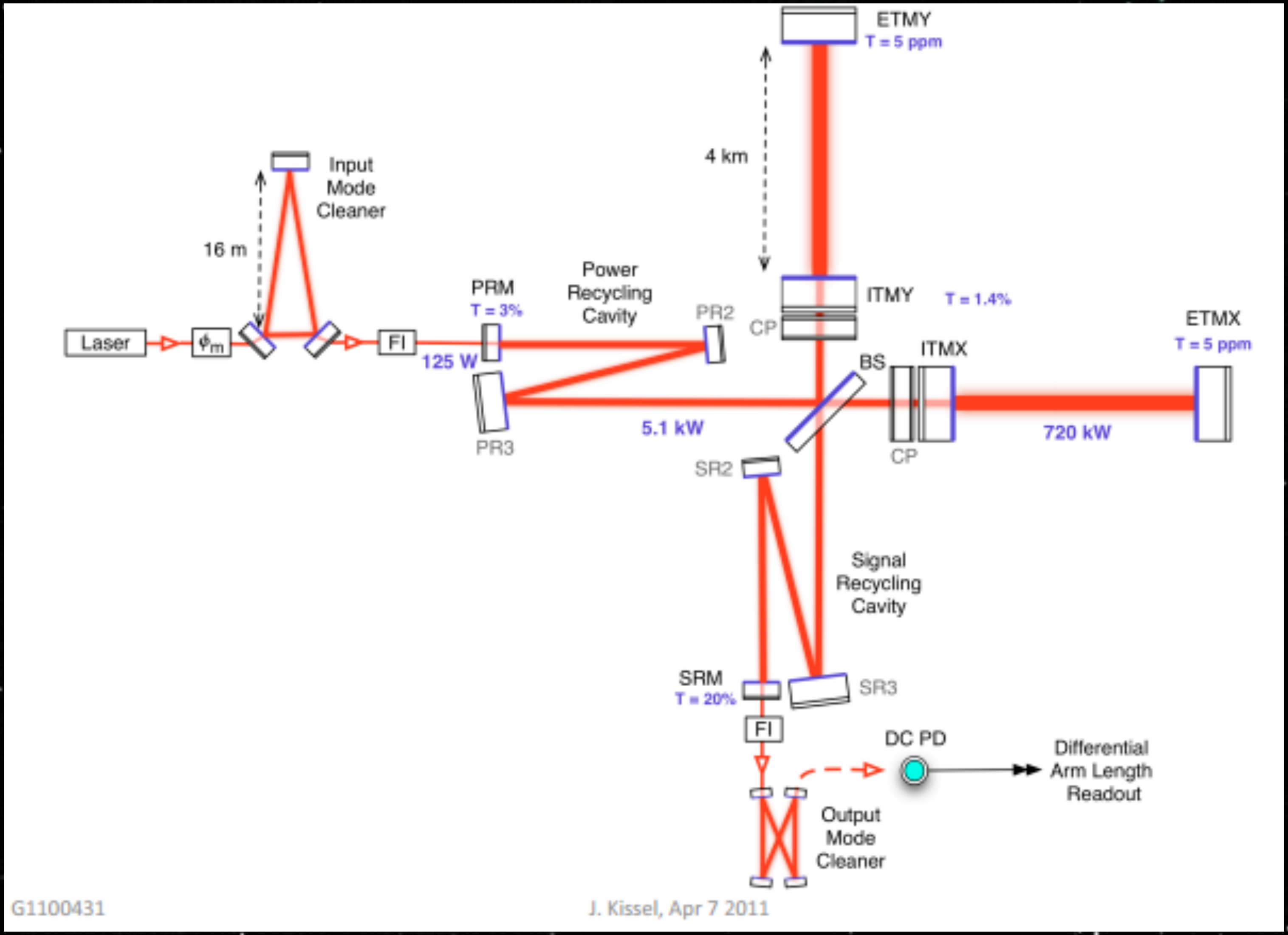

Advanced LIGO seismic isolation instrumentation

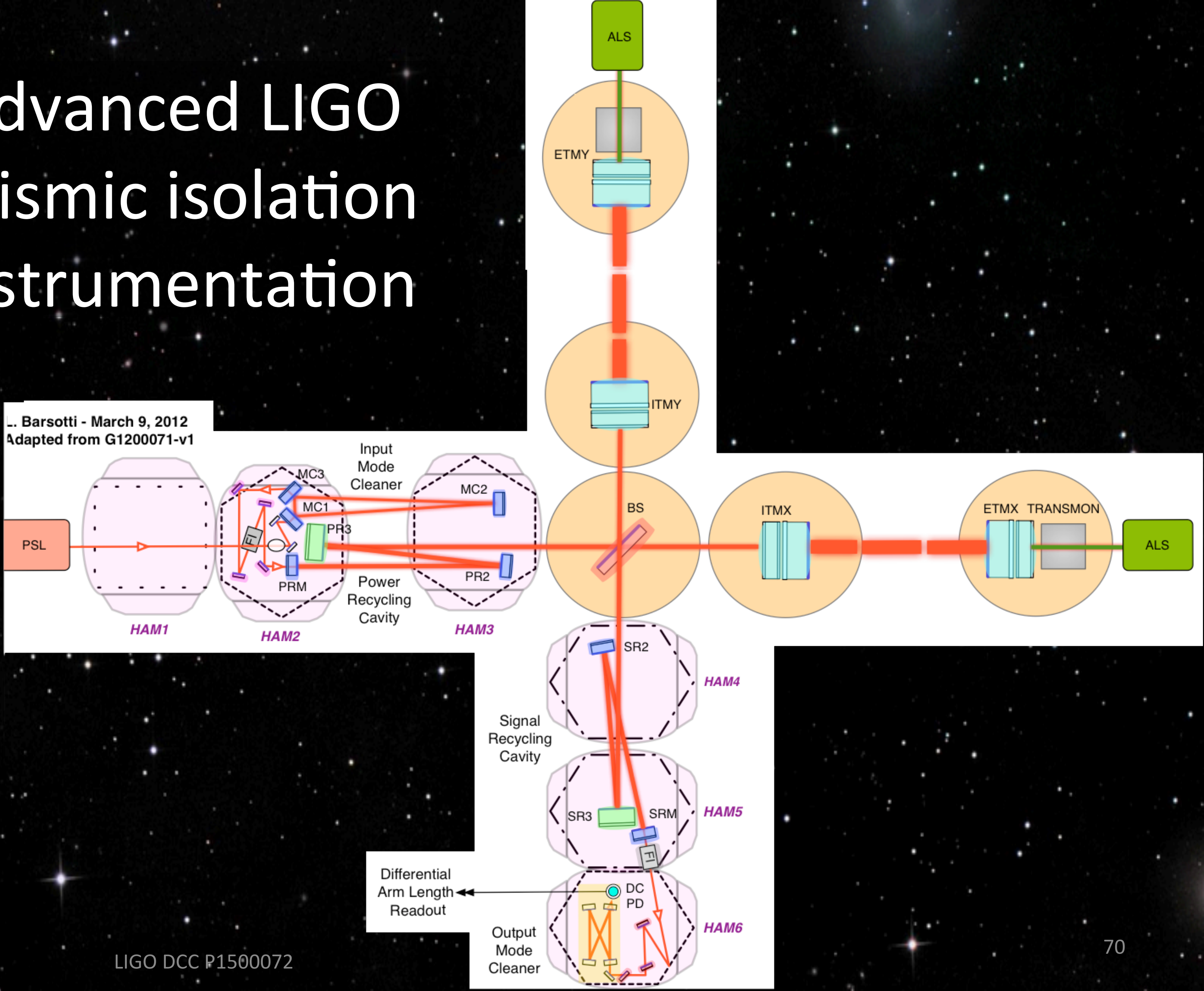

LIGO DCC P1500072